nature chemistry

SUPPLEMENTARY INFORMATION

DOI: 10.1038/NCHEM.2195

Iterative design of a helically folded aromatic oligoamide sequence for the selective encapsulation of fructose

Nagula Chandramouli,[1,2] Yann Ferrand,[1,2] Guillaume Lautrette,[1,2] Brice Kauffmann,[3,4,5] Cameron Mackereth,[6,7] Michel Laguerre,[1,2] Didier Dubreuil,[8,9] Ivan Huc[1,2]

[1] Univ. Bordeaux, CBMN (UMR 5248), Institut Européen de Chimie Biologie, 2 rue Escarpit 33600 Pessac, France.

[2] CNRS, CBMN (UMR 5248), France.

[3] Univ. Bordeaux, IECB (UMS 3033/US 001), Institut Européen de Chimie Biologie, 2 rue Escarpit 33600 Pessac, France.

[4] CNRS, IECB (UMS 3033), France.

[5] INSERM, IECB (US 001), France.

[6] Univ. Bordeaux, ARNA (U 869), Institut Européen de Chimie Biologie, 2 rue Escarpit 33600 Pessac, France.

[7] INSERM, ARNA (U869).

[8] Univ. Nantes, CEISAM (UMR6230), Faculté des Sciences et des Techniques, 2 rue de la Houssinière, BP 92208, 44322 Nantes Cedex 3, France.

[9] CNRS, CEISAM (UMR6230), France.

Table of contents **Page**

1. Methods for NMR, X-ray crystallography and Modelling

Nuclear magnetic resonance spectroscopy

NMR spectra were recorded on 3 different NMR spectrometers: (1) an Avance II NMR spectrometer (Bruker Biospin) with a vertical 7.05T narrow-bore/ultrashield magnet operating at 300 MHz for ^{1}H observation, 282 MHz for ^{19}F observation and 75 MHz for ^{13}C observation by means of a 5-mm direct BBO H/X probe with Z gradient capabilities; (2) an Avance III NMR spectrometer (Bruker Biospin) with a vertical 16.45T narrow-bore/ultrashield magnet operating at 700 MHz for ^{1}H observation by means of a 5-mm TXI ^{1}H/^{13}C/^{15}N probe with Z gradient capabilities. (3) an Avance III NMR spectrometer (Bruker Biospin) with a Standard Bore Cryo Probe operating at 800 MHz for ^{1}H observation by means of a 5-mm TCI ^{1}H/^{13}C/^{15}N probe with Z gradient capabilities. Chemical shifts are reported in part per million (ppm, δ) relative to the ^{1}H residual signal of the deuterated solvent used. ^{1}H NMR splitting patterns with observed first-order coupling are designated as singlet (s), doublet (d), triplet (t), quartet (q) or broad singlet (bs) . Coupling constants (*J*) are reported in hertz. Samples were not degassed. Data processing was performed with Topspin 2.0 software.

X-ray crystallography

Crystallographic data for host-guest complexes **1**⊃α–**8a**, **1**⊃α–**13a**, **3**⊃β–**7a** were collected at the IECB x-ray facility (UMS 3033 – UMS001) on a Rigaku MM007 rotating anode (0.8 kW). Data were collected at the copper kα wavelength with a partial chi goniometer. The x-ray source is equipped with high flux Osmic Varimax mirrors and a RAPID SPIDER image plate detector. Crystallographic data for host-guest complexes **1**⊃β–**7a**, **1**⊃β–**9a** and **5**⊃β–**7a** were collected at the BM30A (ESRF) beamline at 0.8, 0.78 and 0.85 Å, respectively. Phi-scans were performed and data recorded with a large ADSC Q315r CCD detector. The Rigaku CrystalClear suite was used to index and integrate the home source data with a multiscan absorption correction. Data collected at the synchrotron were processed with the XDS package[1].

All structures were solved by charge-flipping with Superflip[2] and refined by full-matrix least-squares methods using WinGX[3] software, which utilizes the SHELXH 2013 module[4]. The SQUEEZE procedure[5] implemented in PLATON was used for all structures in order to treat the regions with highly disordered solvent molecules (mainly chloroform, water, methanol and *n*-hexane molecules).

In all cases, the positions of carbon-bound and nitrogen-bound hydrogen atoms from the capsule were calculated and refined as riding on the parent carbon atoms with UH=1.2 UC. For some isobutoxy side chains the terminal methyl groups were refined with two idealized positions (HFIX 123). For complexes **1**⊃β–**9a** and **1**⊃α–**13a** constraints of type AFIX 116 were applied for some naphthyridine and quinoline residues. SHELX SIMU and DELU restraints were used in the refinement strategy, as listed in the cif files, mostly for the main chain of the foldamers. These are restraints on Displacement Parameters that take into account that atoms, which are bound to one another, move similarly, both in direction and amount. EADP constraints were applied for some side chains. This constraint forces atoms to have identical Atomic Displacement Parameters.

Every time where solvent or side chain disorder could be modelled with partial occupation, it was so. However, more often than not, no simple models of the side chains and solvents can be obtained because multiple positions exists and because complexity is introduced by the swapping of side chains and solvent molecules at some positions, leading to unstable refinement. Introducing too many restraints on the side chains destabilizes the main chain and thus also has to be ruled out. Under such circumstances, an approach that many crystallographers would follow would be to squeeze out the disordered areas that cannot be modelled. However, we did not use this approach which amounts to removing information from our data and which does affect the main chain displacement parameters. Instead, the side chains are modelled using the EADP constraints (equal atomic displacement parameters) and in most cases refined with isotropic atomic displacement parameters. The outcome is a view of the side chains in an average position which, in our opinion represents a real information contained in the data. Such modelling is efficient at avoiding negative displacement parameters and thus well takes into account the measured electron density.

All sugar guests were refined according to the experimental electron density observed in the different capsules. Hydrogen atoms for all guest molecules except for complex **5**⊃β–**7a** were positioned on theoretical basis and refined as riding on the parent carbon atoms. As shown in supplementary Figs. S58 and S59 structural information about H positions on the fructose molecule of complex **5**⊃β–**7a** can be extracted from the experimental data. All C-bound H positions has been confirmed by calculating Fourier difference omit-maps and compare to the dynamic calculation results. Unfortunately, experimental electron density for H atoms of hydroxyl groups are hardly visible at a reasonable signal over noise level in the density maps and were kept in the calculated positions in the final model.

The final cif files were checked using IUCR's checkcif algorithm. Due to the characteristics of the crystals mentioned above (large volume fractions of disordered solvent molecules and side chains, weak diffraction intensity, incompleteness of the data and moderate resolution), and due to the choices made for refining some disordered side chains to use EADP contraints (instead of squeezing them out when valid models could not be established), a number of A-level and B-level alerts remain in the check cif file. These alerts are explicitly listed below and have been divided into two groups. They are inherent to the data and refinement procedures and do not reflect errors. Rather, they illustrate the limited practicality of the checkcif tool for medium size molecule crystallography.

GROUP 1 ALERTS

THETM01_ALERT_3_A : diffrn_reflns_theta_max is greater than expected
RFACR01_ALERT_3_B : refine_ls_wR_factor_ref is within expected limits
RINTA01_ALERT_3_B : diffrn_reflns_av_R_equivalents is within expected limits
PLAT019_ALERT_1_B : diffrn_measured_fraction_theta_max/full consistency
PLAT029_ALERT_3_A : diffrn_measured_fraction_theta_full
PLAT084_ALERT_3_B : Test for reasonable wR2
PLAT088_ALERT_3_A : reasonable Data / parameter ratio
PLAT020_ALERT_3_B : Check Rint
PLAT026_ALERT_3_B : Check for weak data

All these alerts in fact point to the same and unique problem which is the overall weak quality of the data and refinement statistics if compared to that expected for small molecule structures from highly diffracting

crystals. They are inherent to the best quality crystals that can be grown from such host-guest complexes. Large units cells, especially when several independent complexes are found in the asymmetric unit (for **1**⊃**7a** and **1**⊃**9a**), high fraction volume of disordered solvent and side chain content contribute to low average statistics. Data collection using synchrotron radiation (**1**⊃**7a, 1**⊃**9a** and **5**⊃**7a**) brings the benefit of improving diffraction intensity and collecting at higher resolution, but it also has drawbacks such as radiation damage or beamline data collection geometry which may preclude to collect at high θ_{max} values and which also limits data completeness as most beam lines are equipped with a single axis goniometer.

GROUP 2 ALERTS

PLAT201_ALERT_2_B : Test for isotropic non-H atoms in anion ? or solvent ?
PLAT211_ALERT_2_A : Test for NPD ADP's (1.0)
PLAT213_ALERT_2_A and B : Test ratio adp max/min
PLAT222_ALERT_3_A : Uiso(max)/Uiso(Min) range for H atoms in non-solvent
PLAT234_ALERT_4_A and B : Hirshfeld Rigid-Bond Test
PLAT360_ALERT_2_A and B : short C4 - C4 (Angstrom Difference)
PLAT241_ALERT_2_B : unusually high U(eq) as compared with bonded neighbors
PLAT242_ALERT_2_B : unusually Low U(eq) as compared with bonded neighbors
PLAT230_ALERT_2_B :Hirshfeld Rigid-Bond Test
PLAT340_ALERT_3_B : Bond Precision for C-C in Light Atom Structures
PLAT360_ALERT_2_A : Test for short C4 - C4 (Angstrom Difference)
PLAT369_ALERT_2_B : long C3 - C3 (Angstrom Difference)
PLAT410_ALERT_2_A : Test for short non-bonding intra H..H contacts
PLAT412_ALERT_2_A : Test for short non-bonding intra H..H contacts (involving XH3)
PLAT417_ALERT_2_A and B : Test for short non-bonding inter D-H..H-D contacts
PLAT420_ALERT_2_B : Test for D-H without acceptor
PLAT430_ALERT_2_B : Test for short non-bonding inter D...A contacts
PLAT782_ALERT_2_B : Test for Unusual C-NO2 an C-CO2 moiety Bond geometry
PLAT306_ALERT_2_B : Test for isolated Oxygen Atoms

These A and B alerts are related to geometrical and atomic displacement parameters problems, all concerning side chains and solvent molecules, that result from the way these have been treated (see above) when they have not been squeezed out. Many of these alerts are redundant: for example, a “unusually high U(eq) as compared with bonded neighbors” generally goes with one or several “unusually low U(eq) as compared with bonded neighbors”.

Modelling

Calculation of cavity volumes. Cavity volume of complexes **1**⊃**7a**, **1**⊃**8a**, **1**⊃**9a**, **1**⊃**13a**, **3**⊃**7a** and **5**⊃**7a** were estimated using the SURFNET software.[11] PDB-format files were generated from the x-ray data after modelling all the hydrogens of hydroxyl groups and were used directly to calculate volumes. The volume of guest molecules, cavity size and gaps (> 10 $Å^3$) between the guest and the inner wall of the capsule were generated by fitting spheres into the spaces generated between atoms (coordinate of the PDB files). Typically, the diameter of the probe used in this study was 1 Å. The calculation of cavity volumes was performed after the removal of all the atoms the atoms of the carbohydrates. Packing coefficient is defined as the ratio between the volume of the guest and the volume of the cavity. The volumes for complexes **1**⊃**7a**, **1**⊃**8a**, **1**⊃**9a**, **1**⊃**13a**, **3**⊃**7a** and **5**⊃**7a** are reported in Table S12.

2. Methods for chemical synthesis

All reactions were carried out under a dry nitrogen atmosphere. Commercial reagents were purchased from Sigma-Aldrich, Alfa-Aesar or TCI and were used without further purification unless otherwise specified. ^{13}C labeled carbohydrates were purchased from Omicron Biochemicals Inc.. Tetrahydrofurane (THF) and dichloromethane (CH_2Cl_2) were dried over alumina columns; chloroform, triethylamine and diisopropylethylamine (DIEA) were distilled over calcium hydride (CaH_2) prior to use. Reactions were monitored by thin layer chromatography (TLC) on Merck silica gel 60-F254 plates and observed under UV light. Column chromatography purifications were carried out on Merck GEDURAN Si60 (40-63 µm). Melting points were measured on a Büchi B-540. ESI and MALDI mass spectra were obtained on a Waters LCT Premier and from the Mass Spectrometry Laboratory at the European Institute of Chemistry and Biology (UMS 3033 - IECB), Pessac, France.

2.1 Synthesis of "**H**" monomer

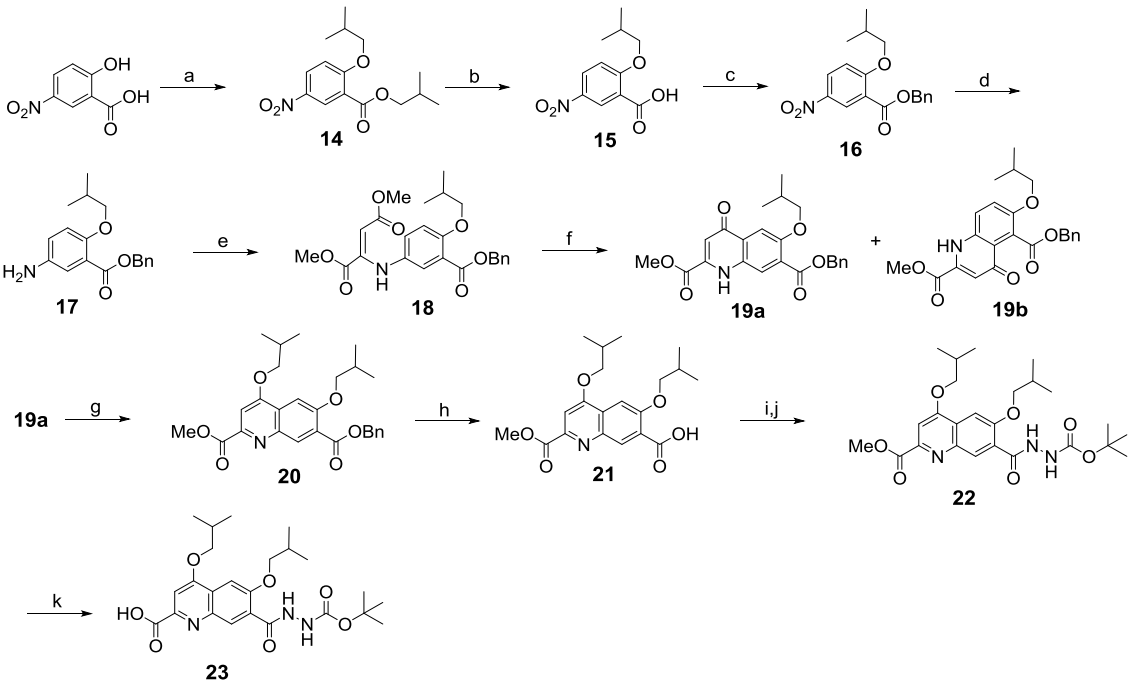

Supplementary Scheme S1. Synthesis of **H** monomer **23**: (a) K_2CO_3, *i*BuI, TBAB, DMF, 80-85°C; (b) NaOH, DMF, 0 °C, room temperature; (c) thionyl chloride, BnOH, Et_3N, $CHCl_3$; (d) $CuSO_4.5xH_2O$, $NaBH_4$, CH_2Cl_2:MeOH, 0 °C; (e) dimethyl acetylenedicarboxylate, MeOH, reflux; (f) PhOPh, reflux; (g) *i*BuOH, DIAD, PPh_3, THF, 0 °C - room temperature; (h) H_2, Pd/C, EtOAc; (i) oxalyl chloride, $CHCl_3$; (j) NH_2NHBoc, DIEA, $CHCl_3$; (k) NaOH, THF, MeOH, H_2O, 0 °C, room temperature.

2.2 Synthesis of aromatic amide oligomers **1**, **2**, **3**, **4**, **5** and **6**

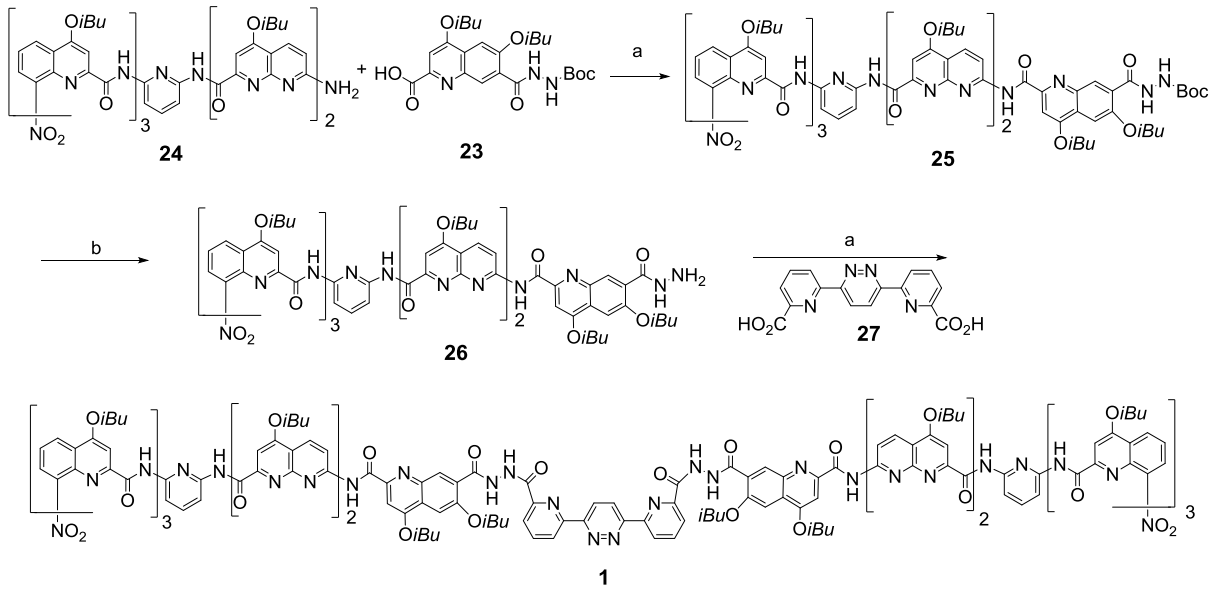

Supplementary Scheme S2. Synthesis of capsule **1**: (a) PyBOP, DIEA, $CHCl_3$, room temperature then 40 °C; (b) TFA, $CHCl_3$, 0 °C, room temperature.

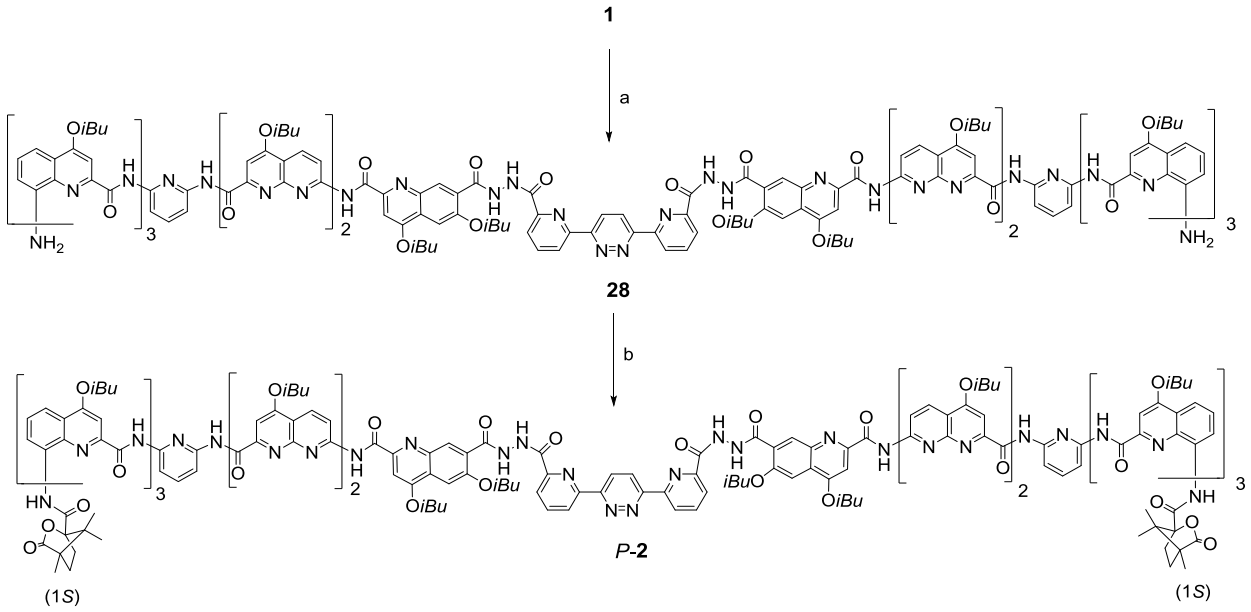

Supplementary Scheme S3. Synthesis of capsule **2**: (a) 10% Pd/C, NH_4CO_2H, cat. NH_4VO_3, EtOAc, EtOH and H_2O, room temperature then 90 °C; (b) (1*S*)-(-)-camphanic chloride, DIEA, $CHCl_3$, room temperature then 40 °C.

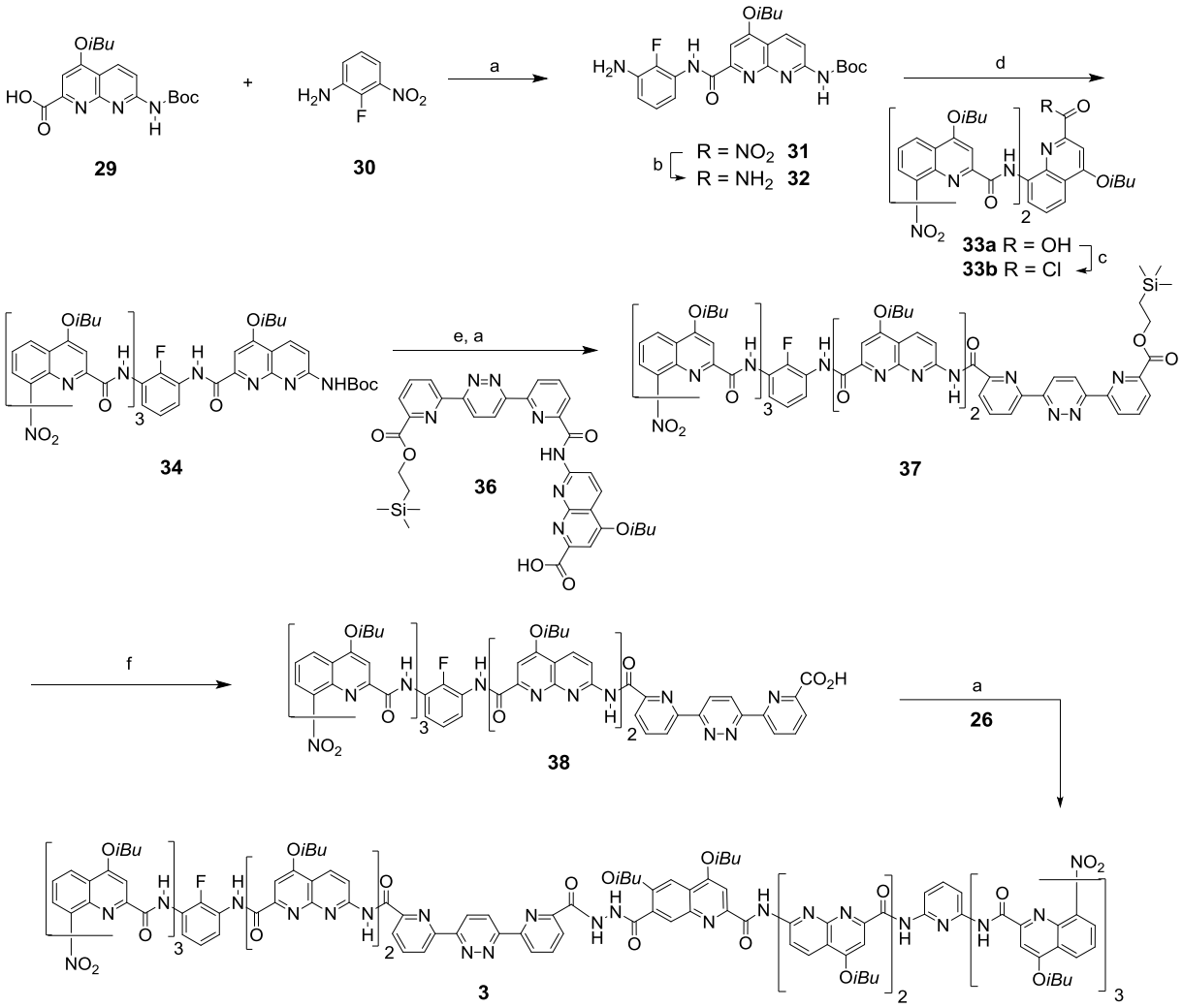

Supplementary Scheme S4. Synthesis of capsule **3**: (a) PyBOP, DIEA, $CHCl_3$, room temperature then 40 °C; (b) H_2, 10% Pd/C, EtOAc; (c) $(COCl)_2$, $CHCl_3$, room temperature; (d) DIEA, $CHCl_3$, 0 °C then room temperature; (e) TFA, $CHCl_3$, room temperature; (f) TBAF, THF, room temperature.

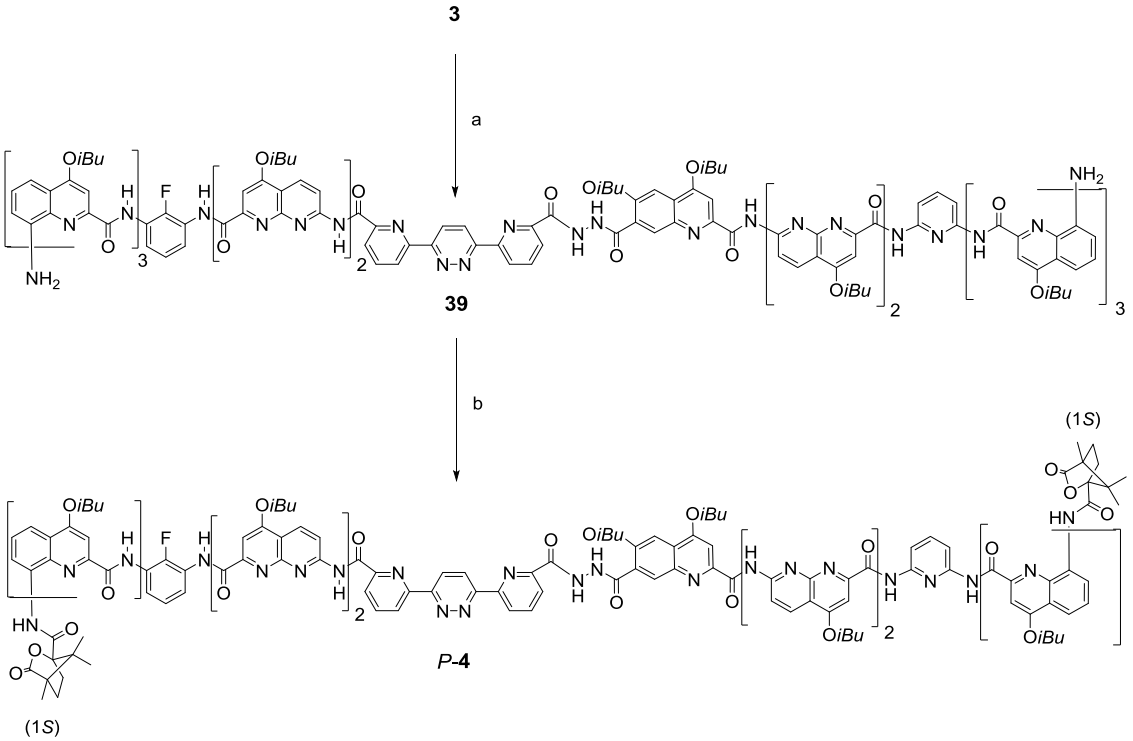

Supplementary Scheme S5. Synthesis of capsule **4**: (a) 10% Pd/C, NH_4CO_2H, cat. NH_4VO_3, EtOAc, EtOH and H_2O, room temperature then 90 °C; (b) (1*S*)-(-)-camphanic chloride, DIEA, $CHCl_3$, room temperature then 40 °C.

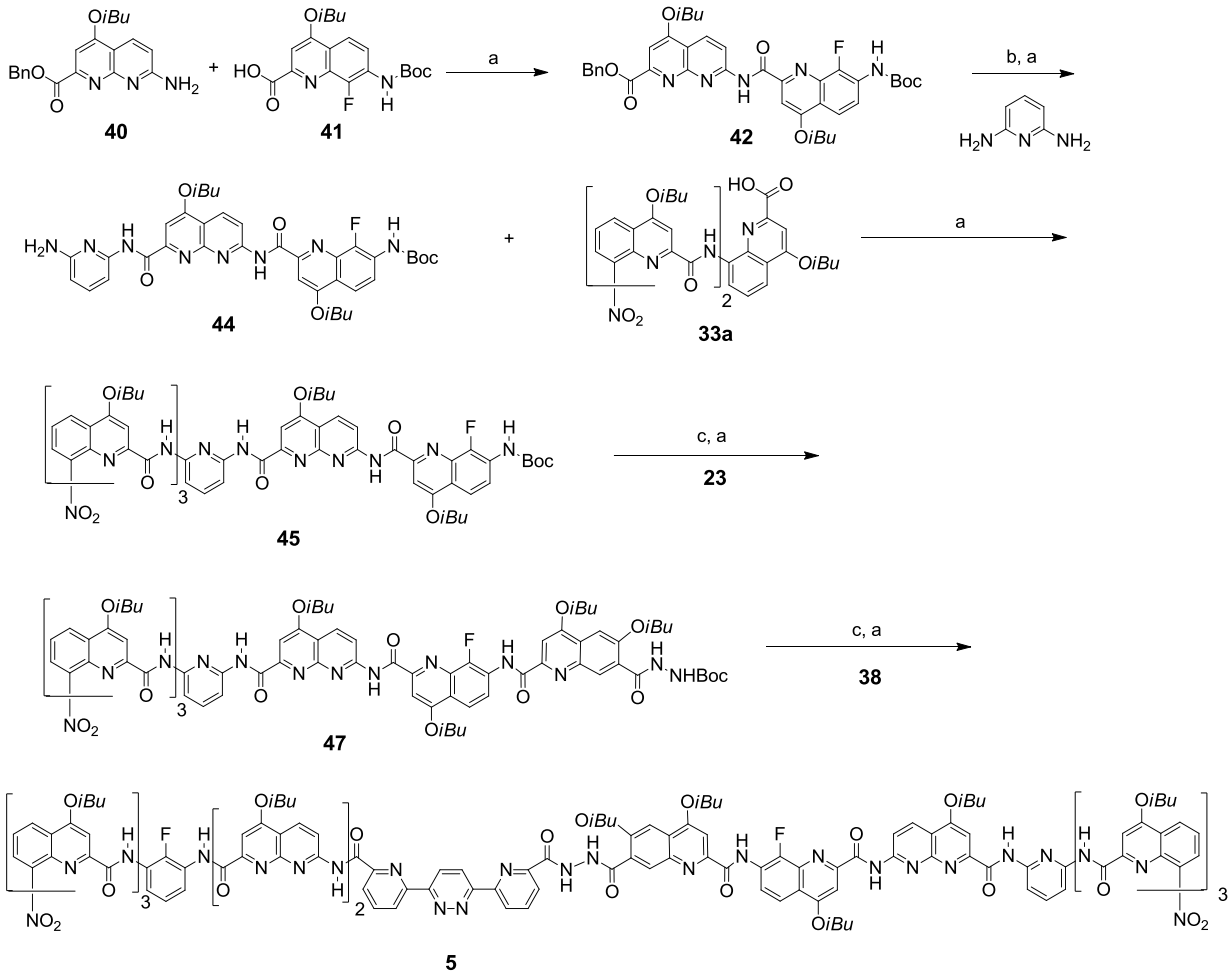

Supplementary Scheme S6. Synthesis of capsule **4**: (a) PyBOP, DIEA, $CHCl_3$, room temperature then 40 °C; (b) H_2, 10% Pd/C, EtOAc; (c) TFA, $CHCl_3$, 0 °C, room temperature.

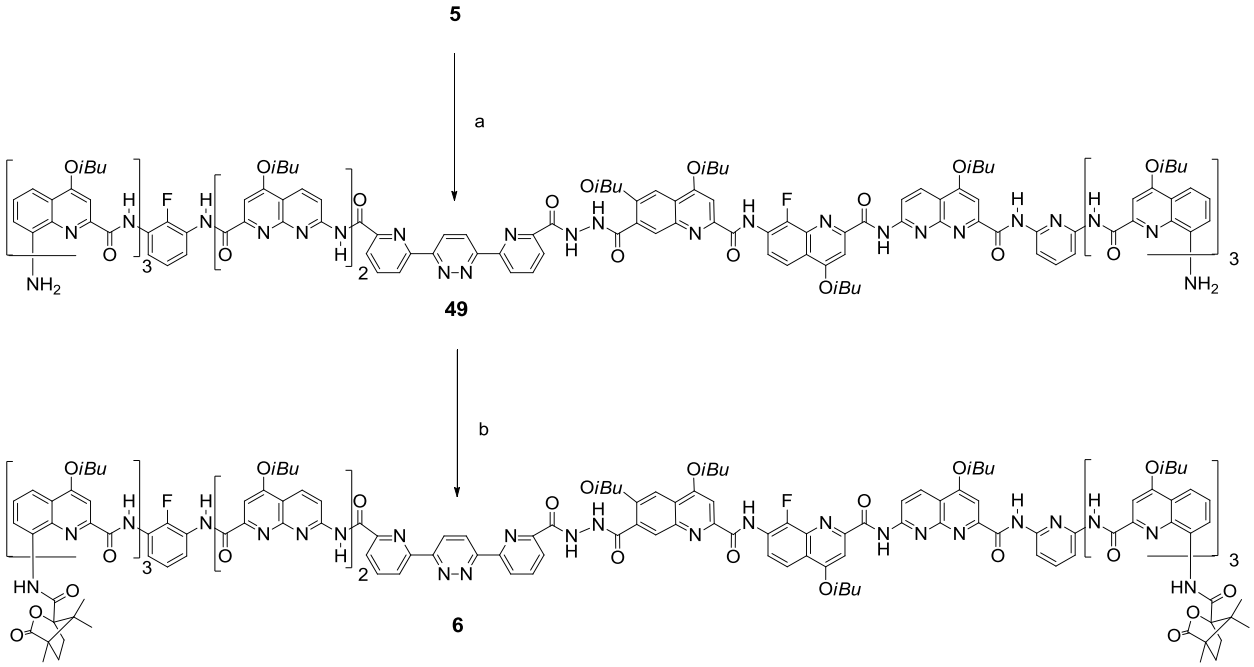

Supplementary Scheme S7. Synthesis of capsule **6**: (a) 10% Pd/C, NH_4CO_2H, cat. NH_4VO_3, EtOAc, EtOH and H_2O, room temperature then 90 °C; (b) (1*S*)-(-)-camphanic chloride, DIEA, $CHCl_3$, room temperature then 40 °C.

2.3 Experimental procedures

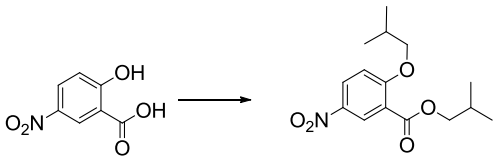

14

2-isobutoxy-5-nitroisobutyl benzoate 14. To the mixture of 5-nitrosalicilic acid (25 g, 0.137 m mol) and K_2CO_3 (38.3 g, 0.683 mmol) in DMF (200 mL) was added isobutyl iodide (39.3 mL, 0.342 mmol). The reaction mixture was stirred for 48 hours. After completion of the reaction, the mixture was diluted with water and extracted with EtOAc. The organic layer was washed with 0.5 N HCl, brine, dried over Na_2SO_4, filtered and concentrated. The residue was purified by column chromatography eluting with EtOAc:cyclohexane (30:70 vol/vol) to give isobutyl-2-isobutoxy-5-nitro benzoate **14** (82 %, 33 g) as a yellow viscous oil. ^{1}H NMR (300 MHz, $CDCl_3$) δ ppm = 8.68 (d, *J* = 2.99, 1H); 8.33 (dd, *J* = 9.22, 1H); 7.02, (d, *J* = 9.22, 1H), 4.12 (d, *J* = 6.98, 2H); 3.90, (d, *J* = 6.58, 2H), 2.19-2.09 (m, 2H); 1.07 (d, *J* = 6.72, 6H); 1.01 (d, *J* = 6.72, 6H). ^{13}C NMR (75 MHz, $CDCl_3$) δ ppm = 164.7, 163.4, 140.6, 128.9, 127.9, 121.2, 112.9, 76.2, 71.9, 28.4, 28.0, 19.4, 19.3. HRMS (ESI$^+$): *m/z* calcd for $C_{15}H_{21}NO_5Na$ $[M+Na]^+$ 318.1317 found 318.1312.

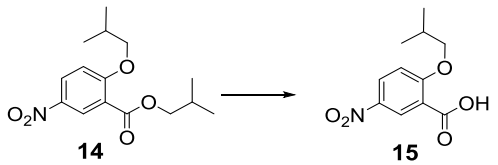

14 **15**

2-isobutoxy-5-nitrobenzoic acid 15. To a solution of 2-isobutoxy-5-nitroisobutyl benzoate **14** (30 g, 0.102 mmol) in 270 mL of THF/MeOH (8:1) at 0 ˚C was added NaOH (12.2 g, 0.304 mmol dissolved in 30 mL of water). The reaction was monitored by TLC and the resulting slurry was stirred at room temperature for 3 hours, quenched by addition of 1N HCl, and then solvents were evaporated. The residue was dissolved in 500 mL dichloromethane, and then the organic layer was washed twice with 500 mL distilled water and with saturated NaCl. The organic layer was dried over $MgSO_4$ and filtered. Solvent was evaporated and dried under high vacuum to give acid derivative **15** as a white solid (94 %, 23 g). mp 142-143°C. ^{1}H NMR (300 MHz, $CDCl_3$) δ ppm = 9.01 (d, *J* = 2.69, 1H); 8.41 (dd, *J* = 9.13, 1H); 7.14, (d, *J* = 9.18, 1H), 4.09 (d, *J* = 6.39, 2H); 2.27 (m, 1H); 1.12 (d, *J* = 6.72, 6H). ^{13}C NMR (75 MHz, $CDCl_3$) δ ppm = 166.5, 163.0, 141.6, 130.1, 129.5, 119.2, 113.3, 77.2, 28.4, 19.3. HRMS (ESI$^-$): *m/z* calcd for $C_{11}H_{12}NO_5$ $[M-H]^-$ 238.0721 found 238.0710.

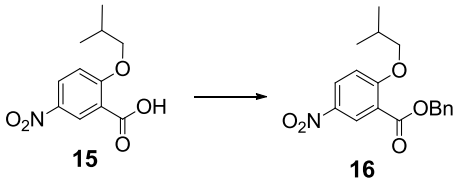

Benzyl 2-isobutoxy-5-nitrobenzoate 16. A suspension of 2-isobutoxy-5-nitrobenzoic acid **15** (9 g, 0.037 mmol) in 10 mL of thionyl chloride and 0.2 mL of DMF was heated at reflux for 2 h and then evaporated to afford 2-isobutoxy-5-nitrobenzoyl chloride as a yellow solid. A solution of benzyl alcohol (4.57 mL, 0.045 mmol) and triethylamine (10.2 mL, 0.075 mmol) dissolved in 100 mL of dichloromethane was added to the crude acid chloride and stirred under nitrogen for 12 h. Dichloromethane (100 mL) then water (200 mL) were added to the reaction mixture, and the organic phase was extracted, washed with saturated aqueous $NaHCO_3$, dried over Na_2SO_4 and filtered. The solvent was removed under reduced pressure and the residue was purified by precipitation in diethyl ether to give benzyl 2-isobutoxy-5-nitrobenzoate **16** as white solid (97 %, 12 g). mp 84-85°C; ^{1}H NMR (300 MHz, $CDCl_3$) δ ppm = 8.71 (d, *J* = 2.95, 1H); 8.32 (dd, *J* = 9.14, 1H); 7.46-7.34, (m, 5H), 7.00 (d, *J* = 9.21, 1H); 5.37, (s, 2H), 3.87 (d, *J* = 6.48, 2H); 2.11 (m, 1H); 1.00 (d, *J* = 6.69, 6H). ^{13}C NMR (75 MHz, $CDCl_3$) δ ppm = 164.6, 163.6, 140.7, 135.8, 129.1, 128.9, 128.9, 128.8, 128.2, 120.9, 112.9, 76.3, 67.6, 28.5, 19.3. MS (ESI$^+$): *m/z* calcd for $C_{36}H_{39}N_2O_{10}$ $[2M+H]^+$ 659.2 found 659.2.

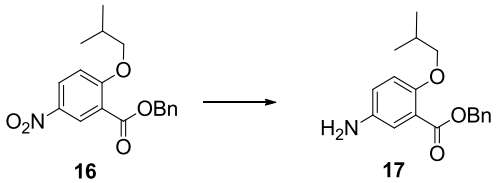

Benzyl 2-isobutoxy-5-aminobenzoate 17. Benzyl 2-isobutoxy-5-nitrobenzoate **16** (11.8 g, 0.036 mmol) was dissolved in 100 mL of dichloromethane. Then, $NaBH_4$ (6.22 g, 0.165 mmol) was added slowly at 0 °C followed by $CuSO_4.5H_2O$ (20.5 g, 0.082 mmol) in methanol (20 mL). The reaction mixture was stirred 45 min. at 0 °C then concentrated by evaporation. The resulting residue was purified by silica gel column chromatography eluting with EtOAc:CH_2Cl_2 (20:80 vol/vol) to give **17** as solid (90 %, 9.7 g). ^{1}H NMR (300 MHz, $CDCl_3$) δ ppm = 7.45-7.31, (m, 5H), 7.16 (s, 1H); 6.78 (d, *J* = 1.59, 2H); 5.33 (s, 2H); 3.67, (d, *J* = 6.49, 2H), 3.46 (bs, 2H); 2.02 (m, 1H); 0.95 (d, *J* = 6.98, 6H). ^{13}C NMR (75 MHz, $CDCl_3$) δ ppm = 166.5, 139.8, 136.3, 128.5, 128.5, 128.4, 128.2, 120.9, 120.5, 117.9, 115.5, 76.4, 66.6, 28.5, 19.3. HRMS (ESI$^+$): *m/z* calcd for $C_{18}H_{21}NO_3Na$ $[M+Na]^+$ 322.1419 found 322.1414.

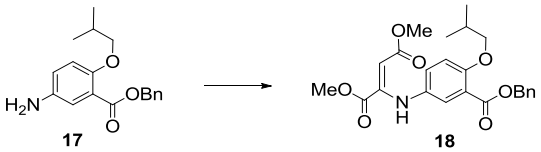

Fumarate derivative 18. To a solution of amine derivative **17** (9.7 g, 0.032 mmol) in 100 mL of methanol was added dimethylacetylene dicarboxylate (5.1 g, 0.035 mmol). The resulting mixture was heated at reflux for 12 h, then the solution was cooled and the solvent was evaporated down to ca. 50 mL. The flask was placed at -18 °C for 4 h for crystallization. The resulting yellow prisms were collected by filtration, washed several times with cold methanol (ca. 50 mL at -18°C) and dried under reduced pressure to give the fumarate derivative **18** as light yellow solid (91 %, 13 g). mp 71-72 °C; ^{1}H NMR (300 MHz, $CDCl_3$) δ ppm = 9.57 (s, 1H); 7.45-7.30, (m, 5H), 7.01 (dd, *J* = 8.90, 1H); 6.87 (s, 1H); 6.84 (s, 1H); 5.34 (s, 1H); 5.31 (s, 2H); 3.74, (m, 4H), 3.61 (s, 3H); 2.06 (m, 1H); 0.97 (d, *J* = 6.74, 6H). ^{13}C NMR (75 MHz, $CDCl_3$) δ ppm = 170.3, 165.7, 164.8, 156.4, 148.7, 136.2, 132.9, 128.8, 128.7, 128.5, 126.9, 125.1, 120.7, 114.1, 93.0, 75.8, 67.1, 53.1, 51.5, 28.6, 19.5. HRMS (ESI$^+$): *m/z* calcd for $C_{24}H_{27}NO_7Na$ $[M+Na]^+$ 464.1685 found 464.1680.

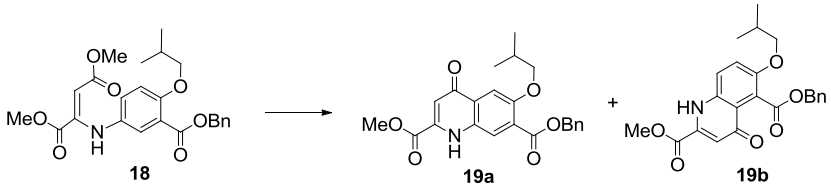

Quinolone 19a. The fumarate derivative **18** (13 g, 0.029 mmol) was added directly to refluxing diphenylether (325 mL and let at this temperature for 20 min). The reaction mixture was allowed to cool to room temperature and then poured onto petroleum ether (3 L). The precipitated was triturated, filtered and washed with one more litre of petroleum ether. Isomer **19a** was separated from **19b** using successive precipitations from hot MeOH to yield a yellow solid (51 %, 6.2 g). mp 207-208 °C; ^{1}H NMR (300 MHz, $CDCl_3$) δ ppm = 9.08 (s, 1H); 7.90 (s, 1H); 7.75 (s, 1H); 7.48-7.33, (m, 5H), 6.94 (d, *J* = 1.68, 1H); 5.39 (s, 2H); 4.03, (s, 3H), 3.89 (d, *J* = 6.42, 2H); 2.10 (m, 1H); 0.98 (d, *J* = 6.72, 6H). ^{13}C NMR (75 MHz, $CDCl_3$) δ ppm = 178.8, 165.8, 163.6, 155.3, 136.6, 135.8, 132.8, 129.7, 128.9, 128.8, 128.7, 127.4, 122.7, 110.7, 107.2, 77.5, 75.9, 67.8, 54.2, 28.5, 19.5. HRMS (ESI$^+$): *m/z* calcd for $C_{23}H_{24}NO_6$ $[M+H]^+$ 410.1604 found 410.1598.

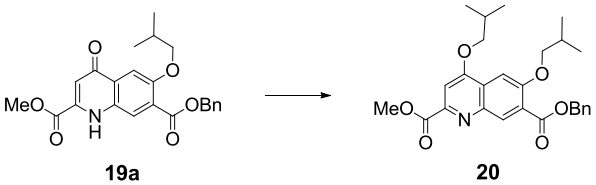

Quinoline 20. Quinolone **19a** (6.2 g, 0.015 mmol), 2-methyl propanol (2 mL, 0.023 mmol) and triphenylphosphine (5.96 g, 0.023 mmol) were suspended in 120 mL of anhydrous THF (**19a** was not soluble in THF before the addition of diisopropyl azodicarboxylate). Diisopropyl azodicarboxylate (4.6 g, 0.023 mmol) was added to the reaction mixture at 0 °C and let to stir for 30 min. at this temperature, then at room temperature for 24 h. Solvents were removed by evaporation. The residue was recrystallized from methanol

and the product was dried under reduced pressure to give compound **20** as a white powder (91 %, 6.4 g). mp 98-99°C; ^{1}H NMR (300 MHz, $CDCl_3$) δ ppm = 8.62 (s, 1H); 7.55 (s, 1H); 7.47-7.31, (m, 6H), 5.39 (s, 2H); 4.06-4.04, (m, 5H), 3.91 (d, *J* = 6.44, 2H); 2.38-2.11 (m, 2H); 1.13 (d, *J* = 6.65, 6H), 1.05 (d, *J* = 6.66, 6H). ^{13}C NMR (75 MHz, $CDCl_3$) δ ppm = 166.4, 165.5, 161.4, 156.8, 147.7, 143.0, 135.9, 134.5, 128.8, 128.8, 128.6, 126.7, 125.6, 102.2, 101.3, 77.5, 75.4, 67.4, 53.5, 28.5, 28.3, 19.6, 19.5. HRMS (ESI$^+$): *m/z* calcd for $C_{27}H_{32}NO_6$ $[M+H]^+$ 466.2230 found 466.2224.

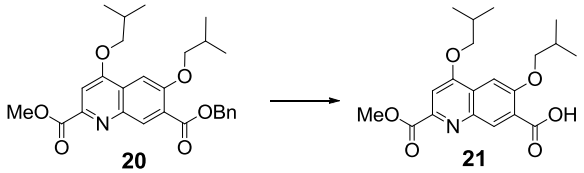

Quinoline acid 21. To a solution of **20** (3 g, 0.006 mmol) in 50 mL of EtOAc was added 10% Pd/C (150 mg). The flask was evacuated then filled with hydrogen gas and the reaction mixture was vigorously stirred for 12 h at room temperature. The Pd catalyst was removed by filtration, washed with dichloromethane and the filtrate was evaporated under reduced pressure to give the corresponding acid **21** as a white solid (99 %, 2.4 g). mp 160-161°C; ^{1}H NMR (300 MHz, $CDCl_3$) δ ppm = 10.79 (bs, 1H); 9.13 (s, 1H); 7.63 (s, 1H), 7.61 (s, 1H); 4.16 (d, *J* = 6.43, 2H), 4.09-4.07, (m, 5H), 2.33 (m, 2H); 1.16 (d, *J* = 2.66, 6H), 1.14 (d, *J* = 2.71, 6H). ^{13}C NMR (75 MHz, $CDCl_3$) δ ppm = 166.3, 165.2, 161.6, 155.5, 148.9, 143.6, 137.7, 126.2, 123.3, 102.7, 102.3, 77.5, 76.7, 75.7, 53.7, 28.4, 19.6, 19.5. HRMS (ESI$^+$): *m/z* calcd for $C_{20}H_{26}NO_6$ $[M+H]^+$ 376.1760 found 376.1755.

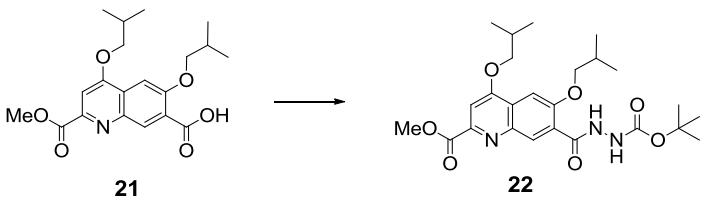

Quinoline hydrazide 22. A solution of acid **21** (4 g, 0.011 mmol), HBTU (*O*-benzotriazole-*N,N,N',N'*-tetramethyl-uronium-hexafluoro-phosphate) (6 g, 0.016 mmol) and DIEA (2.6 mL, 0.016 mmol) dissolved in 50 mL of anhydrous DMF was stirred for 15 min. then *tert*-butyl carbazate (1.7 g, 0.013 mmol) was added. The mixture was stirred at room temperature 12 h under nitrogen, then ice and EtOAc were added to the solution. The organic layer was washed with brine, dried over $MgSO_4$ and solvent was removed under reduced pressure. After purification by flash column chromatography eluting with EtOAc/cyclohexane (50:50 vol/vol) **22** was obtained as a white solid (90 %, 4.7 g). mp 182-183°C; ^{1}H NMR (300 MHz, $CDCl_3$) δ ppm = 9.73 (bs, 1H); 9.13 (s, 1H); 7.58 (s, 1H), 7.56 (s, 1H); 7.08 (bs, 1H); 4.07, (m, 7H), 2.34 (m, 2H); 1.50 (s, 9H); 1.16 (d, *J* = 3.76, 6H), 1.14 (d, *J* = 3.76, 6H). ^{13}C NMR (75 MHz, $CDCl_3$) δ ppm = 166.5, 162.9, 161.5, 155.5, 155.1, 148.4, 143.7, 136.4, 125.5, 124.9, 102.3, 101.7, 82.0, 77.5, 76.3, 75.5, 53.6, 28.5, 28.4, 19.8, 19.6. HRMS (ESI$^+$): *m/z* calcd for $C_{25}H_{36}N_3O_7$ $[M+H]^+$ 490.2553 found 490.2548.

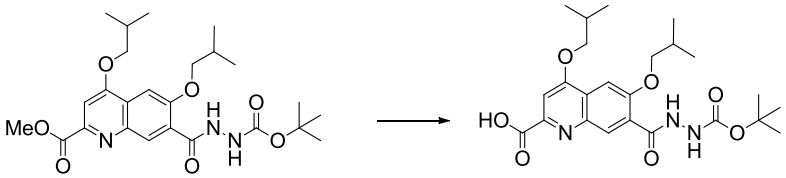

22 23

Acid derivative 23. NaOH (0.17 g, 0.004 mmol, dissolved in 3 mL of water) was added to a solution of ester **22** (1 g, 0.002 mmol) in 27 mL of THF/MeOH (8:1). The resulting slurry was stirred for 2 h at room temperature and the reaction was monitored by TLC. The reaction was then quenched by a 5% aqueous citric acid solution, and solvents were removed by evaporation. The residue was dissolved in dichloromethane and washed with distilled water and saturated NaCl. Organic layer was dried over $MgSO_4$ and filtered. Solvent was evaporated to dryness and the residue was dried under vacuum to give monomer acid **23** as a white solid (95 %, 0.92 g). mp 197-198 °C; ^{1}H NMR (300 MHz, $CDCl_3$) δ ppm = 10.35 (bs, 1H); 9.92 (bs, 1H); 9.16 (s, 1H), 8.10 (bs, 1H); 7.66 (s, 1H); 7.55 (s, 1H); 4.11 (d, *J* = 6.74, 2H), 4.07 (d, *J* = 6.51, 2H), 2.34 (m, 2H); 1.49 (s, 9H); 1.14 (m, 12H). ^{13}C NMR (75 MHz, $CDCl_3$) δ ppm = 163.7, 162.3, 155.9, 155.2, 148.0, 139.8, 133.2, 126.1, 125.4, 102.3, 100.8, 82.1, 77.5, 76.6, 76.4, 28.5, 28.3, 28.3, 19.7, 19.5. HRMS (ESI$^+$): *m/z* calcd for $C_{24}H_{34}N_3O_7$ $[M+H]^+$ 476.2397 found 476.2391.

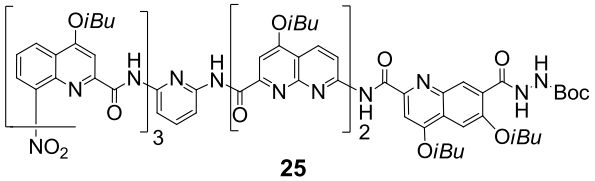

25

O_2N-Q_3PN_2H-Boc 25. Acid derivative **23** (79 mg, 0.166 mmol), hexamer amine **24**[6] (150 mg, 0.111 mmol) and PyBOP (173 mg, 0.332 mmol) were dissolved in 5 mL of dry chloroform. Then, DIEA (0.06 mL, 0.332 mmol) was added to the reaction mixture which was stirred at room temperature for 24 h. The solvents were removed under reduced pressure and the residue was purified by precipitation from MeOH to give heptamer **25** as a yellow solid (95 %, 190 mg). ^{1}H NMR (300 MHz, $CDCl_3$) δ ppm = 11.99 (s, 1H); 11.73 (s, 1H); 11.37, (s, 1H), 11.10 (s, 1H); 10.24, (s, 1H), 9.88 (s, 1H); 9.29 (bs, 1H); 8.93 (d, *J* = 9.11, 1H); 8.76 (m, 4H); 8.47 (d, *J* = 7.96, 2H); 8.23 (s, 1H); 8.13 (d, *J* = 7.34, 1H); 7.81-7.70 (m, 7H); 7.38-7.27 (m, 4H); 7.19 (s, 1H); 6.95 (m, 2H); 6.88 (s, 2H); 6.34 (t, *J* = 7.97, 1H); 4.24-3.83 (m, 13H); 3.34 (bs, 2H); 2.47-2.16 (m, 6H); 1.87 (m, 1H); 1.37 (s, 9H); 1.25-1.18 (m, 38H); 1.10 (d, *J* = 6.38, 6H); 0.78 (m, 6H). ^{13}C NMR (75 MHz, $CDCl_3$) δ ppm = 164.5, 164.1, 163.8, 163.5, 163.2, 163.0, 162.4, 161.7, 161.5, 161.4, 154.9, 154.8, 154.6, 154.5, 153.8, 153.6, 152.8, 151.3, 149.8, 149.0, 147.6, 145.2, 141.9, 139.9, 139.2, 139.1, 138.8, 135.1, 134.7, 134.2, 128.1, 126.9, 126.1, 125.8, 124.8, 124.2, 123.9, 123.6, 122.7, 121.4, 118.2, 117.1, 115.7, 115.5, 115.1, 114.9, 114.4, 109.9, 108.6, 101.7, 100.9, 99.6, 99.3, 98.3, 98.2, 97.5, 81.1, 77.5, 76.3, 75.9, 75.7, 75.4, 75.1, 31.4, 29.9, 28.3, 28.0, 19.6, 19.5. HRMS (ESI$^+$): *m/z* calcd for $C_{97}H_{104}N_{18}O_{18}Na$ $[M+Na]^+$ 1832.770 found 1832.769.

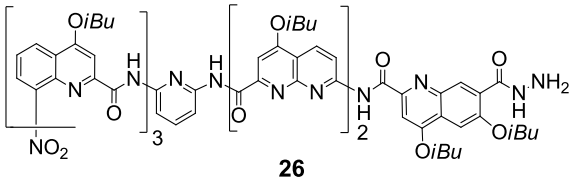

26

O_2N-Q_3PN_2H-NH_2 26. Trifluoroacetic acid (0.6 mL) was added dropwise to a solution of **25** (150 mg, 0.083 mmol) in 2 mL of $CHCl_3$ under nitrogen at 0 °C. Then, the resulting mixture was stirred at room temperature for 2 h. The solvents were removed under reduced pressure to give a solid which was dissolved in dichloromethane and washed twice with a saturated aqueous solution of $NaHCO_3$, distilled water and then with brine. The organic layer was dried over $MgSO_4$ and the solvent was evaporated. The product was precipitated from MeOH to give the amine derivative **26** as a yellow solid (97 %, 136 mg). ^{1}H NMR (300 MHz, $CDCl_3$) δ ppm = 11.98 (s, 1H); 11.79 (s, 1H); 11.44, (s, 1H), 11.13 (s, 1H); 10.25, (s, 1H), 9.90 (s, 1H); 8.92 (d, *J* = 9.19, 1H); 8.77 (m, 3H); 8.70 (d, *J* = 7.80, 1H); 8.48 (m, 3H); 8.24 (s, 1H); 8.13 (d, *J* = 8.08, 1H); 7.80-7.60 (m, 7H); 7.39-7.30 (m, 4H); 7.19 (s, 1H); 6.91 (m, 3H); 6.34 (t, *J* = 7.99, 1H); 4.25-3.83 (m, 16H); 3.29 (m, 2H); 3.16 (m, 4H); 2.45-2.12 (m, 7H); 1.81 (m, 5H); 1.25-1.19 (m, 34H); 1.07 (d, *J* = 6.34, 6H); 0.76 (m, 6H). ^{13}C NMR (75 MHz, $CDCl_3$) δ ppm = 164.5, 164.5, 164.0, 163.7, 163.5, 163.2, 163.2, 163.0, 162.4, 161.6, 161.3, 154.9, 154.8, 154.6, 154.5, 154.4, 153.8, 153.5, 152.7, 151.3, 149.8, 149.0, 148.8, 147.6, 145.1, 141.9, 139.9, 139.2, 139.0, 138.7, 135.0, 134.6, 134.1, 128.2, 126.9, 126.0, 125.9, 124.7, 124.4, 124.2, 123.6, 122.7, 121.3, 118.1, 117.1, 115.6, 115.0, 114.9, 114.4, 109.9, 108.5, 101.4, 101.0, 99.6, 99.1, 98.3, 98.2, 97.5, 77.5, 76.0, 75.7, 75.4, 75.4, 75.1, 29.9, 28.4, 28.4, 28.3, 27.9, 19.6, 19.5. MS (ESI$^+$): *m/z* calcd for $C_{92}H_{97}N_{18}O_{16}$ $[M+H]^+$ 1709.73 found 1709.73.

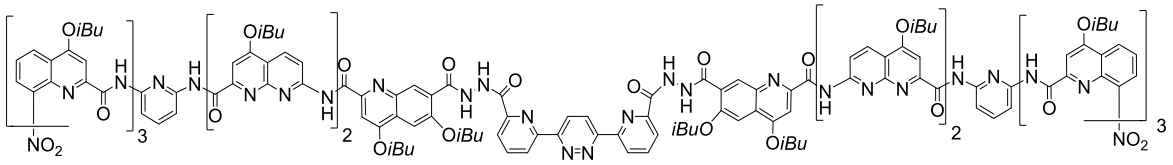

1

Capsule 1. Diacid **27**[6] (19 mg, 0.058 mmol) and heptamer amine **26** (200 mg, 0.117 mmol) were dissolved in dry $CHCl_3$ (5 mL). Then, DIEA (0.05 mL, 0.292 mmol) and PyBOP (152 mg, 0.292 mmol) were added at room temperature and the reaction mixture was heated to 40 °C. After two days, the solvents were removed under reduced pressure and the residue was purified by precipitation from a minimum amount of MeOH to yield capsule **1** as a yellow solid (83 %, 180 mg). ^{1}H NMR (300 MHz, $CDCl_3$) δ ppm = 11.69 (s, 1H); 11.45 (s, 1H); 11.06, (s, 1H), 10.32 (d, *J* = 8.72, 1H); 9.97 (s, 1H), 9.61 (s, 1H); 9.55 (s, 1H); 9.26 (d, *J* = 7.56, 1H); 8.91 (d, *J* = 7.85, 1H); 8.62 (s, 1H); 8.54 (m, 4H); 8.19 (d, *J* = 8.43, 1H); 8.13-8.08 (m, 2H); 8.00 (d, *J* = 7.27, 1H); 7.95 (d, *J* = 6.98, 1H); 7.78 (s, 1H); 7.39 (s, 2H); 7.30 (s, 2H); 7.19-7.05 (m, 4H); 6.95 (s, 1H); 6.77 (m, 1H); 6.68 (m, 2H); 6.52 (m, 3H); 5.72 (t, *J* = 7.78, 1H); 4.25-3.94 (m, 7H); 3.83-3.52 (m, 7H); 2.91 (bs, 1H); 2.64 (bs, 1H); 2.53-2.33 (m, 4H); 2.22-2.03 (m, 4H); 1.37-1.17 (m, 30H); 1.09 (d, *J* = 6.48, 6H); 1.03 (d, *J* = 6.48, 6H); 0.43 (bs, 3H); 0.08 (bs, 3H). HRMS (ESI$^+$): *m/z* calcd for $C_{200}H_{198}N_{40}O_{34}Na_2$ $[M+2Na]^{2+}$ 1875.7428 found 1875.7434.

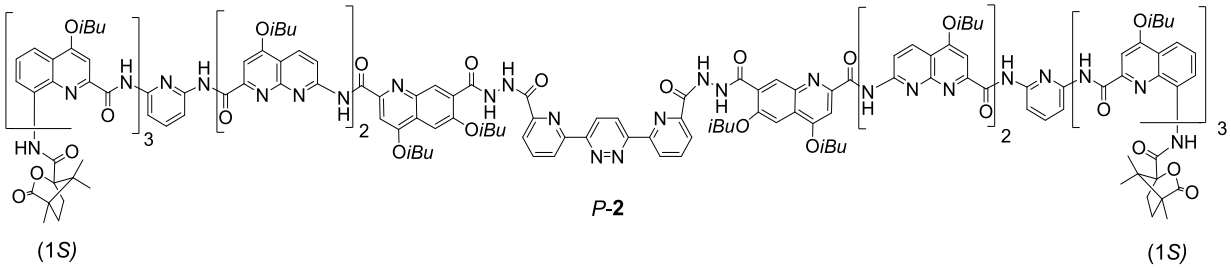

P-**2**

Capsule 2. To a solution of capsule **1** (45 mg, 0.012 mmol) in EtOAc/MEOH (4:1, 5 mL), 10% Pd/C (50 mg) and NH_4VO_3 (2 mg) was slowly added an aqueous solution of ammonium formate (200 mg in 0.4 ml of water). The mixture was stirred at 90 °C 24 h. Then, the solution was cooled down and filtered through celite. The evaporation of solvents gave the diamino derivative **28** as a pale yellow solid. Diamine **28** (40 mg, 0.011 mmol) was dissolved in dry $CHCl_3$ (3 mL) containing DIEA (0.03 mL, 0.165 mmol), then the commercially available 1*S*-(-)-camphanic chloride (24 mg, 0.109 mmol) was added as a solid to the solution. The reaction mixture was stirred at room temperature overnight and the solvents were removed under reduced pressure. The residue was purified by column chromatography eluting with EtOAc:CH_2Cl_2 (10:90 vol/vol) to give **2** as a pale yellow solid (72 %, 35 mg). ^{1}H NMR (300 MHz, $CDCl_3$) δ ppm = 11.75 (s, 1H); 11.71 (s, 1H); 10.94, (s, 1H), 10.25 (d, *J* = 9.53, 1H), 10.03 (s, 1H); 9.56 (s, 1H); 9.29 (s, 2H); 9.24 (d, *J* = 9.53, 1H); 8.92 (d, *J* = 7.87, 1H); 8.58-8.46 (m, 4H); 8.11 (t, *J* = 7.74, 1H); 8.02-7.98 (m, 2H); 7.91 (d, *J* = 7.46, 1H); 7.66 (s, 1H); 7.62 (d, *J* = 8.30, 1H); 7.49 (d, *J* = 7.47, 1H); 7.37 (s, 1H); 7.31 (s, 1H); 7.20 (d, *J* = 8.30, 1H); 7.14 (d, *J* = 7.19, 1H); 7.11 (s, 1H); 6.95-6.77 (m, 4H); 6.63 (s, 1H); 6.40-6.26 (m, 3H); 5.81 (m, 1H); 4.20-3.94 (m, 6H); 3.78-3.59 (m, 4H); 3.45 (t, *J* = 8.85, 1H); 3.01-2.88 (m, 2H); 2.42 (m, 3H); 2.17 (m, 2H); 2.03 (m, 1H); 1.33-1.18 (m, 24H); 1.10 (dd, *J* = 9.13, 6H); 1.01 (dd, *J* = 6.64, 6H); 0.49-0.44 (m, 6H); 0.06 (s, 2H); 0.03 (d, *J* = 6.64, 2H). HRMS (ESI$^+$): *m/z* calcd for $C_{220}H_{226}N_{40}O_{36}Na_2$ $[M+2Na]^{2+}$ 2025.8473 found 2025.8478.

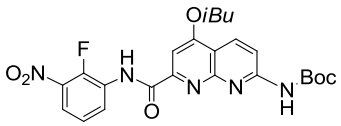

31

O_2N-FN-Boc (31). Acid **29**[7] (0.254 g, 0.704 mmol) and amine **30**[8] (0.100 g, 0.640 mmol) were dissolved in dry chloroform (5 mL). Then, DIEA (0.33 mL, 1.92 mmol) and PyBOP (0.666 g, 1.28 mmol) were added at room temperature and the reaction mixture was heated at 45°C for 24 hours. Then, the solvents were removed under reduced pressure and the residue was purified by flash chromatography (SiO_2) eluting with EtOAc:dichloromethane (10:90 vol/vol) and by precipitation from minimum amount of MeOH to obtain **31** as a white solid (72 %, 0.230 g). ^{1}H NMR (300 MHz, $CDCl_3$) δ ppm = 10.61 (s, 1H); 8.83 (t, *J* = 6.7, 1H); 8.58 (d, *J* = 9.1, 1H); 8.36 (d, *J* = 9.1, 1H); 7.82 (t, *J* = 6.9, 1H); 7.71 (s, 2H); 7.35 (t, *J* = 8.3, 1H); 4.11 (d, *J* = 6.5, 2H); 2.31 (m, 1H); 1.57 (s, 9H); 1.14 (d, *J* = 6.7, 6H). ^{13}C NMR (100 MHz, $CDCl_3$) δ ppm = 164.3; 162.8; 155.6; 154.7; 152.7; 152.3; 148.0; 145.3; 137.7; 134.2; 128.7; 128.6; 126.9; 124.4; 124.3; 120.3;

114.4; 114.3; 98.7; 82.2; 75.9; 28.3; 28.2; 19.3. HRMS (ESI$^+$): *m/z* calcd for $C_{24}H_{26}FN_5O_6$ $[M+H]^+$: 500.1946 found 500.1950.

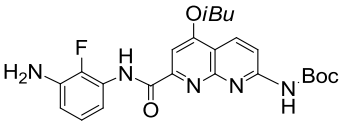

32

H_2N-FN-Boc (32). To a solution of dimer **31** (0.200 g, 0.4 mmol) in EtOAc (30 mL) was added Pd/C (20 mg) under nitrogen. Then the reaction mixture was vigorously stirred under hydrogen atmosphere at room temperature for 16 h. The mixture was filtered through a pad of Celite which was washed with dichloromethane and the filtrate was concentrated under vacuum. The residue was purified by flash chromatography (SiO_2) eluting with EtOAc:dichloromethane (20:80 vol/vol) to obtain **32** as a white solid (90 %, 0.170 g). ^{1}H NMR (300 MHz, $CDCl_3$) δ ppm = 10.31 (s, 1H); 8.57 (d, *J* = 9.1, 1H); 8.33 (d, *J* = 9.1, 1H); 7.81 (t, *J* = 7.4, 1H); 7.75 (s, 1H); 7.69 (s, 1H); 6.98 (t, *J* = 8.1, 1H); 6.60 (t, *J* = 8.2, 1H); 4.10 (d, *J* = 6.5, 2H); 3.78 (s, 2H); 2.29 (m, 1H); 1.56 (s, 9H); 1.13 (d, *J* = 6.7, 6H). ^{13}C NMR (75 MHz, $CDCl_3$) δ ppm = 164.2; 162.4; 155.4; 154.9; 154.0; 152.4; 144.6; 141.4; 134.8; 134.6; 134.3; 126.5; 126.4; 124.4; 114.2; 113.9; 112.9; 111.7; 99.0; 82.1; 75.9; 28.4; 28.3; 19.4. HRMS (ESI$^+$): *m/z* calcd for $C_{24}H_{28}FN_5O_4$ $[M+H]^+$: 470.2204 found 470.2206.

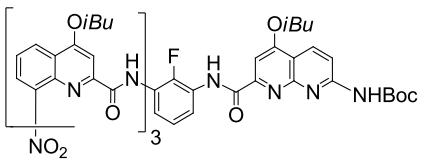

34

O_2N-Q_3FN-Boc (34). Acid **33a**[9] (0.930 g, 1.2 mmol) was suspended in anhydrous $CHCl_3$ (10 mL). Oxalyl chloride (0.52 mL, 6 mmol) was added and the reaction was stirred at room temperature for 2 h. The solvents were removed under vacuum and the residue was dried under vacuum for at least 1 h to yield acid chloride **33b** as a yellow solid. To a solution of dimer amine **32** (0.563 g, 1.2 mmol) and distilled DIEA (1 mL, 6 mmol) in dry $CHCl_3$ (5 mL) was added dropwise at 0 °C a solution of the freshly prepared diacid chloride **33b** in dry $CHCl_3$ (5 mL). The reaction was allowed to proceed at room temperature 12 h. The solvents were removed under reduced pressure and the residue was purified by flash chromatography (SiO_2) eluting with EtOAc:dichloromethane (5:95 vol/vol) and by precipitation from minimum amount of MeOH to obtain **34** as a yellow solid (75 %, 1.1 g). ^{1}H NMR (300 MHz, $CDCl_3$) δ ppm = 11.98 (s, 1H); 11.67 (s, 1H); 9.85 (d, *J* = 3.1, 1H); 9.55 (s, 1H); 9.09 (d, *J* = 6.8, 1H); 8.70 (s, 1H); 8.67 (s, 1H); 8.52 (d, *J* = 9.6, 1H); 8.44 (d, *J* = 9.0, 1H); 8.04 (d, *J* = 7.4, 1H); 7.97 (m, 2H); 7.91 (s, 1H); 7.75 (m, 4H); 7.54 (d, *J* = 6.3, 1H); 7.38 (t, *J* = 8.0, 1H); 7.31 (s, 1H); 7.14 (t, *J* = 8.3, 1H); 7.06 (s, 1H); 6.53 (t, *J* = 8.0, 1H); 4.18 (d, *J* = 6.5, 2H); 4.13 (d, *J* = 6.7, 2H); 4.04 (d, *J* = 6.5, 2H); 3.97 (d, *J* = 6.5, 2H); 2.31 (m, 4H); 1.60 (s, 9H); 1.24 (d, *J* = 6.7, 6H); 1.19 (d, *J* = 6.7, 12H); 1.09 (d, *J* = 6.7, 6H). ^{13}C NMR (100 MHz, $CDCl_3$) δ ppm = 164.0; 163.5; 163.4; 163.2; 163.1; 162.6; 161.7; 160.9; 154.9; 154.8; 154.0; 153.9; 152.3; 150.8; 148.1; 145.3; 145.2; 142.8; 139.4; 139.3; 139.2; 134.9; 134.3; 134.2; 128.3; 128.2; 126.9; 126.3; 126.2; 126.0; 125.9;

124.5; 124.0; 123.7; 122.4; 119.9; 118.7; 118.4; 116.6; 116.0; 115.5; 114.2; 113.6; 99.9; 99.7; 98.9; 97.9; 82.2; 75.9; 75.7; 75.5; 75.4; 28.4; 28.3; 28.2; 19.5; 19.4; 19.3; 19.2. HRMS (ESI$^+$): *m/z* calcd for $C_{66}H_{68}FN_{11}O_{12}$ [M+Na]$^+$: 1248.4931 found 1248.4923.

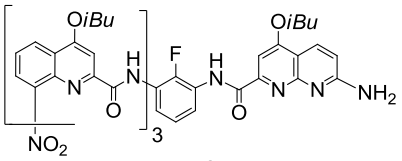

35

O_2N-Q_3FN-NH_2 (35). Trifluoroacetic acid (1.2 mL) was added dropwise to a solution of **34** (0.4 g, 0.326 mmol) in 6 mL of chloroform under nitrogen at room temperature. Then, the resulting mixture was stirred at room temperature for 5 h. The solvents were removed under reduced pressure to give a solid which was dissolved in dichloromethane and washed with a saturated solution of $NaHCO_3$, distilled water and then with brine. The organic layer was dried over Na_2SO_4 then filtered and concentrated under reduced pressure to give the amine derivative **35** as yellow solid (98 %, 0.358 g). ^{1}H NMR (300 MHz, $CDCl_3$) δ ppm = 11.99 (s, 1H); 11.70 (s, 1H); 9.87 (d, *J* = 3.0, 1H); 9.74 (s, 1H); 9.13 (d, *J* = 6.8, 1H); 8.65 (d, *J* = 6.8, 1H); 8.53 (d, *J* = 7.0, 1H); 8.33 (d, *J* = 8.9, 1H); 8.09 (t, *J* = 7.5, 1H); 8.06 (d, *J* = 7.2, 1H); 7.95 (t, *J* = 7.1, 1H); 7.76 (d, *J* = 8.0, 1H); 7.69 (s, 1H); 7.64 (s, 1H); 7.56 (d, *J* = 6.2, 1H); 7.40 (t, *J* = 8.2, 2H); 7.31 (s, 1H); 7.15 (t, *J* = 8.1, 1H); 7.09 (s, 1H); 6.71 (d, *J* = 8.9, 1H); 6.59 (t, *J* = 8.1, 1H); 5.46 (s, 2H); 4.14 (d, *J* = 6.5, 2H); 4.06 (d, *J* = 6.4, 2H); 3.98 (d, *J* = 6.5, 4H); 2.36 (m, 3H); 2.17 (m, 1H); 1.25 (d, *J* = 6.7, 6H); 1.19 (m, 12H); 1.03 (d, *J* = 6.8, 6H). ^{13}C NMR (100 MHz, $CDCl_3$) δ ppm = 164.0; 163.7; 163.5; 163.2; 163.1; 161.4; 160.9; 160.7; 156.1; 154.1; 152.3; 150.7; 148.2; 145.3; 144.8; 142.4; 139.4; 139.2; 139.1; 135.1; 134.1; 132.9; 128.4; 128.2; 126.9; 126.5; 126.4; 126.1; 125.9; 124.5; 124.4; 123.7; 122.4; 119.5; 118.1; 117.5; 116.5; 116.4; 115.0; 112.4; 110.7; 100.0; 99.4; 98.0; 97.4; 75.8; 75.5; 75.4; 75.2; 28.4; 28.3; 28.1; 19.5; 19.4; 19.3; 19.2. HRMS (ESI$^+$): *m/z* calcd for $C_{61}H_{60}FN_{11}O_{10}$ [M+H]$^+$: 1126.4588 found 1126.4580.

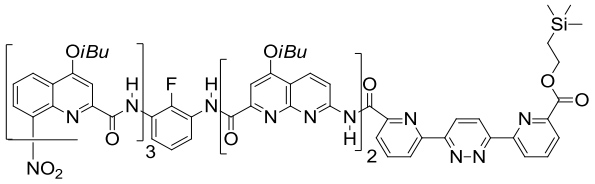

37

O_2N-Q_3FN_2PyrPyzPyr-TMSE (37). Acid **36**[10] (0.260 g, 0.390 mmol) and amine **35** (0.40 g, 0.355 mmol) were dissolved in dry chloroform (6 mL). Then, DIEA (0.25 mL, 1.42 mmol) and PyBOP (0.369 g, 0.710 mmol) were added at room temperature and the reaction mixture was heated at 45 °C for 72 h. Then, the solvent was removed under reduced pressure and the residue was purified by flash chromatography (SiO_2) eluting with EtOAc:dichloromethane (5:95 vol/vol) and by precipitation from minimum amount of MeOH to obtain **37** as a yellow solid (75 %, 0.473 g). ^{1}H NMR (300 MHz, $CDCl_3$) δ ppm = 11.71 (s, 1H); 11.44 (s, 1H); 11.30 (s, 1H); 10.91 (s, 1H); 10.35 (d, *J* = 2.4, 1H); 9.59 (d, *J* = 3.8, 1H); 9.05 (d, *J* = 9.0, 1H); 8.84 (m, 4H); 8.68 (d, *J* = 8.9, 1H); 8.39 (m, 7H); 8.06 (t, *J* = 7.8, 1H); 7.88 (m, 5H); 7.77 (t, *J* = 7.8, 1H); 7.40 (d, *J* = 6.2, 1H); 7.31 (d, *J* = 8.0, 1H); 7.23 (t, *J* = 7.1, 1H); 7.14 (t, *J* = 8.1, 1H); 7.08 (s, 1H); 6.98 (m, 2H); 6.78 (s,

1H); 6.29 (t, *J* = 8.0, 1H); 4.09 (m, 10H); 3.31 (m, 2H); 2.39 (m, 4H); 1.64 (m, 1H); 1.25 (m, 24H); 0.88 (t, *J* = 9.9, 2H); 0.74 (s, 3H); 0.48 (s, 3H); -0.24 (s, 9H). ^{13}C NMR (100 MHz, $CDCl_3$) δ ppm = 164.6; 164.3; 164.2; 163.9; 163.6; 163.3; 163.2; 162.9; 162.8; 161.7; 161.2; 158.5; 157.3; 156.1; 155.2; 155.0; 154.4; 153.9; 153.8; 153.7; 152.7; 152.6; 152.1; 150.6; 148.8; 147.9; 147.4; 144.8; 143.9; 141.4; 139.2; 138.9; 138.4; 138.3; 137.6; 134.6; 134.3; 128.3; 127.8; 126.7; 126.6; 126.1; 126.0; 125.9; 125.5; 125.4; 125.3; 124.9; 124.5; 124.3; 124.1; 123.9; 123.8; 122.8; 122.0; 119.0; 117.4; 116.5; 115.9; 115.4; 112.9; 114.4; 113.3; 101.1; 99.6; 98.5; 98.4; 97.4; 76.1; 76.0; 75.7; 75.6; 63.8; 28.5; 28.4; 28.3; 28.2; 28.0; 19.5; 19.4; 19.3; 17.4; -1.7. HRMS (ESI$^+$): *m/z* calcd for $C_{95}H_{93}FN_{18}O_{15}Si$ $[M+H]^+$: 1773.6894 found 1773.6901.

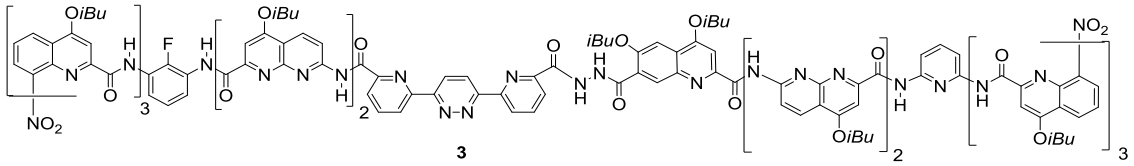

3

Capsule 3. Oligomer **37** (55 mg, 0.031 mmol) was reacted with tetrabutylammonium fluoride 1M (0.062 mL) in THF (2 mL) for 24 h. The solvent was removed under reduced pressure to give a solid which was dissolved in dichloromethane and washed with 5% aqueous citric acid solution, distilled water and brine. Heptamer acid **38** was used directly in subsequent reaction without further purification. Heptamer acid **38** (49 mg, 0.029 mmol) and heptamer amine **26** (50 mg, 0.029 mmol) were dissolved in dry $CHCl_3$ (4 mL). Then, DIEA (0.02 mL, 0.102 mmol) and PyBOP (53 mg, 0.102 mmol) were added at room temperature and the reaction mixture was heated at 40 °C. After 48 hours, the solvents were removed and the residue was purified by precipitation from minimum amount of MeOH which gave capsule **3** as a pale yellow solid (81 %, 80 mg). ^{1}H NMR (300 MHz, $CDCl_3$) δ ppm = 11.59 (s, 1H); 11.40 (s, 1H); 11.34, (s, 1H), 11.28 (s, 1H); 11.22 (s, 1H), 10.94 (s, 1H); 10.62 (d, *J* = 9.37, 1H); 10.24 (d, *J* = 2.96, 1H); 9.88 (s, 1H); 9.84 (s, 1H); 9.69 (s, 1H); 9.48 (d, *J* = 3.45, 1H); 9.33 (s, 1H); 9.28 (d, *J* = 9.53, 1H); 8.93 (s, 2H); 8.62-8.53 (m, 3H); 8.46 (d, *J* = 9.06, 2H); 8.33-7.88 (m, 15H); 7.78-7.75 (m, 2H); 7.52-7.48 (m, 2H); 7.41 (s, 1H); 7.35 (d, *J* = 8.24, 1H); 7.21-7.08 (m, 6H); 7.04 (s, 1H); 7.01 (s, 1H); 6.99-6.66 (m, 8H); 6.59 (s, 1H); 6.54 (s, 1H); 6.45 (t, *J* = 6.42, 1H); 6.37-6.34 (m, 3H); 5.85 (t, *J* = 8.24, 1H); 5.80 (t, *J* = 7.96, 1H); 4.33-3.57 (m, 17H); 3.49 (d, *J* = 5.56, 1H); 2.85 (t, *J* = 8.98, 1H); 2.72 (t, *J* = 9.05, 1H); 2.63-2.19 (m, 9H); 2.1 (m, 1H); 1.42-1.09 (m, 54H); 0.98 (d, *J* = 6.63, 6H); 0.49 (d, *J* = 6.60, 3H); 0.45 (d, *J* = 6.60, 3H); 0.31 (d, *J* = 6.60, 3H); 0.23 (d, *J* = 6.60, 3H). HRMS (ESI$^+$): *m/z* calcd for $C_{182}H_{175}FN_{36}O_{30}Na_2$ $[M+2Na]^{2+}$ 1705.1 found 1705.6.

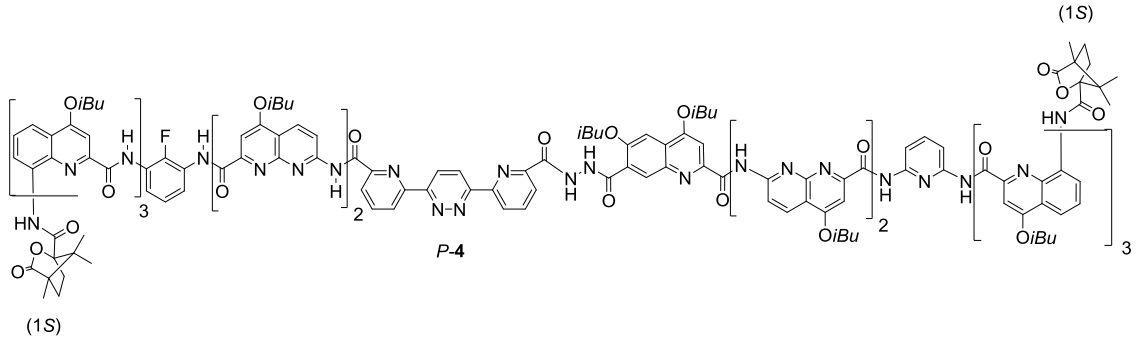

Capsule 4. To a solution of capsule **3** (45 mg, 0.013 mmol) in EtOAc/MEOH (4:1, 5 mL), 10% Pd/C (30 mg) and NH_4VO_3 (2 mg) was slowly added an aqueous solution of ammonium formate (250 mg in 0.3 ml of water). The mixture was let to stir at 90 °C 24 h. Then, the solution was cooled down and filtered through celite. The evaporation of solvents gave the diamino derivative **39** as a pale yellow solid. Diamine **39** (40 mg, 0.011 mmol) was dissolved in dry $CHCl_3$ (3 mL) containing DIEA (0.03 mL, 0.165 mmol), then the commercially available 1*S*-(-)-camphanic chloride (26 mg, 0.109 mmol) was added as a solid to the solution. The reaction mixture was stirred at room temperature overnight and the solvents were removed under reduced pressure. The residue was purified by column chromatography (SiO_2), eluting with EtOAc:dichloromethane (10:90 vol/vol) to give **4** as a pale yellow solid (76 %, 37 mg). ^{1}H NMR (300 MHz, $CDCl_3$) δ ppm = 11.71 (s, 1H); 11.60 (s, 1H); 11.47, (s, 1H), 11.37 (s, 1H); 10.94 (s, 1H), 10.60 (d, *J* = 9.27, 1H); 10.15 (m, 2H); 9.63 (d, *J* = 8.11, 2H); 9.44 (s, 2H); 9.38 (s, 1H); 9.30 (m, 2H); 8.91 (s, 2H); 8.60-8.45 (m, 5H); 8.33 (d, *J* = 8.96, 1H); 8.23 (d, *J* = 7.45, 1H); 8.18 (s, 1H); 8.15-7.90 (m, 10H); 7.78-7.71 (m, 4H); 7.65 (d, *J* = 7.98, 1H); 7.58 (d, *J* = 7.71, 2H); 7.51 (s, 1H); 7.43 (d, *J* = 8.51, 1H); 7.13-6.89 (m, 8H); 6.85 (d, *J* = 6.69, 2H); 6.74 (t, *J* = 7.90, 1H); 6.62 (t, *J* = 8.17, 1H); 6.57-6.51 (m, 3H); 6.47 (d, *J* = 7.90, 1H); 6.32-6.27 (m, 3H); 5.89 (m, 2H); 4.33-3.56 (m, 21H); 2.96-2.67 (m, 5H); 2.54-2.04 (m, 12H); 1.41-1.18 (m, 60H); 1.10 (t, *J* = 6.73, 9H); 0.98 (d, *J* = 6.73, 6H); 0.53-0.45 (m, 1H); 0.40 (d, *J* = 6.23, 6H); 0.33 (d, *J* = 6.81, 3H); 0.24 (d, *J* = 6.73, 3H); 0.01 (d, *J* = 3.32, 6H). MS (ESI$^+$): *m/z* calcd for $C_{202}H_{203}FN_{36}O_{32}Na_2$ $[M+2Na]^{2+}$ 1855.7 found 1855.7.

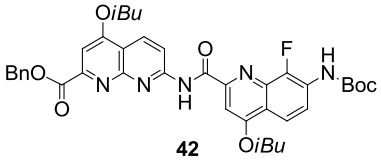

42

Bn-NQ^f-Boc 42. Acid **41**[8] (, 0.322 g, 0.850 mmol) and amine **40**[7] (0.300 g, 0.850 mmol) were dissolved in dry chloroform (10 mL). Then, DIEA (0.59 mL, 3.40 mmol) and PyBOP (0.885 g, 1.70 mmol) were added at room temperature and the reaction mixture was heated at 45 °C for 12 h. Then, the solvents were removed under reduced pressure and the residue was purified by flash chromatography (SiO_2) eluting with EtOAc:dichloromethane (10:90 vol/vol) to obtain **42** as a white solid (91 %, 0.551 g). ^{1}H NMR (300 MHz, $CDCl_3$) δ ppm = 11.21 (s, 1H); 8.82 (d, *J* = 9.0, 1H); 8.68 (d, *J* = 9.0, 1H); 8.50 (m, 1H); 8.00 (d, *J* = 7.9, 1H); 7.70 (s, 1H); 7.56 (m, 3H); 7.37 (m, 3H); 7.11 (d, *J* = 3.2, 1H); 5.53 (s, 2H); 4.01 (m, 4H); 2.31 (m, 2H); 1.60

(s, 9H); 1.14 (d, *J* = 6.7, 12H). ^{13}C NMR (75 MHz, $CDCl_3$) δ ppm = 165.8; 163.8; 163.5; 163.4; 163.3; 155.7; 154.4; 152.4; 152.3; 150.9; 137.9; 137.7; 135.9; 134.2; 128.9; 128.6; 128.4; 127.9; 127.8; 120.2; 119.0; 117.7; 117.6; 115.5; 115.0; 101.4; 97.9; 81.8; 75.7; 75.6; 67.9; 28.4; 28.3; 19.4; 19.3. HRMS (ESI$^+$): *m/z* calcd for $C_{39}H_{42}FN_5O_7$ $[M+H]^+$: 712.3147 found 712.3142.

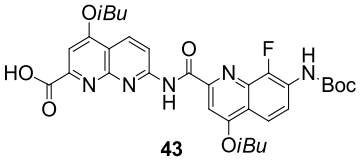

43

HO_2C-NQ^f-Boc 43. To a solution of dimer **42** (0.515 g, 0.72 mmol) in DMF (20 mL) was added Pd/C (52 mg) under nitrogen. Then the reaction mixture was vigorously stirred under hydrogen atmosphere at room temperature for 24 h. The mixture was filtered through a pad of Celite which was washed with dichloromethane and concentrated under vacuum to obtain **43** as a yellow solid (74 %, 0.379 g). ^{1}H NMR (300 MHz, $CDCl_3$) δ ppm = 11.14 (s, 1H); 8.91 (d, *J* = 9.1, 1H); 8.74 (d, *J* = 9.1, 1H); 8.52 (t, *J* = 8.5, 1H); 8.01 (d, *J* = 9.2, 1H); 7.70 (s, 2H); 7.09 (s, 1H); 4.12 (m, 4H); 2.32 (m, 2H); 1.60 (s, 9H); 1.15 (m, 12H). ^{13}C NMR (75 MHz, $CDCl_3$) δ ppm = 164.9; 164.3; 163.9; 163.4; 155.0; 154.3; 152.3; 150.7; 147.2; 143.9; 137.8; 134.8; 128.0; 127.9; 120.3; 119.0; 117.7; 116.1; 115.5; 99.8; 98.0; 81.9; 76.3; 75.6; 28.4; 28.3; 19.4; 19.3. HRMS (ESI$^+$): *m/z* calcd for $C_{32}H_{36}FN_5O_7$ $[M+H]^+$: 622.2678 found 622.2674.

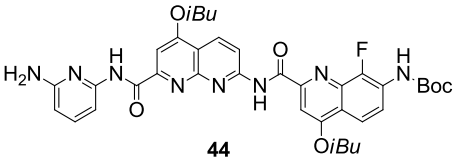

44

H_2N-PNQ^f-Boc 44. Acid **43** (0.366 g, 0.590 mmol) and 2,6-diaminopyridine (0.644 g, 5.9 mmol) were dissolved in dry chloroform (40 mL). Then, DIEA (0.41 mL, 2.36 mmol) and PyBOP (0.614 g, 1.18 mmol) were added at room temperature and the reaction mixture was heated at 45 °C for 48 h. The volatiles were removed under reduced pressure to give a solid which was dissolved in dichloromethane. The solution was washed with water and then with brine. The organic layer was dried over Na_2SO_4 then concentrated under reduce pressure. The residue was purified by precipitation from minimum amount of MeOH to obtain **44** as a yellow solid (74 %, 0.310 g). ^{1}H NMR (300 MHz, $CDCl_3$) δ ppm = 11.17 (s, 1H); 10.47 (s, 1H); 8.84 (d, *J* = 9.0, 1H); 8.73 (d, *J* = 9.0, 1H); 8.50 (t, *J* = 9.2, 1H); 8.02 (d, *J* = 9.3, 1H); 7.82 (s, 1H); 7.76 (d, *J* = 7.8, 1H); 7.72 (s, 1H); 7.53 (t, *J* = 7.9, 1H); 7.10 (d, *J* = 3.0, 1H); 6.31 (d, *J* = 7.9, 1H); 4.33 (s, 2H); 4.13 (m, 4H); 2.32 (m, 2H); 1.60 (s, 9H); 1.15 (m, 12H). ^{13}C NMR (100 MHz, $CDCl_3$) δ ppm = 164.1; 163.9; 163.4; 163.3; 162.4; 157.4; 155.0; 154.5; 154.3; 152.4; 150.9; 149.8; 146.9; 144.4; 139.9; 137.9; 137.7; 134.6; 127.9; 127.8; 120.2; 119.0; 117.7; 117.6; 115.3; 115.0; 104.7; 103.8; 99.3; 98.1; 81.8; 75.9; 75.6; 28.5; 28.3; 19.4; 19.3. HRMS (ESI$^+$): *m/z* calcd for $C_{37}H_{41}FN_8O_6$ $[M+H]^+$: 713.3212 found 713.3204.

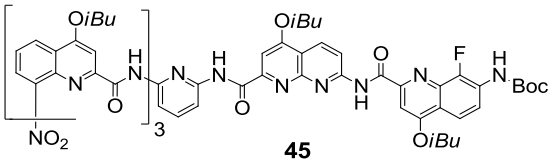

45

O_2N-Q_3PNQ^f-Boc 45. Acid **33a**[9] (0.272 g, 0.350 mmol) and amine **44** (0.250 g, 0.350 mmol) were dissolved in dry chloroform (15 mL). Then, DIEA (0.24 mL, 1.4 mmol) and PyBOP (0.364 g, 0.7 mmol) were added at room temperature and the reaction mixture was heated at 45 °C for 24 h. Then, the solvents were removed under reduced pressure and the residue was purified by flash chromatography (SiO_2) eluting with EtOAc:dichloromethane (5:95 vol/vol) and by precipitation from minimum amount of MeOH to obtain **45** as a yellow solid (66 %, 0.340 g). ^{1}H NMR (300 MHz, $CDCl_3$) δ ppm = 12.04 (s, 1H); 11.98 (s, 1H); 10.96 (s, 1H); 9.86 (s, 1H); 9.72 (s, 1H); 9.29 (d, *J* = 7.1, 1H); 8.87 (d, *J* = 9.0, 1H); 8.70 (d, *J* = 9.0, 1H); 8.64 (m, 1H); 8.54 (m, 2H); 8.16 (d, *J* = 7.7, 1H); 8.05 (m, 3H); 7.87 (d, *J* = 2.7, 1H); 7.84 (s, 1H); 7.76 (m, 3H); 7.67 (d, *J* = 7.8, 1H); 7.57 (d, *J* = 6.3, 1H); 7.37 (t, *J* = 8.1, 1H); 7.32 (s, 1H); 7.04 (s, 1H); 6.95 (d, *J* = 7.4, 1H); 6.48 (t, *J* = 8.0, 1H); 4.24 (s, 2H); 4.13 (m, 4H); 3.96 (m, 2H); 3.79 (m, 2H); 2.38 (m, 4H); 1.79 (m, 1H); 1.67 (s, 9H); 1.22 (m, 24H); 0.73 (s, 3H); 0.53 (s, 3H). ^{13}C NMR (75 MHz, $CDCl_3$) δ ppm = 164.0; 163.8; 163.7; 163.6; 163.3; 163.2; 163.1; 162.4; 161.5; 161.1; 154.8; 154.5; 154.1; 153.9; 152.9; 151.1; 150.8; 149.7; 148.7; 147.9; 147.2; 145.4; 143.8; 139.9; 139.5; 139.3; 139.1; 137.9; 137.8; 135.4; 134.6; 134.4; 128.8; 128.6; 128.3; 128.1; 126.2; 126.0; 124.4; 123.7; 122.5; 122.4; 121.0; 119.1; 118.8; 117.5; 116.3; 115.8; 115.0; 114.9; 110.2; 108.7; 100.5; 100.4; 99.8; 98.9; 97.9; 97.8; 81.6; 76.0; 75.8; 75.7; 75.4; 75.1; 28.6; 28.4; 28.3; 28.2; 28.1; 28.0; 19.5; 19.4; 19.3; 19.2. HRMS (ESI$^+$): *m/z* calcd for $C_{79}H_{81}FN_{14}O_{14}$ $[M+H]^+$: 1469.6120 found 1469.6113.

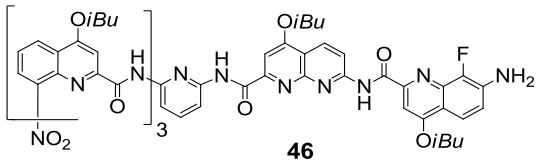

46

O_2N-Q_3PNQ^f-NH_2 46. Trifluoroacetic acid (0.8 mL) was added dropwise to a solution of **45** (0.135 g, 0.092 mmol) in 2 mL of $CHCl_3$ under nitrogen at room temperature. Then, the resulting mixture was stirred at room temperature for 5 h. The volatiles were removed under reduced pressure to give a solid which was dissolved in dichloromethane. The solution was washed with a saturated solution of $NaHCO_3$, distilled water and then with brine. The organic layer was dried over Na_2SO_4 then removed under reduced pressure to give the amine derivative **46** as a yellow solid (98 %, 0.123 g). ^{1}H NMR (300 MHz, $CDCl_3$) δ ppm = 12.06 (s, 1H); 11.93 (s, 1H); 11.11 (s, 1H); 9.81 (s, 1H); 9.72 (s, 1H); 9.23 (d, *J* = 7.2, 1H); 8.85 (d, *J* = 9.0, 1H); 8.78 (d, *J* = 9.0, 1H); 8.55 (d, *J* = 7.4, 2H); 8.16 (d, *J* = 7.9, 1H); 8.05 (d, *J* = 8.3, 1H); 8.02 (S, 1H); 7.90 (d, *J* = 9.2, 1H); 7.83 (s, 1H); 7.76 (m, 2H); 7.66 (d, *J* = 7.9, 1H); 7.61 (S, 1H); 7.57 (d, *J* = 6.4, 1H); 7.39 (t, *J* = 8.1, 1H); 7.31 (s, 1H); 7.18 (t, *J* = 8.1, 1H); 7.05 (s, 1H); 6.96 (d, *J* = 7.5, 1H); 6.45 (t, *J* = 8.0, 1H); 4.57 (s, 2H); 4.24 (d, *J* = 6.7, 2H); 4.10 (m, 4H); 3.96 (d, *J* = 6.6, 2H); 3.80 (s, 2H); 2.36 (m, 4H); 1.81 (m, 1H); 1.21 (m, 24H); 0.65 (s, 6H). ^{13}C NMR (75 MHz, $CDCl_3$) δ ppm = 164.1; 164.0; 163.8; 163.7; 163.6; 163.5; 163.4;

163.2; 162.6; 161.6; 161.3; 154.9; 154.6; 154.3; 154.0; 151.1; 150.5; 149.9; 148.8; 148.0; 145.4; 142.1; 139.9; 139.5; 139.4; 139.2; 138.9; 138.8; 136.1; 135.9; 135.5; 134.6; 134.4; 128.3; 128.2; 126.2; 126.1; 124.5; 123.8; 122.6; 122.5; 120.0; 119.1; 117.8; 117.5; 116.4; 116.1; 115.9; 115.0; 110.4; 108.8; 100.6; 99.8; 98.9; 98.0; 96.4; 76.0; 75.8; 75.5; 75.4; 75.2; 29.9; 28.5; 28.4; 28.1; 19.6; 19.5; 19.4; 19.3. HRMS (ESI$^+$): *m/z* calcd for $C_{74}H_{73}FN_{14}O_{12}$ $[M+H]^+$: 1369.5595 found 1369.5599.

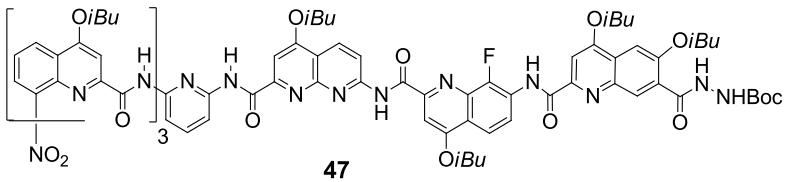

47

O_2N-Q_3PNQ^{F}H-Boc 47. To the acid derivative **23** (42 mg, 0.088 mmol) dissolved in dry chloroform (2 mL) was added at 0 °C 1-chloro-*N*,*N*-2-trimethylpropenylamine (0.04 mL, 0.292 mmol). The reaction mixture was maintained at room temperature for 2 h then the solvent was evaporated to provide the acid chloride. The amine derivative **46** (100 mg, 0.073 mmol) in dry chloroform (2 mL) containing DIEA (0.05 mL, 0.292 mmol) was added to a solution of the acid chloride in dry chloroform (2 mL) and the reaction mixture was let to stir at room temperature for 12 h. The solvents were removed under reduced pressure and the residue was purified by precipitation in MeOH to give heptamer **47** as yellow solid (71 %, 95 mg). ^{1}H NMR (300 MHz, $CDCl_3$) δ ppm = 12.01 (s, 1H); 11.73 (s, 1H); 11.20, (bs, 1H), 10.85 (s, 1H); 10.21, (s, 1H), 9.94 (s, 1H); 9.37 (bs, 1H); 9.06 (t, *J* = 7.36, 1H); 8.89 (d, *J* = 7.36, 1H); 8.78 (s, 2H); 8.48 (t, *J* = 8.76, 2H); 8.22-8.18 (m, 2H); 8.11 (d, *J* = 7.36, 1H); 7.79-7.71 (m, 4H); 7.65 (s, 1H); 7.40 (m, 2H); 7.34-7.27 (m, 2H); 7.21 (s, 1H); 7.00 (t, *J* = 8.06, 1H); 6.89 (s, 1H); 6.85 (d, *J* = 8.41, 1H); 6.33 (t, *J* = 8.06, 1H); 4.33-3.90 (m, 10H); 3.82 (d, *J* = 6.14, 2H); 3.44 (m, 2H); 2.46-2.21 (m, 6H); 1.94 (m, 1H); 1.36 (s, 9H); 1.26-1.12 (m, 35H); 0.82 (m, 6H). ^{13}C NMR (75 MHz, $CDCl_3$) δ ppm = 164.3, 163.9, 163.6, 163.4, 163.3, 163.0, 162.9, 161.8, 155.4, 154.9, 154.8, 154.6, 153.9, 151.3, 150.9, 150.0, 149.7, 149.2, 147.9, 145.4, 142.2, 140.1, 139.4, 139.2, 135.3, 134.8, 134.4, 128.2, 127.4, 126.1, 126.0, 125.1, 124.4, 123.8, 122.8, 121.8, 121.4, 119.9, 118.8, 117.9, 117.3, 115.5, 115.2, 114.7, 110.1, 108.7, 101.9, 100.6, 99.7, 99.5, 98.5, 97.9, 97.6, 81.4, 77.5, 76.6, 76.1, 75.9, 75.7, 75.5, 75.2, 30.0, 28.5, 28.4, 28.2, 19.8, 19.6. HRMS (ESI$^+$): *m/z* calcd for $C_{98}H_{104}FN_{17}O_{18}Na$ $[M+Na]^+$ 1849.7661 found 1849.7651.

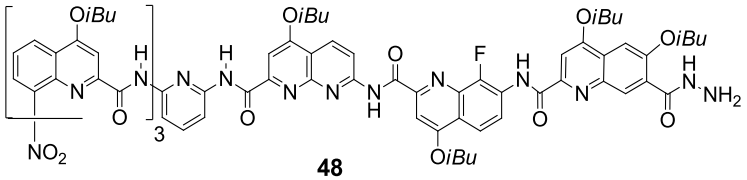

48

O_2N-Q_3PNQ^{F}H-NH_2 48. Trifluoroacetic acid (0.5 mL) was added dropwise to a solution of **47** (80 mg, 0.044 mmol) in chloroform (2 mL) under nitrogen at 0 °C. Then, the resulting mixture was stirred at room temperature for 2 h. The volatiles were removed under reduced pressure to give a solid which was dissolved in dichloromethane. The solution was washed twice with a saturated solution of $NaHCO_3$, distilled water and then with brine. The organic layer was dried over $MgSO_4$, filtered then removed under reduce pressure

and a precipitation from MeOH gave the amine derivative **48** as pale yellow solid (98 %, 74 mg). ^{1}H NMR (300 MHz, $CDCl_3$) δ ppm = 11.96 (s, 1H); 11.70 (s, 1H); 11.14, (s, 1H), 10.80 (s, 1H); 10.10, (s, 1H), 9.90 (s, 1H); 9.04 (dd, *J* = 6.44, 1H); 8.79 (d, *J* = 7.73, 1H); 8.76 (s, 2H); 8.59 (s, 1H); 8.44 (t, *J* = 7.09, 2H); 8.17 (d, *J* = 9.66, 1H); 8.14 (s, 1H); 8.06 (d, *J* = 6.44, 1H); 7.77-7.72 (m, 3H); 7.66-7.62 (m, 3H); 7.38-7.35 (m, 1H); 7.30-7.20 (m, 5H); 6.92 (t, *J* = 7.77, 1H); 6.83-6.79 (m, 2H); 6.33 (t, *J* = 8.13, 1H); 4.24-3.78 (m, 16H); 3.44 (bs, 2H); 2.46-2.15 (m, 7H); 1.99-1.81 (m, 3H); 1.26-1.08 (m, 44H); 0.87-0.84 (m, 3H). ^{13}C NMR (75 MHz, $CDCl_3$) δ ppm = 164.8, 164.2, 163.9, 163.6, 163.4, 163.2, 163.0, 162.6, 162.5, 161.7, 161.4, 154.7, 154.6, 154.6, 153.9, 153.8, 151.2, 150.9, 149.9, 149.5, 149.2, 148.7, 147.7, 145.3, 142.1, 140.0, 139.3, 139.2, 139.0, 138.0, 135.2, 134.8, 134.3, 134.2, 130.0, 128.2, 128.0, 127.9, 127.3, 126.1, 125.9, 125.0, 124.6, 124.3, 123.8, 122.7, 121.7, 121.3, 119.9, 118.6, 117.9, 117.3, 115.5, 115.1, 115.1, 114.7, 110.1, 108.6, 101.7, 100.4, 99.7, 99.2, 98.5, 97.9, 97.6, 77.5, 76.2, 76.1, 75.9, 75.8, 75.6, 75.5, 75.2, 30.0, 28.5, 28.4, 28.2, 19.8, 19.6. MS (ESI$^+$): *m/z* calcd for $C_{93}H_{97}FN_{17}O_{16}$ $[M+H]^+$ 1727.7 found 1727.7.

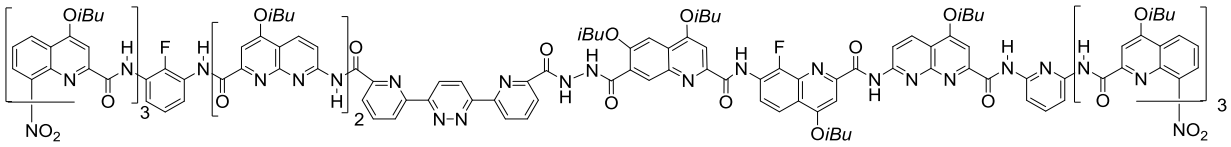

5

Capsule 5. Oligomer **37** (65 mg, 0.037 mmol) was reacted with tetrabutylammonium fluoride 1M (0.074 mL) in THF (2 mL) for 24 h. The solvent was removed under reduced pressure to give a solid which was dissolved in dichloromethane and washed with 5% aqueous citric acid solution, distilled water and brine. Heptamer acid **38** was used directly in subsequent reaction without further purification. Heptamer acid **38** (58 mg, 0.035 mmol) and heptamer amine **46** (60 mg, 0.035 mmol) were dissolved in dry chloroform (5 mL). Then, DIEA (0.02 mL, 0.087 mmol) and PyBOP (45 mg, 0.087 mmol) were added at room temperature and the reaction mixture was heated at 40 °C. After 48 h, the solvents were evaporated and the residue was purified by precipitation from minimum amount of MeOH which gave capsule **5** as a pale yellow solid (77 %, 90 mg). ^{1}H NMR (300 MHz, $CDCl_3$) δ ppm = 11.59 (s, 1H); 11.54 (s, 1H); 11.38, (s, 1H), 11.20 (s, 1H); 11.18 (s, 1H), 10.60 (d, *J* = 3.68, 1H); 10.17 (d, *J* = 2.94, 1H); 10.11 (d, *J* = 9.27, 1H); 10.00 (s, 1H); 9.72-9.68 (m, 3H); 9.55 (s, 1H); 9.44 (d, *J* = 3.30, 1H); 9.24 (dd, *J* = 9.00, 1H); 8.70 (d, *J* = 8.83, 1H); 8.61 (d, *J* = 8.83, 1H); 8.52 (d, *J* = 8.50, 2H); 8.45 (d, *J* = 7.77, 1H); 8.37 (d, *J* = 9.18, 1H); 8.27 (d, *J* = 8.12, 1H); 8.18-7.89 (m, 14H); 7.77 (m, 2H); 7.58 (s, 1H); 7.55 (d, *J* = 8.48, 1H); 7.51 (s, 1H); 7.47 (s, 1H); 7.33 (s, 1H); 7.20-7.00 (m, 8H); 6.89-6.73 (m, 4H); 6.64-6.61 (m, 2H); 6.53 (s, 1H); 6.48-6.41 (m, 2H); 6.35 (s, 1H); 6.28 (m, 2H); 5.90 (t, *J* = 7.77, 1H); 5.82 (t, *J* = 8.48, 1H); 4.38-3.44 (m, 24H); 2.98 (m, 2H); 2.74 (t, *J* = 8.81, 1H); 2.60-2.04 (m, 13H); 1.45 (dd, *J* = 6.50, 6H); 1.38-1.10 (m, 58H); 1.00 (dd, *J* = 6.50, 6H); 0.55 (d, *J* = 6.32, 3H); 0.44 (d, *J* = 6.55, 3H); 0.26 (d, *J* = 6.83, 3H); 0.23 (d, *J* = 6.83, 3H). MS (ESI$^+$): *m/z* calcd for $C_{183}H_{175}F_2N_{35}O_{30}Na_2$ $[M+2Na]^{2+}$ 1713.6 found 1713.6.

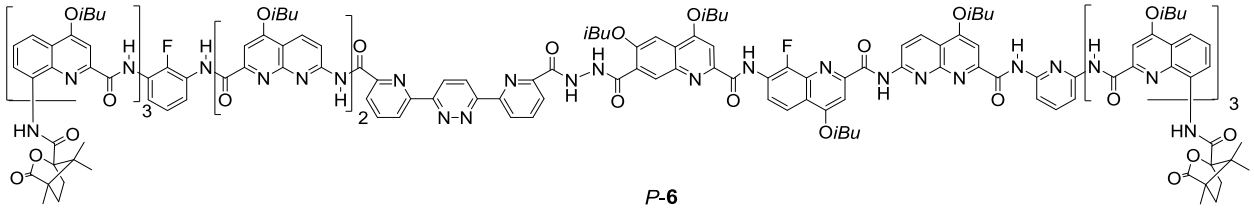

P-**6**

(1*S*) (1*S*)

Capsule 6. To a solution of capsule **5** (55 mg, 0.016 mmol) in EtOAc/MeOH (4:1, 5 mL), 10% Pd/C (30 mg) and NH_4VO_3 (2 mg) was slowly added an aqueous solution of ammonium formate (270 mg in 0.3 ml of water) and the mixture was stirred at 90 °C. After 24 h, the solution was cooled down and filtered through celite. The evaporation of solvents gave the diamino derivative **49** as a pale yellow solid. Diamine **49** (50 mg, 0.015 mmol) was dissolved in dry chloroform (3 mL) containing DIEA (0.04 mL, 0.226 mmol), then the commercially available 1*S*-(-)-camphanic chloride (33 mg, 0.15 mmol) was added as a solid to the solution. The reaction mixture was stirred at room temperature overnight and the solvents were removed under reduced pressure. The residue was purified by column chromatography (SiO_2), eluting with EtOAc:dichloromethane (: vol/vol) to give **6** as a pale yellow solid (78%, 47 mg). ^{1}H NMR (300 MHz, $CDCl_3$) δ ppm = 11.85 (s, 1H); 11.63 (s, 1H); 11.45, (s, 1H), 11.42 (s, 1H); 11.29 (s, 1H), 10.60 (d, *J* = 3.52, 1H); 10.07 (m, 2H); 9.96 (s, 1H); 9.82 (s, 1H); 9.67 (d, *J* = 9.63, 1H); 9.54 (d, *J* = 4.93, 2H); 9.48 (s, 1H); 9.40 (d, *J* = 3.52, 1H); 9.32 (s, 1H); 9.22 (d, *J* = 8.69, 1H); 8.71-8.59 (m, 2H); 8.51 (t, *J* = 7.52, 2H); 8.41 (d, *J* = 7.52, 1H); 8.36 (d, *J* = 9.56, 1H); 8.14-7.95 (m, 11H); 7.89 (s, 1H); 7.80-7.70 (m, 3H); 7.63-7.55 (m, 4H); 7.50 (d, *J* = 8.22, 1H); 7.45 (s, 1H); 7.32 (d, *J* = 9.63, 2H); 7.20 (m, 2H); 7.05-6.79 (m, 8H); 6.67 (t, *J* = 7.99, 1H); 6.60 (s, 1H); 6.55-6.47 (m, 3H); 6.38 (d, *J* = 7.97, 1H); 6.25 (s, 1H); 6.20-6.14 (m, 2H); 5.97 (t, *J* = 7.97, 1H); 5.88 (t, *J* = 7.97, 1H); 4.38-3.45 (m, 23H); 3.21 (m, 1H); 3.07 (t, *J* = 8.96, 1H); 2.80 (t, *J* = 8.96, 1H); 2.69 (m, 1H); 2.59-1.90 (m, 11H); 1.68 (m, 6H); 1.45-1.08 (m, 64H); 0.98 (d, *J* = 6.97, 6H); 0.57 (d, *J* = 6.35, 3H); 0.48-0.39 (m, 13H); 0.26 (t, *J* = 7.06, 6H); 0.02 (d, *J* = 6.01, 6H). MS (ESI$^+$): *m/z* calcd for $C_{203}H_{203}F_2N_{35}O_{32}Na$ $[M+Na]^+$ 3705.5 found 3705.5.

3. Principles of folding

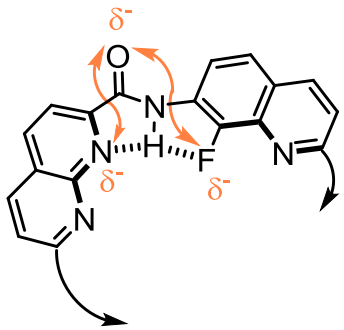

Supplementary Figure S1. Folding patterns of aza-aromatic and fluoro-aromatic foldamers. Conjugation, hydrogen bonds (dashed lines) and electrostatic repulsions (arrows) concur to stabilize a preferred conformation of each aryl-amide and aryl-aryl linkages, resulting in a bent conformation that gives rise to a helix. Intramolecular π–π stacking comes as an additional, solvent dependent, force stabilizing the helix.

4. Binding Studies

4.1 Procedures

Circular Dichroism titrations. Stock solutions of carbohydrates were prepared in DMSO and allowed to equilibrate overnight prior to use. Chloroform was added to the DMSO solution until reaching a 80:20 chloroform/DMSO stock solution and mixed with receptors **1**, **3** and **5** just before the experiment. Then, aliquots of the guest solution were added to the cell with the receptor (2 mL, [**receptor**]$_{initial}$ = 15 or 30 μM) in the same solvent mixture. Homogenization was performed after each addition using a microsyringe and CD spectra were recorded on a Jasco J-815 spectropolarimeter at 298 K. Spectra for the additions of *D*-fructose **7**, D-mannose **8**, D-glucose **9**, D-galactose **10**, D-*N*-acetylglucosamine **11**, D-ribose **12**, D-xylose **13** with **1** are shown in supplementary Figures S2a, S4a, S5a, S6a, S7a, S8a, and S10a, respectively. Spectra for the additions of *D*-fructose **7**, D-mannose **8,** D-glucose **9** and D-ribose **12** with **3** are shown in supplementary Figures S11a, S12a, S13a and S14a, respectively. Spectra for the additions of *D*-fructose **7** and D-mannose **8** with **5** are shown in supplementary Figures S17a and S18a, respectively Changes in ellipticity were analysed according to a 1:1 binding model, using a non-linear least squares curve-fitting program implemented within Microsoft Excel. The programme yields binding constants K_a and limiting $\Delta\varepsilon$ as output. Resulting binding curves (experimental *vs.* calculated data) are shown in supplementary Figures S2b, S4b, S5b, S6b, S7b, S8b, S10b, S11b, S12b, S13b, S14b, S17b and S18b, respectively.

^{1}H NMR titrations. Solutions of carbohydrates were prepared in d_6-DMSO and allowed to equilibrate overnight prior to use. $CDCl_3$ was added to the DMSO solution until reaching a 80:20 $CDCl_3$/DMSO stock solution and mixed with receptors **2**, **4** and **6** just before the experiment. Aliquots were then added to an NMR tube containing the receptor in the same solvent mixture (0.25 mmol in 500 μL, [**receptor**]$_{initial}$ = 0.5 mM). The sample tube was shaken carefully after each addition and ^{1}H NMR spectra were recorded at 298 K. Spectra recorded for the additions of *D*-fructose **7**, D-Mannose **8**, D-glucose **9**, D-galactose **10**, D-*N*-acetylglucosamine **11**, D-ribose **12**, D-xylose **13** with **2** are shown in Figures S19, S21, S23, S25, S27, S28, and S30, respectively. Spectra recorded for the additions of *D*-fructose **7**, D-mannose **8** and D-ribose **12** with **4** are shown in Figures S32, S34 and S35, respectively. Spectra recorded for the additions of *D*-fructose **7**, D-mannose **8** and D-ribose **12** with **6** are shown in Figures S36, S38 and S38, respectively. As free and bound receptor could be observed simultaneously (slow exchange), binding constants K_a were obtained by integration of signals from both against each other. Values were obtained from several spectra and the results averaged. Details are given below.

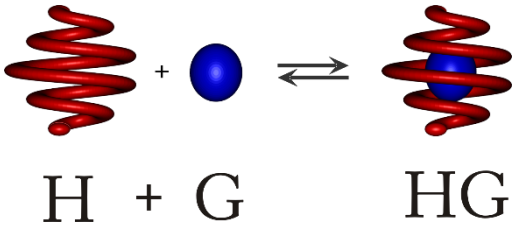

For the equilibrium shown in Eq. 1, the association constant K_a of the receptor is given by Eq. 2.

$$H + G \rightleftharpoons HG \qquad (1)$$

$$K_a = \frac{[HG]}{[H][G]} \qquad (2)$$

where: [HG] = complex concentration; [H] = host concentration; [G] = guest concentration

Alternatively,

$$K_a = \frac{n_{HG} \times V_T}{n_H \times n_G} \qquad (3)$$

where: V_T = total volume of the sample; n_H = number of moles of host (etc.)

From mass balance,

$$n_{H_0} = n_H + n_{HG} \qquad (4)$$

$$n_{G_0} = n_G + n_{HG} \qquad (5)$$

where: n_{H0} = initial number of moles of host; n_{G0} = number of moles of guest added to the sample

Substituting equations (4) and (5) into (3),

$$K_a = \frac{n_{HG} \times V_T}{(n_{H_0} - n_{HG}) \times (n_{G_0} - n_{HG})} \qquad (6)$$

From integration of the NMR spectrum it is possible to obtain the fraction of bound host molecules, x (Eq. 7).

$$x = \frac{n_{HG}}{n_{H_0}} \qquad (7)$$

Using Eq. 7 to eliminate n_{HG} from Eq. 6,

$$K_a = \frac{x \times V_T}{n_{G_0} - (x \times n_{H_0}) - (x \times n_{G_0}) + (x^2 \times n_{H_0})} \qquad (8)$$

4.2 Circular Dichroism Titrations

Titrations with capsule **1**

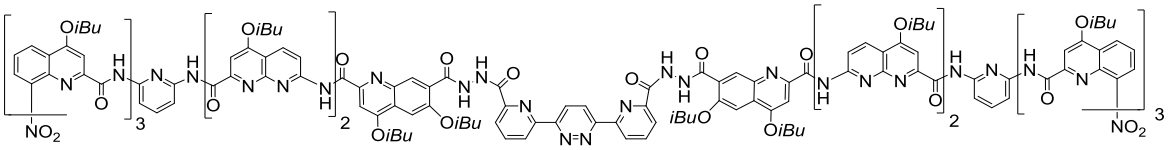

1

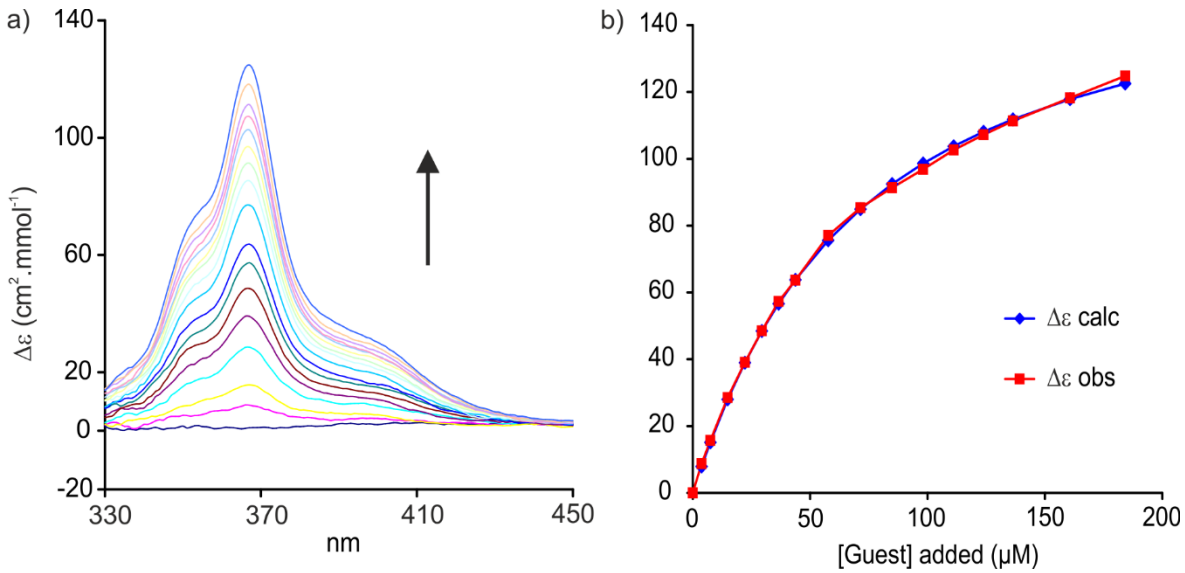

Supplementary Figure S2. (a) CD spectra recorded at 298K for the binding study of receptor **1** vs. D-fructose **7** in $CHCl_3$/DMSO (80:20). $[\mathbf{1}]_{initial}$ = 0.015 mM, $[\mathbf{7}]_{titrant}$ = 1.5 mM. (b) Experimental and calculated values for the ICD binding study of receptor **1** vs. D-fructose **7** in $CHCl_3$/DMSO (80:20). Δε values at 367 nm were used for the analysis. K_a = 16600 L mol^{-1}. Limiting Δε = 164.8 cm^2 $mmol^{-1}$.

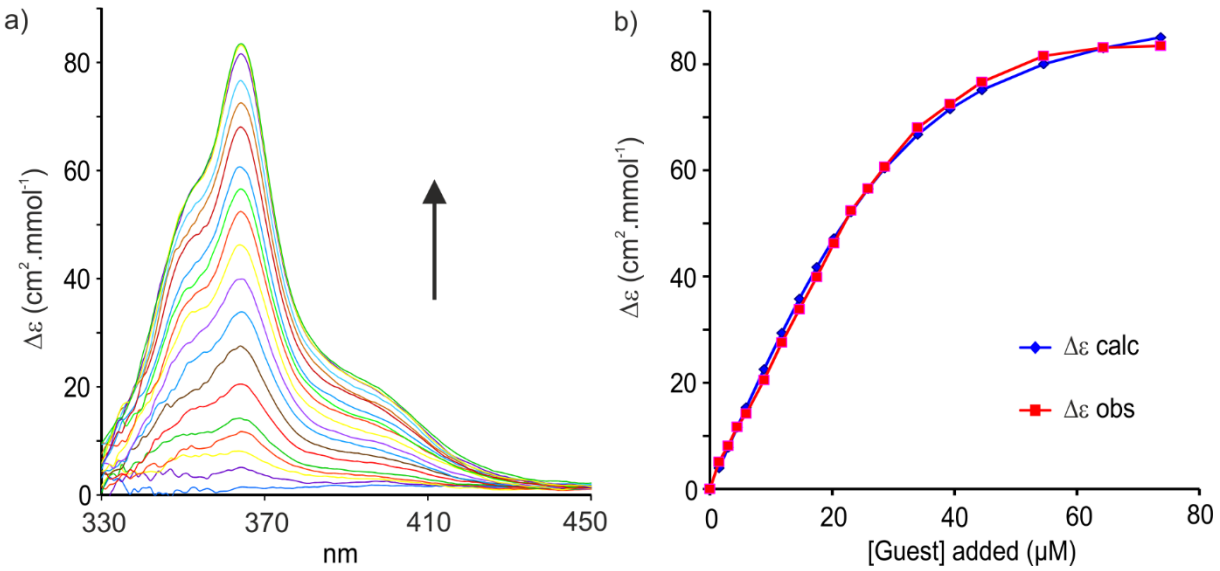

Supplementary Figure S3. (a) CD spectra recorded at 298K for the binding study of receptor **1** vs. D-fructose **7** in $CHCl_3$/DMSO (95:5). $[\mathbf{1}]_{initial}$ = 0.03 mM, $[\mathbf{7}]_{titrant}$ = 0.6 mM. (b) Experimental and calculated values for the ICD binding study of receptor **1** vs. D-fructose **7** in $CHCl_3$/DMSO (95:5). Δε values at 364 nm were used for the analysis. K_a = 165000 L mol^{-1}. Limiting Δε = 95.3 cm^2 $mmol^{-1}$.

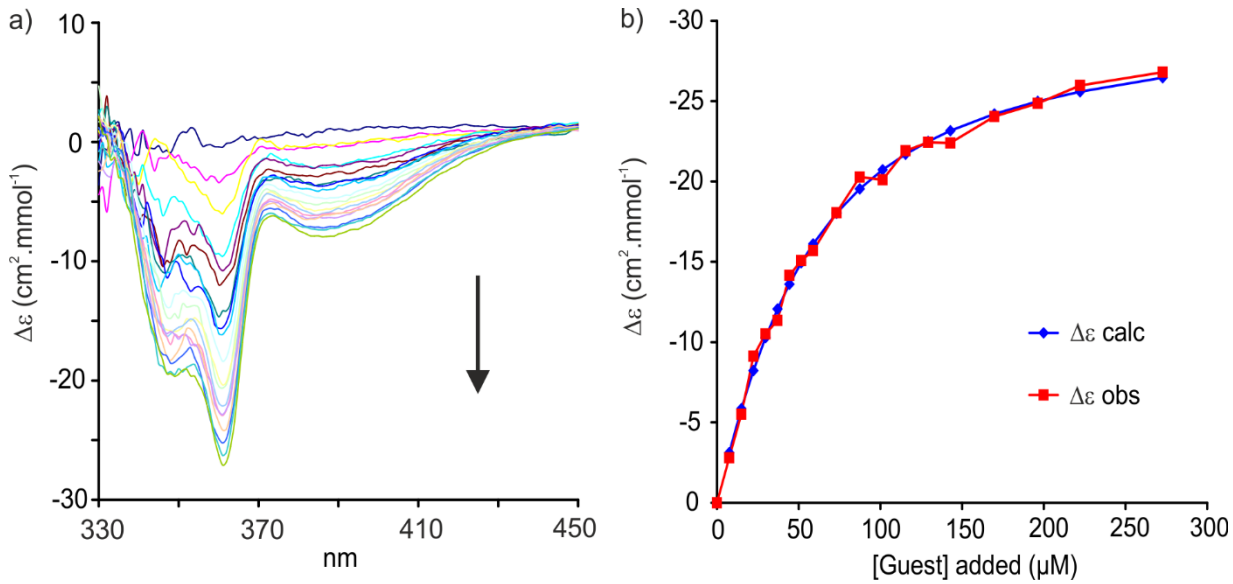

Supplementary Figure S4. (a) CD spectra recorded at 298K for the binding study of receptor **1** vs. D-mannose **8** in $CHCl_3$/DMSO (80:20). $[\mathbf{1}]_{initial}$ = 0.03 mM, $[\mathbf{8}]_{titrant}$ = 3 mM. (b) Experimental and calculated values for the ICD binding study of receptor **1** vs. D-mannose **8** in $CHCl_3$/DMSO (80:20). Δε values at 362 nm were used for the analysis. K_a = 25600 L mol^{-1}. Limiting Δε = -30.6 cm^2 $mmol^{-1}$.

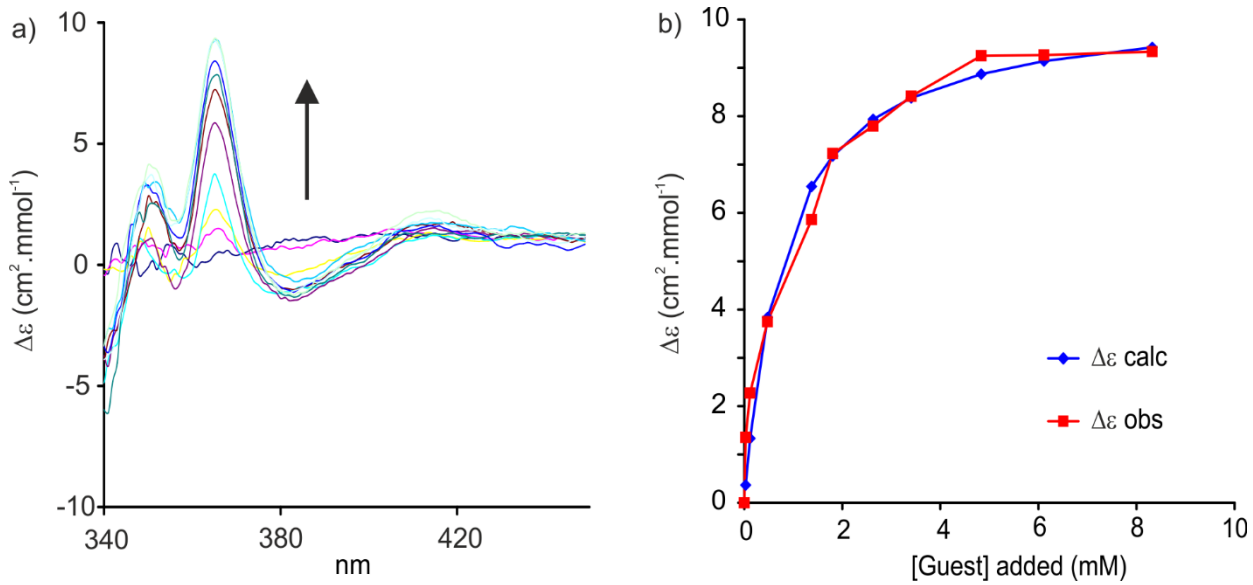

Supplementary Figure S5. (a) CD spectra recorded at 298K for the binding study of receptor **1** vs. D-glucose **9** in $CHCl_3$/DMSO (80:20). $[\mathbf{1}]_{initial}$ = 0.03 mM, $[\mathbf{9}]_{titrant}$ = 3 mM. (b) Experimental and calculated values for the ICD binding study of receptor **1** vs. D-glucose **9** in $CHCl_3$/DMSO (80:20). Δε values at 365 nm were used for the analysis. K_a = 1300 L mol^{-1}. Limiting Δε = 10.3 cm^2 $mmol^{-1}$.

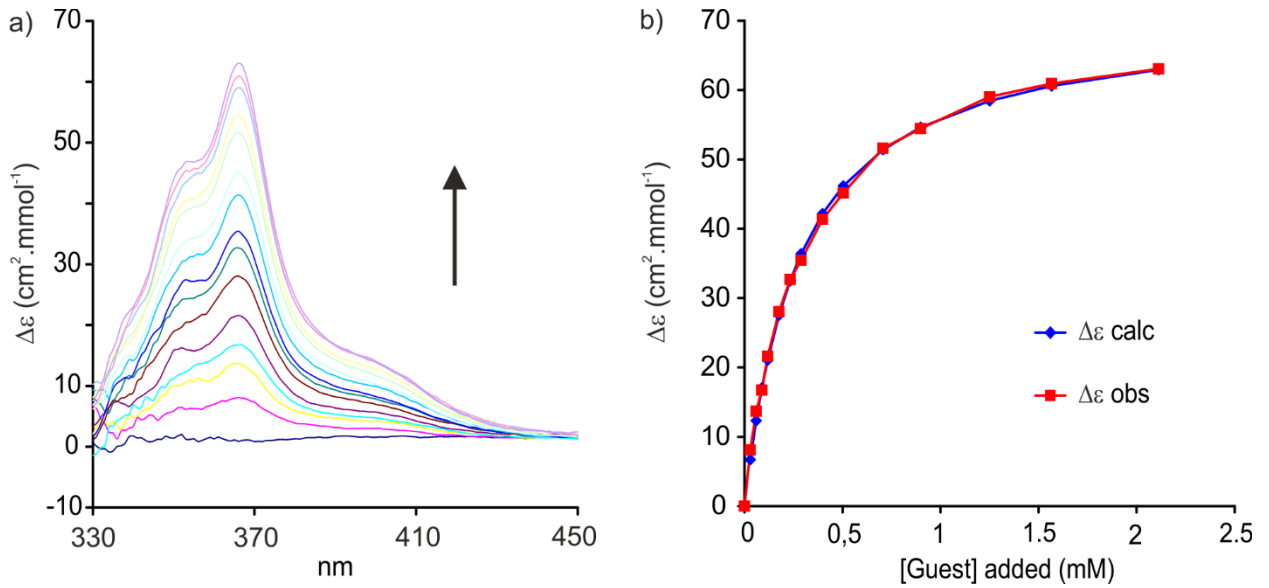

Supplementary Figure S6. (a) CD spectra recorded at 298K for the binding study of receptor **1** vs. D-galactose **11** in $CHCl_3$/DMSO (80:20). $[\mathbf{1}]_{initial}$ = 0.03 mM, $[\mathbf{10}]_{titrant}$ = 1.5 mM. (b) Experimental and calculated values for the ICD binding study of receptor **1** vs. D-galactose **10** in $CHCl_3$/DMSO (80:20). Δε values at 366 nm were used for the analysis. K_a = 3900 L mol^{-1}. Limiting Δε = 70.68 cm^2 $mmol^{-1}$.

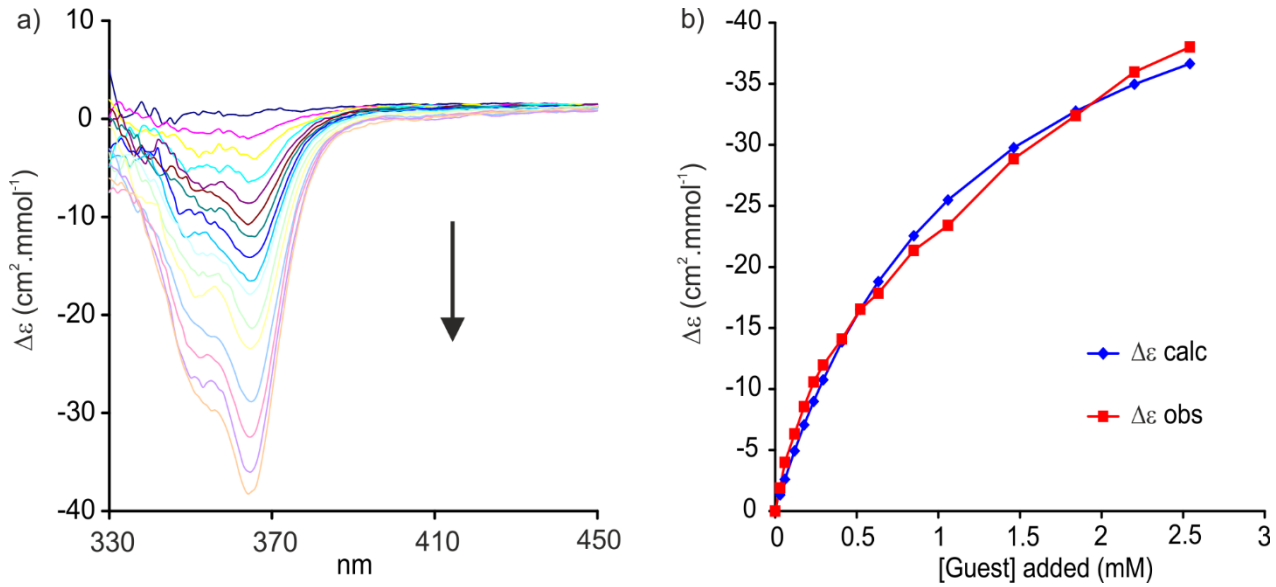

Supplementary Figure S7. (a) CD spectra recorded at 298K for the binding study of receptor **1** vs. D-GlcNAc **11** in $CHCl_3$/DMSO (80:20). $[\mathbf{1}]_{initial}$ = 0.03 mM, $[\mathbf{11}]_{titrant}$ = 1.5 mM. (b) Experimental and calculated values for the ICD binding study of receptor **1** vs. D-GlcNAc **11** in $CHCl_3$/DMSO (80:20). Δε values at 365 nm were used for the analysis. K_a = 880 L mol^{-1}. Limiting Δε = -53.1 cm^2 $mmol^{-1}$.

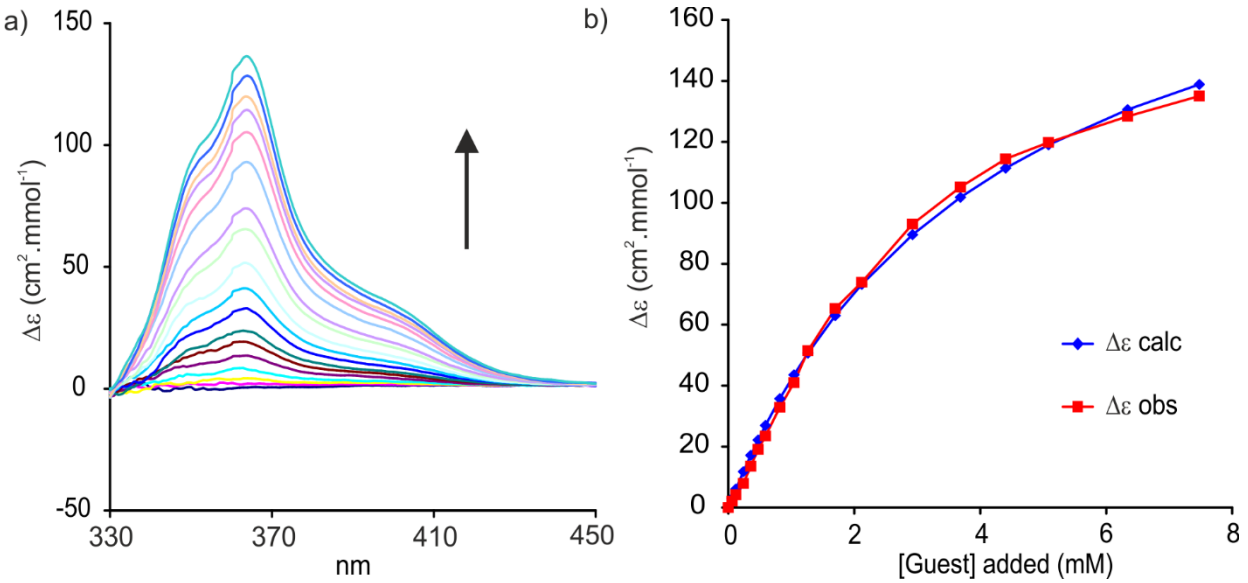

Supplementary Figure S8. (a) CD spectra recorded at 298K for the binding study of receptor **1** vs. D-ribose **12** in $CHCl_3$/DMSO (80:20). $[\mathbf{1}]_{initial}$ = 0.03 mM, $[\mathbf{12}]_{titrant}$ = 30 mM; (b) Experimental and calculated values for the ICD binding study of receptor **1** vs. D-ribose **12** in $CHCl_3$/DMSO (80:20). Δε values at 364 nm were used for the analysis. K_a = 240 L mol^{-1}. Limiting Δε = 151.1 cm^2 $mmol^{-1}$.

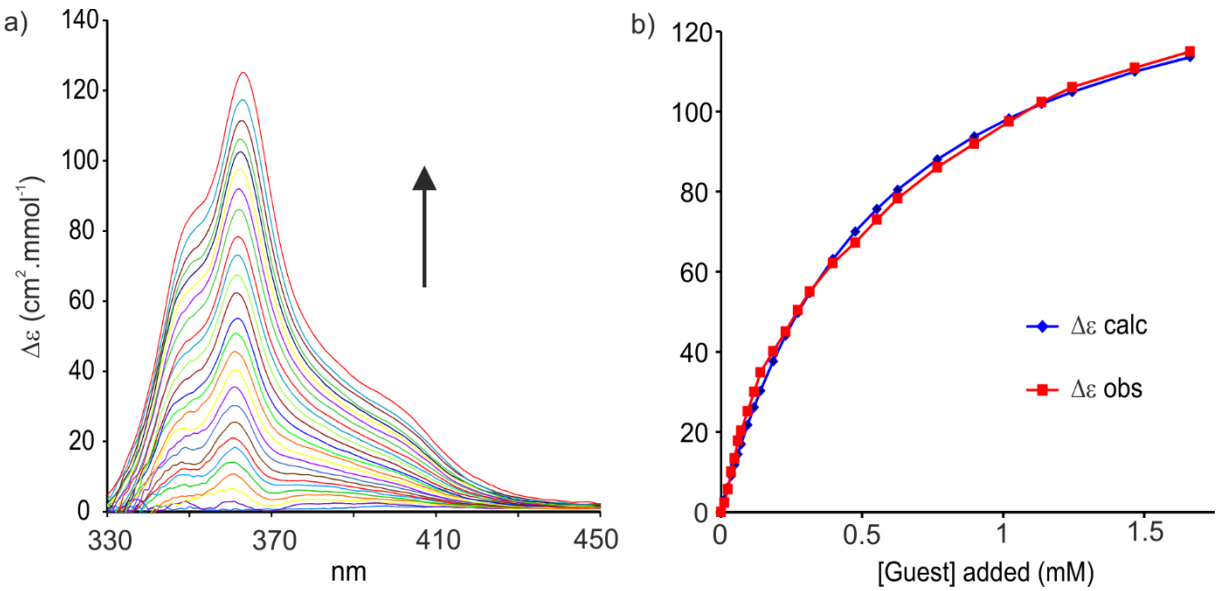

Supplementary Figure S9. a) CD spectra recorded at 298K for the binding study of receptor **1** vs. D-ribose **12** in $CHCl_3$/DMSO (95/5). $[\mathbf{1}]_{initial}$ = 0.03 mM, $[\mathbf{12}]_{titrant}$ = 4.8 mM; b) Experimental and calculated values for the ICD binding study of receptor **1** vs. D-ribose **12** in $CHCl_3$/DMSO (95/5). Δε values at 362 nm were used for the analysis. K_a = 1900 L mol^{-1}. Limiting Δε = 151.1 cm^2 $mmol^{-1}$.

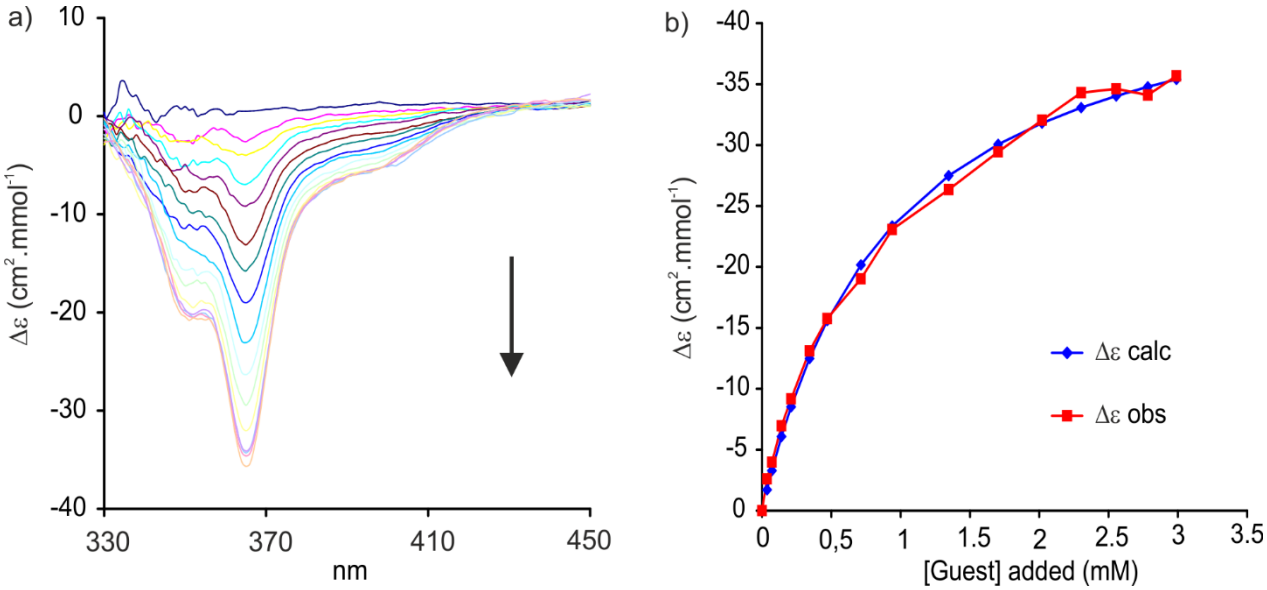

Supplementary Figure S10. (a) CD spectra recorded at 298K for the binding study of receptor **1** vs. D-xylose **13** in $CHCl_3$/DMSO (80:20). $[\mathbf{1}]_{initial}$ = 0.03 mM, $[\mathbf{13}]_{titrant}$ = 7.2 mM; (b) Experimental and calculated values for the ICD binding study of receptor **1** vs. D-xylose **13** in $CHCl_3$/DMSO (80:20). Δε values at 365 nm were used for the analysis. K_a = 1100 L mol^{-1}. Limiting Δε = -46.1 cm^2 $mmol^{-1}$.

Titrations with capsule **3**

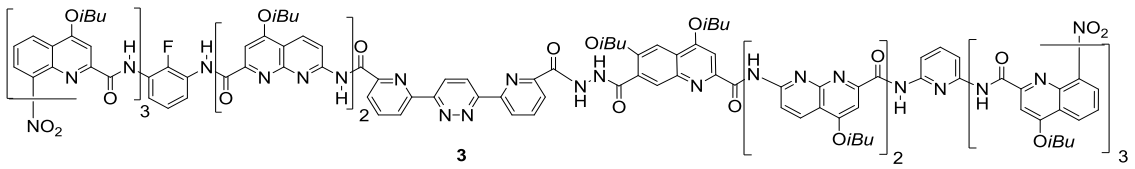

3

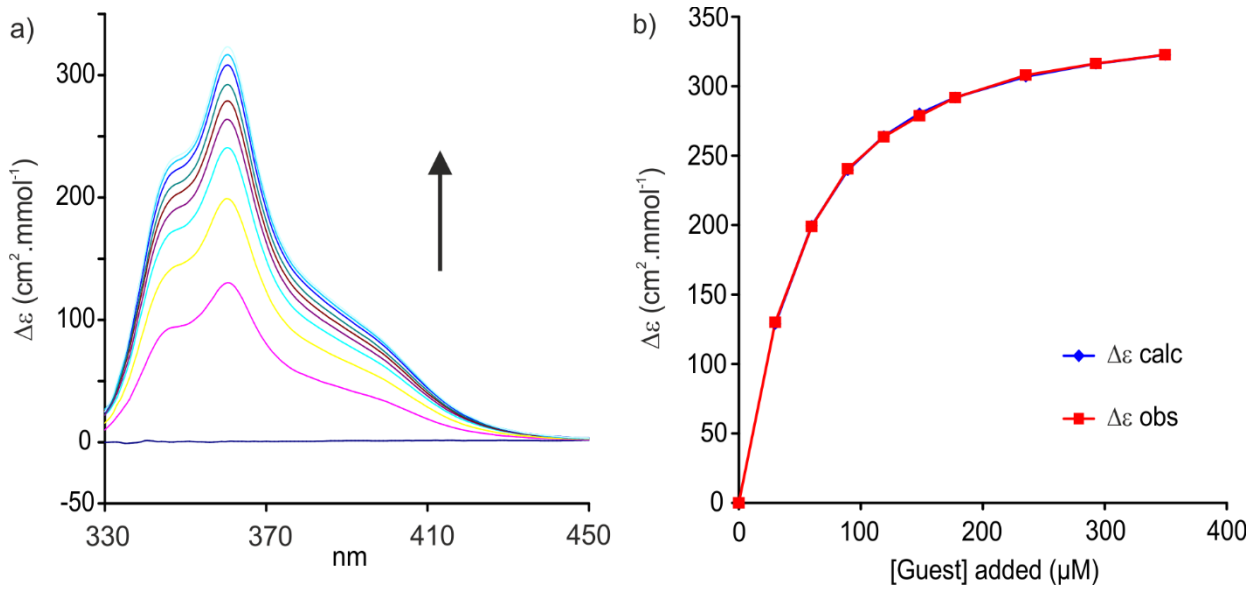

Supplementary Figure S11. (a) CD spectra recorded at 298K for the binding study of receptor **3** vs. D-fructose **7** in $CHCl_3$/DMSO (80:20). $[\mathbf{3}]_{initial}$ = 0.03 mM, $[\mathbf{7}]_{titrant}$ = 12 mM; (b) Experimental and calculated values for the ICD binding study of receptor **3** vs. D-fructose **7** in $CHCl_3$/DMSO (80:20). Δε values at 365 nm were used for the analysis. K_a = 29600 L mol^{-1}. Limiting Δε = 356.1 cm^2 $mmol^{-1}$.

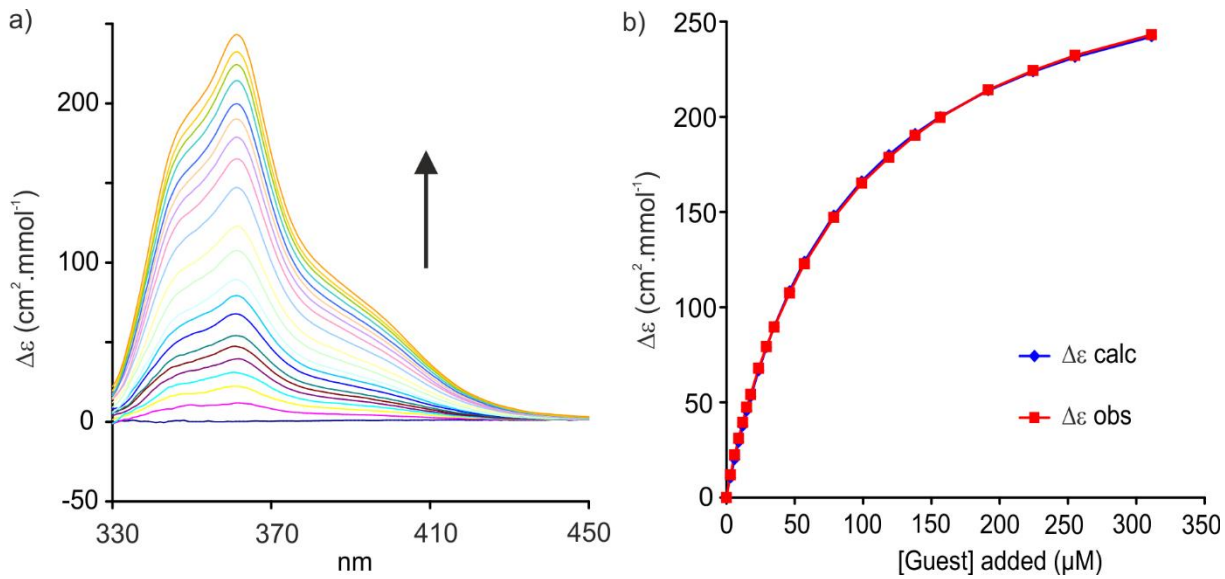

Supplementary Figure S12. (a) CD spectra recorded at 298K for the binding study of receptor **3** vs. D-mannose **8** in $CHCl_3$/DMSO (80:20). $[\mathbf{3}]_{initial}$ = 0.03 mM, $[\mathbf{8}]_{titrant}$ = 12 mM. (b) Experimental and calculated values for the ICD binding study of receptor **3** vs. D-mannose **8** in $CHCl_3$/DMSO (80:20). Δε values at 361 nm were used for the analysis. K_a = 1200 L mol^{-1}. Limiting Δε = 306.5 cm^2 $mmol^{-1}$.

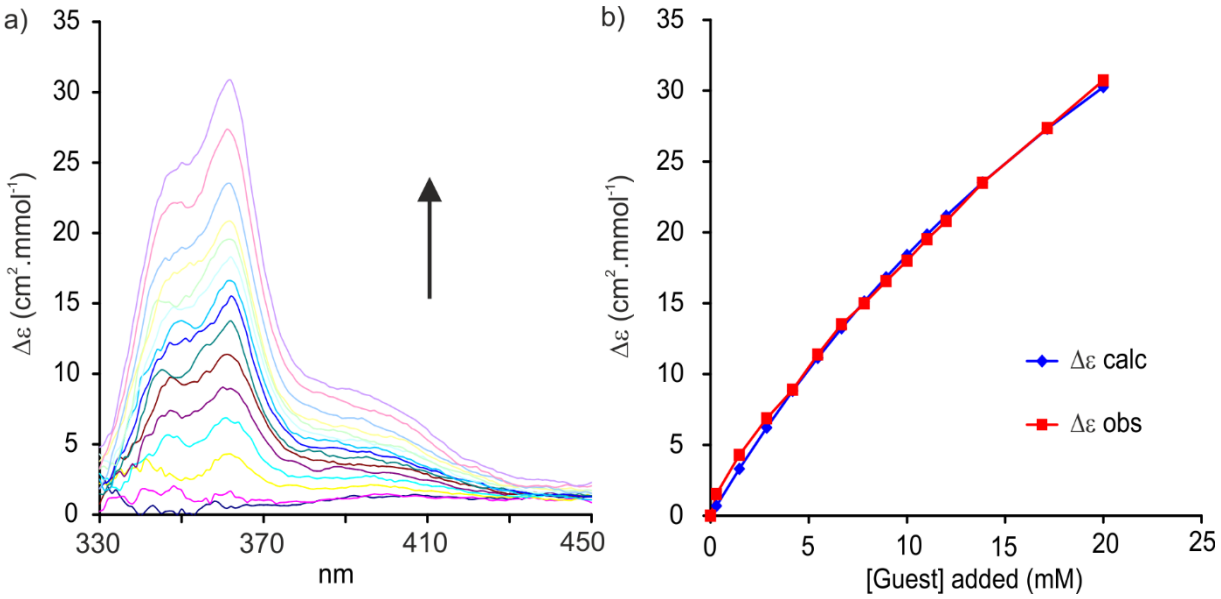

Supplementary Figure S13. (a) CD spectra recorded at 298K for the binding study of receptor **3** vs. D-glucose **9** in $CHCl_3$/DMSO (80:20). $[\mathbf{3}]_{initial}$ = 0.03 mM, $[\mathbf{9}]_{titrant}$ = 60 mM; (b) Experimental and calculated values for the ICD binding study of receptor **3** vs. D-ribose **9** in $CHCl_3$/DMSO (80:20). Δε values at 361 nm were used for the analysis. K_a = 30 L mol^{-1}. Limiting Δε = 84.9 cm^2 $mmol^{-1}$.

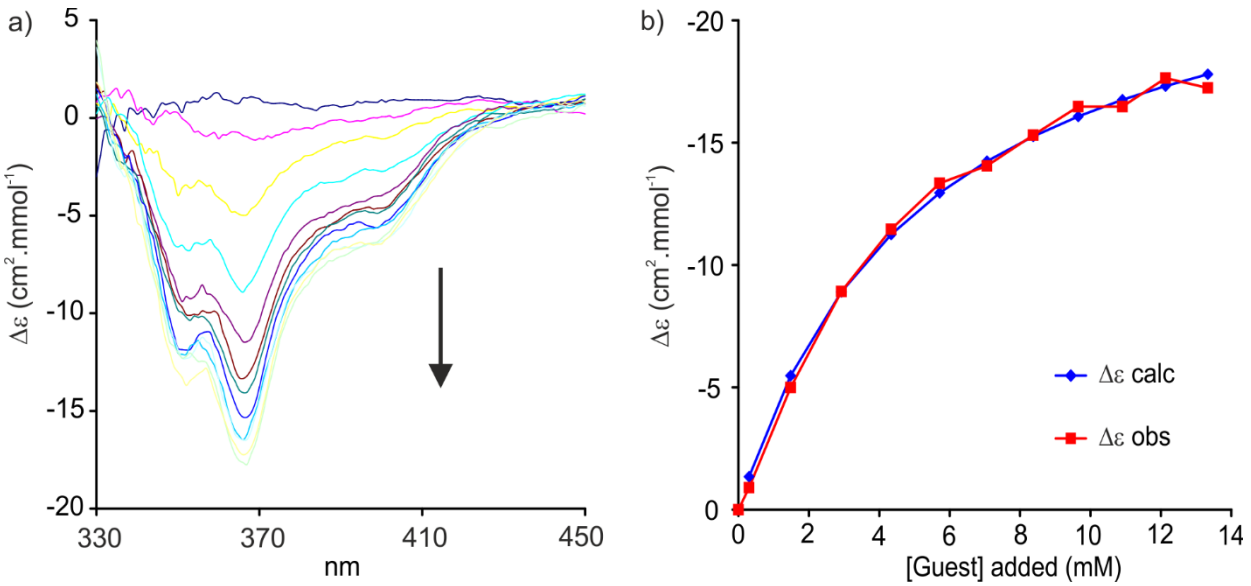

Supplementary Figure S14. (a) CD spectra recorded at 298K for the binding study of receptor **3** vs. D-ribose **12** in $CHCl_3$/DMSO (80:20). $[\mathbf{3}]_{initial}$ = 0.03 mM, $[\mathbf{12}]_{titrant}$ = 120 mM; (b) Experimental and calculated values for the ICD binding study of receptor **3** vs. D-ribose **12** in $CHCl_3$/DMSO (80:20). Δε values at 366 nm were used for the analysis. K_a = 190 L mol^{-1}. Limiting Δε = -24.7 cm^2 $mmol^{-1}$.

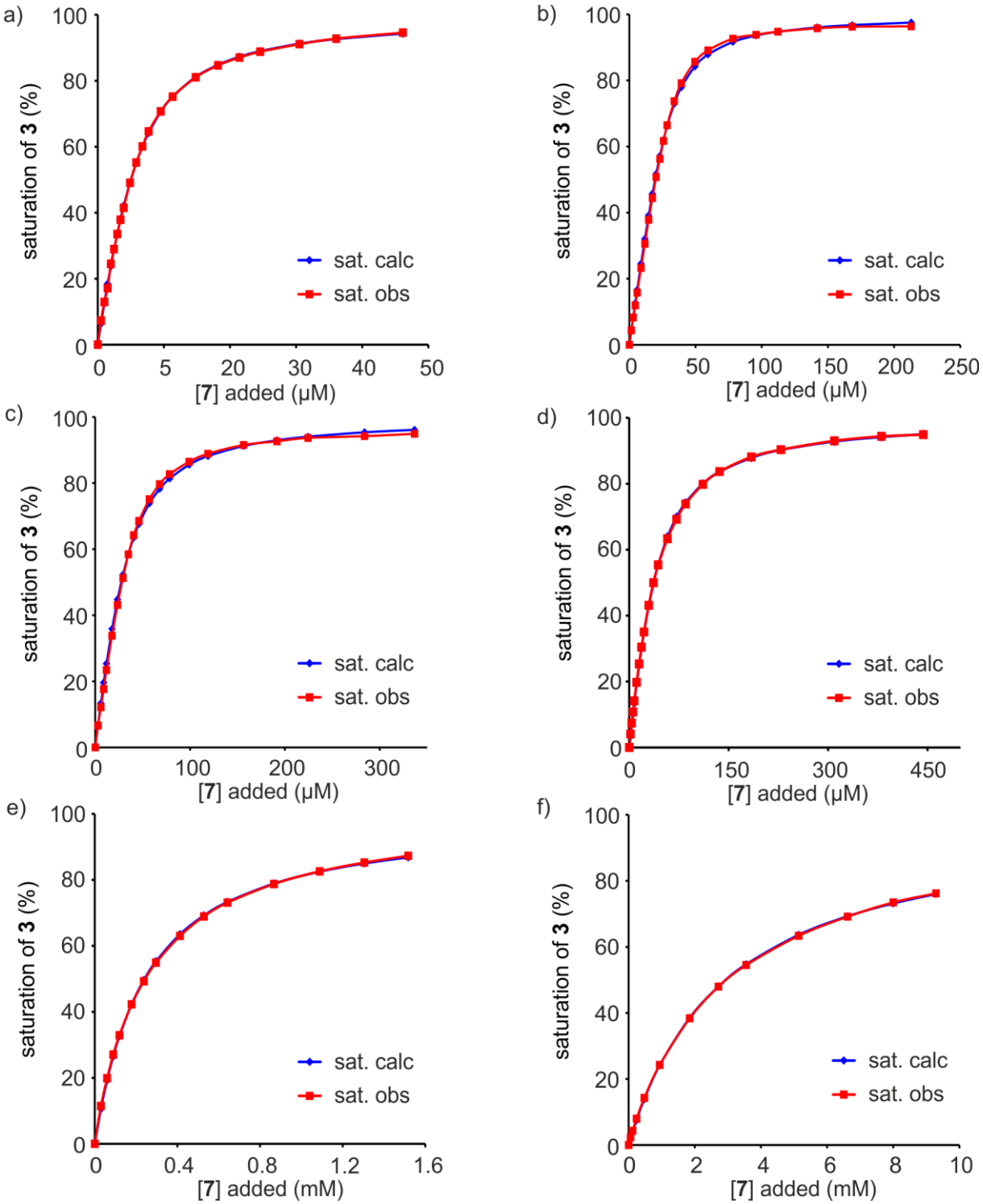

Supplementary Figure S15. Experimental and calculated values for the ICD binding study of receptor **3** vs. D-fructose **7** in the presence of increasing proportions of DMSO: (a) 5%; (b) 7.5%; (c) 10%; (d) 15%; (e) 30% (f) 40%. Ka values are summarized in Table S1.

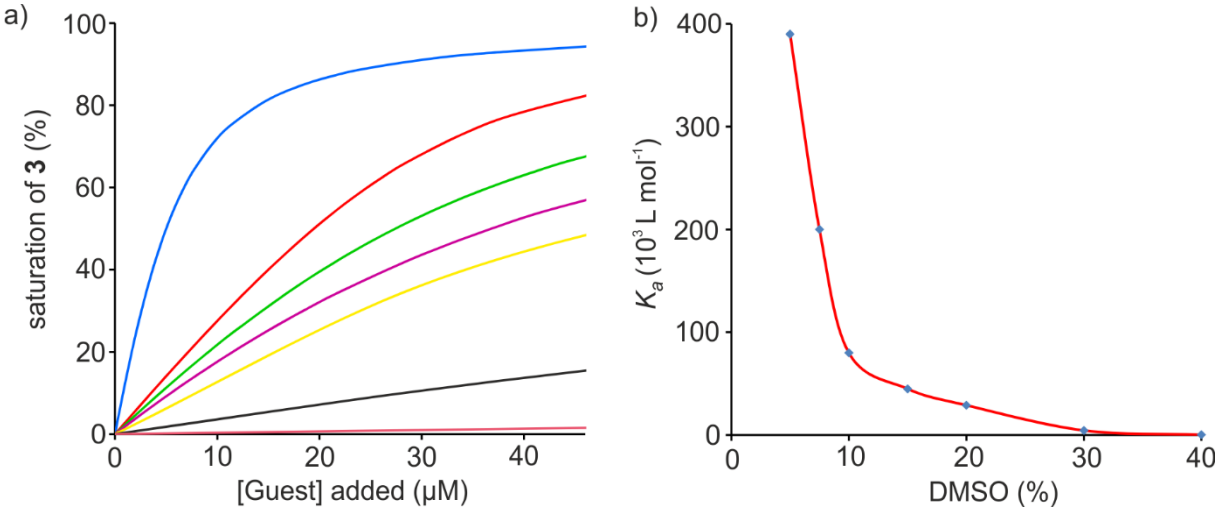

Supplementary Figure S16. (a) Curve fittings of the CD titrations of **3** with **7** in $CHCl_3$ at 298K in the presence of increasing proportions of DMSO: 5% (blue), 7.5% (red), 10% (green), 15% (purple), 20% (yellow), 30% (black) and 40% (pink); (b) Binding constants K_a of receptor **3** to **7** in $CHCl_3$/DMSO solvent mixtures measured by circular dichroism.

Supplementary Table S1. Host-guest association constants for the binding of D-fructose **7** in receptor **3** in the presence of increasing proportions of DMSO.

% of DMSO in $CHCl_3$	5	7.5	10	15	20	30	40
Ka (L.mol^{-1})	390000	200000	80000	45000	29600	4500	350

Titrations with capsule **5**

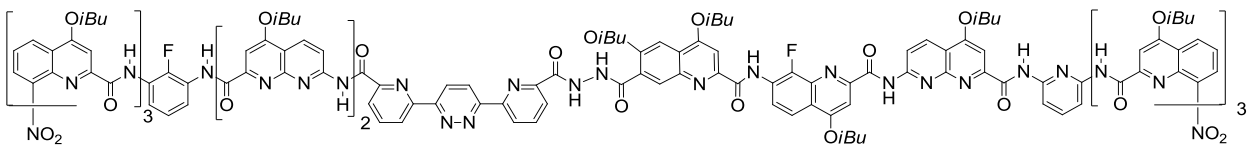

5

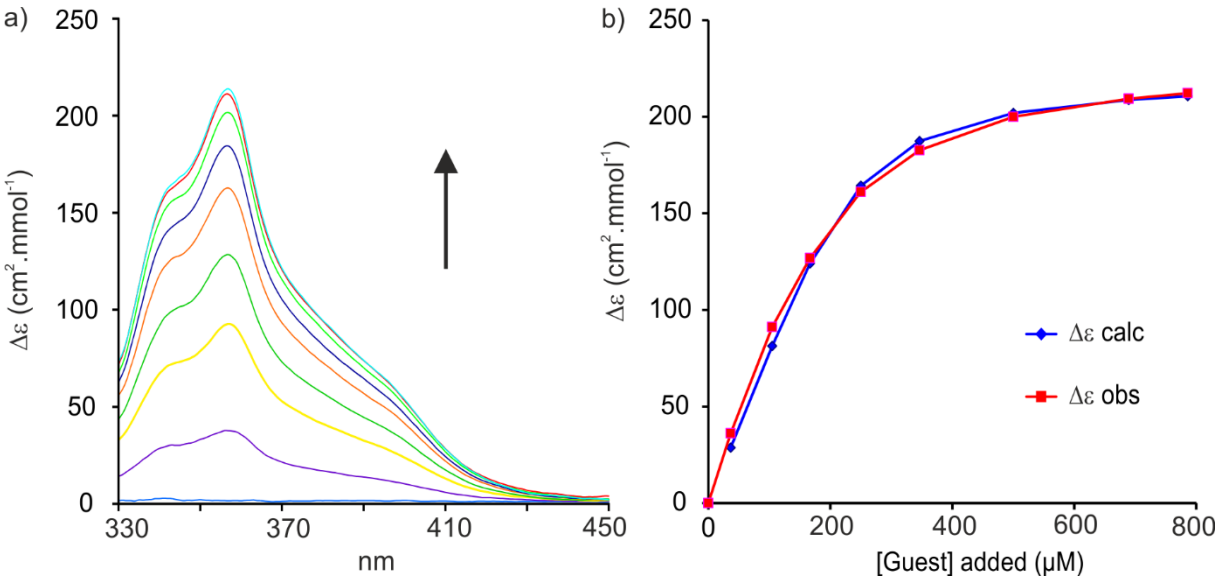

Supplementary Figure S17. (a) CD spectra recorded at 298K for the binding study of receptor **5** vs. D-fructose **7** in $CHCl_3$/DMSO (80:20). $[\mathbf{5}]_{initial}$ = 0.25 mM, $[\mathbf{7}]_{titrant}$ = 1.5 mM; (b) Experimental and calculated values for the ICD binding study of receptor **5** vs. D-fructose **7** in $CHCl_3$/DMSO (80:20). Δε values at 357 nm were used for the analysis. K_a = 30500 L mol^{-1}. Limiting Δε = 222.5 cm^2 $mmol^{-1}$.

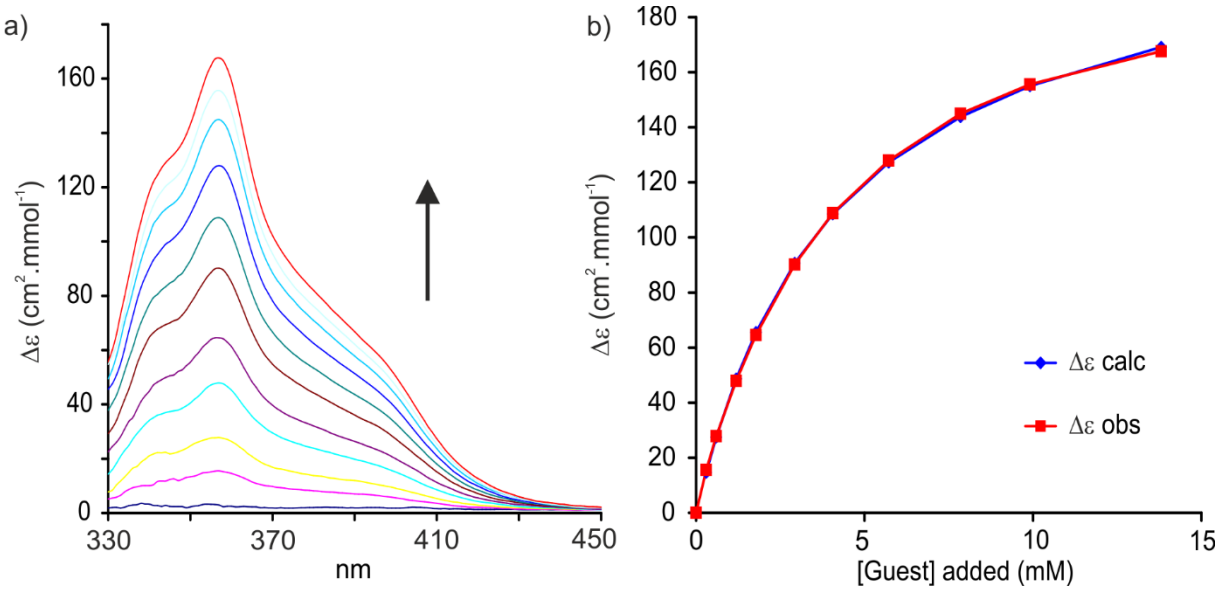

Supplementary Figure S18. (a) CD spectra recorded at 298K for the binding study of receptor **5** vs. D-mannose **8** in $CHCl_3$/DMSO (80:20). $[\mathbf{5}]_{initial}$ = 0.03 mM, $[\mathbf{8}]_{titrant}$ = 120 mM; (b) Experimental and calculated values for the ICD binding study of receptor **5** vs. D-mannose **8** in $CHCl_3$/DMSO (80:20). Δε values at 357 nm were used for the analysis. K_a = 240 L mol^{-1}. Limiting Δε = 220.3 cm^2 $mmol^{-1}$.

4.3 ^{1}H Nuclear Magnetic Resonance Titrations

Titrations with capsule **2**

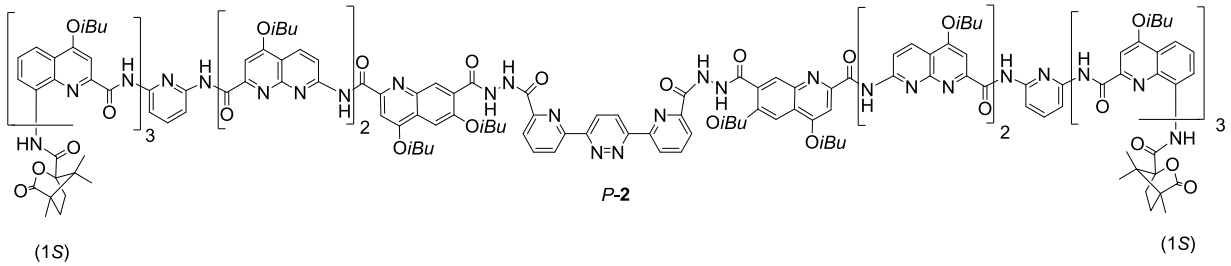

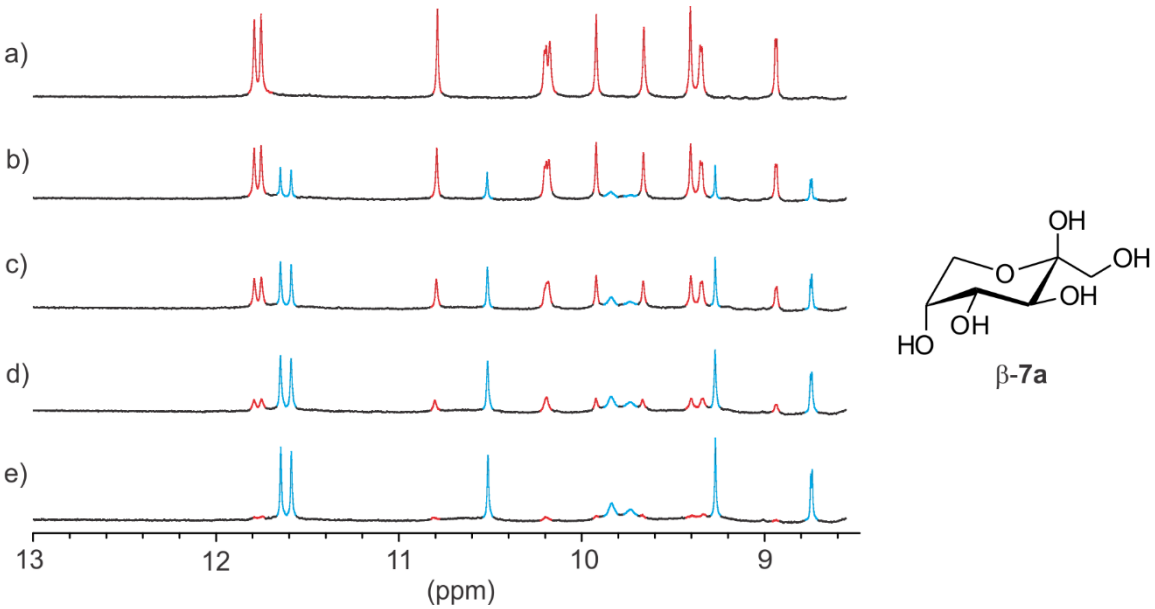

Supplementary Figure S19. Part of the ^{1}H NMR spectrum (800 MHz) at 298K of capsule **2** (0.4 mM) in $CDCl_3$/d_6-DMSO (80:20) in the presence of: (a) 0 equiv.; (b) 0.25 equiv.; (c) 0.75 equiv.; (d) 1.25 equiv.; (e) 3 equiv. of *D*-fructose **7**. Signals of the empty host and of the host–guest complex (**2**⊃β-*D*-fructopyranose) peaks are marked with red and blue colors, respectively. *K*a = 13600 L mol^{-1}.

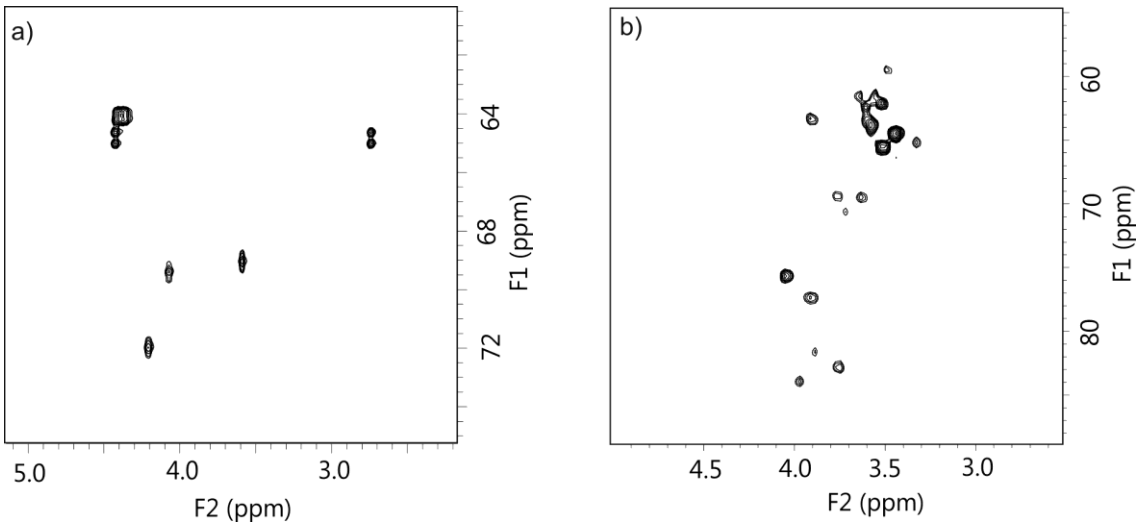

Supplementary Figure S20. (a) Part of the ^{1}H-^{13}C HSQC NMR spectrum (700 MHz) at 298K of capsule **2** (1 mM) in $CDCl_3$/d_3-MeOH (95:5) in the presence of 1 equiv. of *D*-[$^{13}C_6$]fructose **7**. (b) As a reference, part of the ^{1}H-^{13}C HSQC NMR spectrum (700 MHz) at 298K of *D*-[$^{13}C_6$]fructose (2 mM) alone in $CDCl_3$/d_6-DMSO (80:20) after 12 hours of incubation. β-**7a**: 28%; α-**7a**: 5%; β-**7b**: 51%; α-**7b**: 16%. The assignment of the ^{13}C signals to the corresponding carbohydrate tautomer was based on dihedral angle values between CH and OH groups derived from J3-coupling constants, on bidimensionnal NMR experiments (COSY, TOCSY, HSQC), and on comparisons with literature data about assignments in other solvents

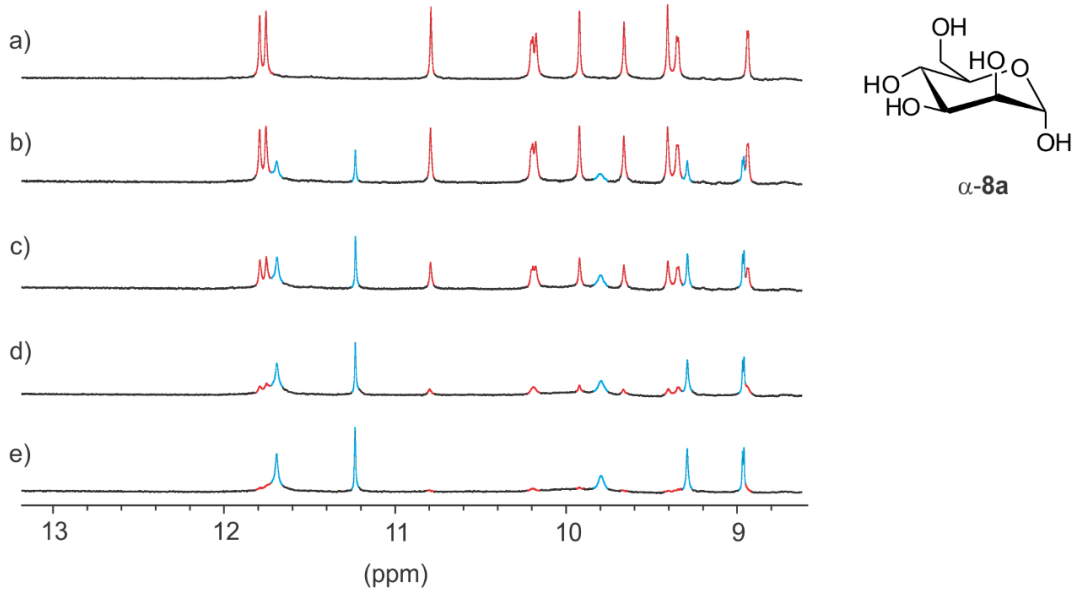

Supplementary Figure S21. Part of the ^{1}H NMR spectrum (800 MHz) at 298K of capsule **2** (0.5 mM) in $CDCl_3$/d6-DMSO (80:20) in the presence of: (a) 0 equiv.; (b) 0.25 equiv.; (c) 0.5 equiv.; (d) 1 equiv.; (e) 2.5 equiv. of *D*-mannose **8**. Signals of the empty host and of the host–guest complex (**2**⊃α-*D*-mannopyranose) peaks are marked with red and blue colors, respectively. *K*a = 28500 L mol^{-1}.

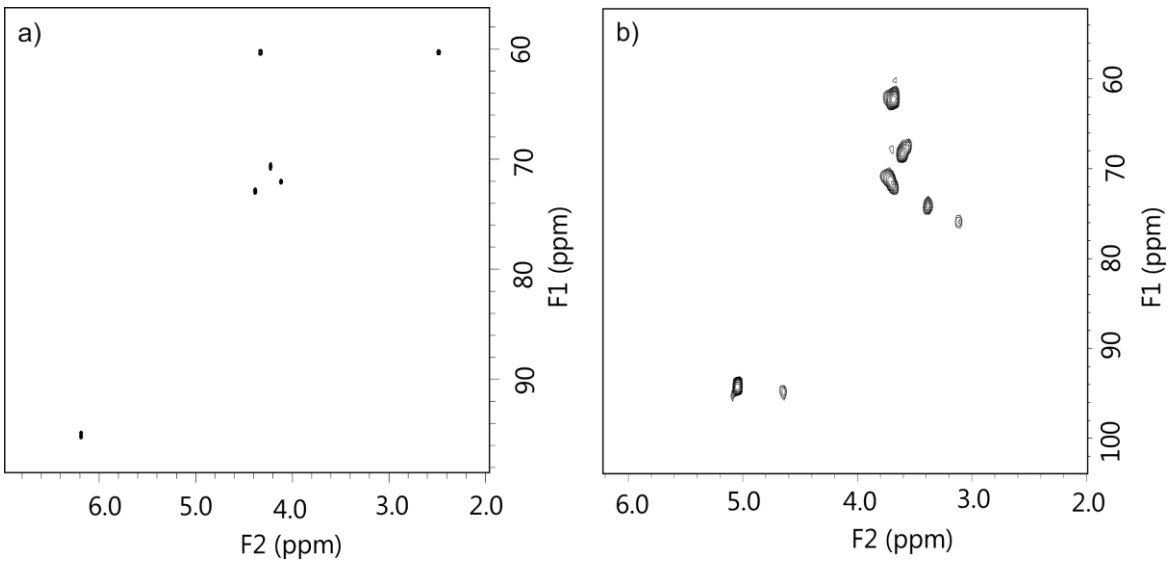

Supplementary Figure S22. (a) Part of the ^{1}H-^{13}C HSQC NMR spectrum (700 MHz) at 298K of capsule **2** (1 mM) in $CDCl_3$/d_3-MeOH (95:5) in the presence of 1 equiv. of *D*-[$^{13}C_6$]mannose **8**. (b) As a reference, part of the ^{1}H-^{13}C HSQC NMR spectrum (700 MHz) at 298K of *D*-[$^{13}C_6$]mannose **8** (2 mM) alone in $CDCl_3$/d_6-DMSO (80:20) after 12 hours of incubation. β-**8a**: 3%; α-**8a**: 97%. The assignment of the ^{13}C signals to the corresponding carbohydrate tautomer was based on dihedral angle values between CH and OH groups derived from ^{3}J-coupling constants, on bidimensionnal NMR experiments (COSY, TOCSY, HSQC), and on comparisons with literature data about assignments in other solvents.

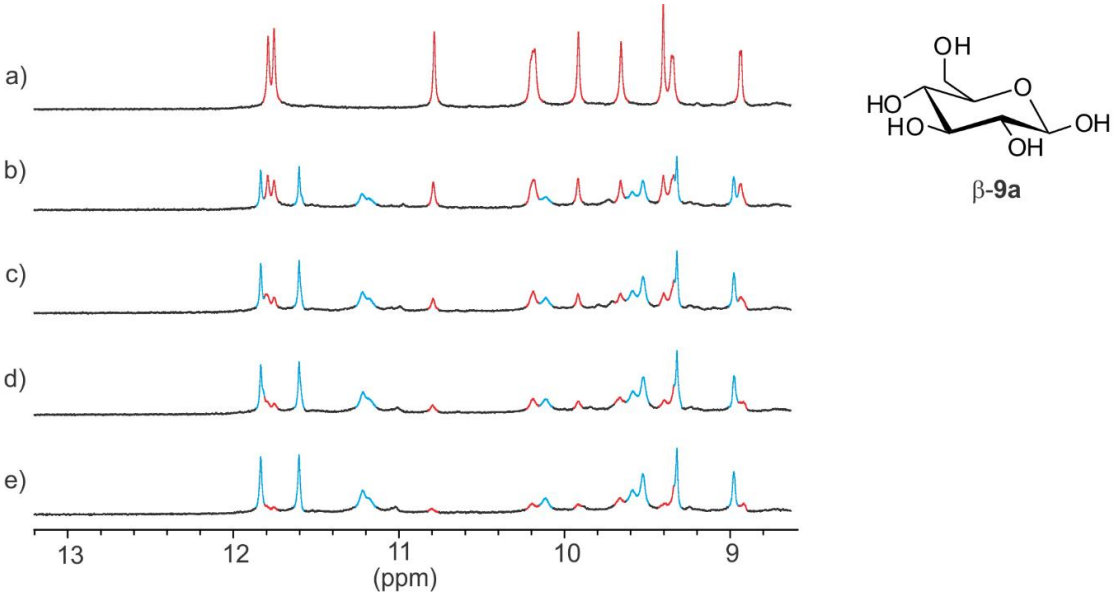

Supplementary Figure S23. Part of the ^{1}H NMR spectrum (800 MHz) at 298K of capsule **2** (0.5 mM) in $CDCl_3$/d6-DMSO (80:20) in the presence of: (a) 0 equiv.; (b) 1 equiv.; (c) 2 equiv.; (d) 3 equiv.; (e) 5 equiv. of *D*-glucose. Signals of the empty host and of the host–guest complex (**2**⊃β-*D*-glucopyranose and **2**⊃α-*D*-glucopyranose) peaks are marked with red and blue colors, respectively. *K*a = 3900 L mol^{-1}.

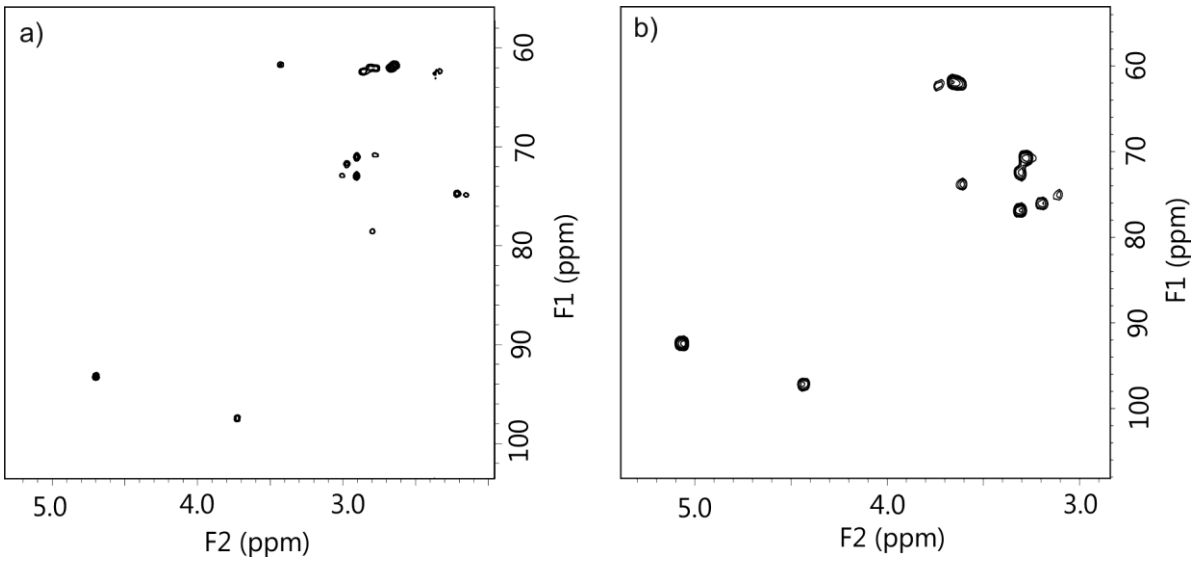

Supplementary Figure S24. (a) Part of the ^{1}H-^{13}C HSQC NMR spectrum (700 MHz) at 298K of capsule **2** (1 mM) in $CDCl_3$/d_3-MeOH (95:5) in the presence of 1 equiv. of *D*-[$^{13}C_6$]glucose **9**. (b) As a reference, part of the ^{1}H-^{13}C HSQC NMR spectrum (700 MHz) at 298K of *D*-[$^{13}C_6$]glucose **9** (2 mM) alone in $CDCl_3$/d_6-DMSO (80:20) after 12 hours of incubation. β-**9a**: 3%; α-**9a**: 97%. The assignment of the ^{13}C signals to the corresponding carbohydrate tautomer was based on dihedral angle values between CH and OH groups derived from ^{3}J-coupling constants, on bidimensionnal NMR experiments (COSY, TOCSY, HSQC), and on comparisons with literature data about assignments in other solvents.

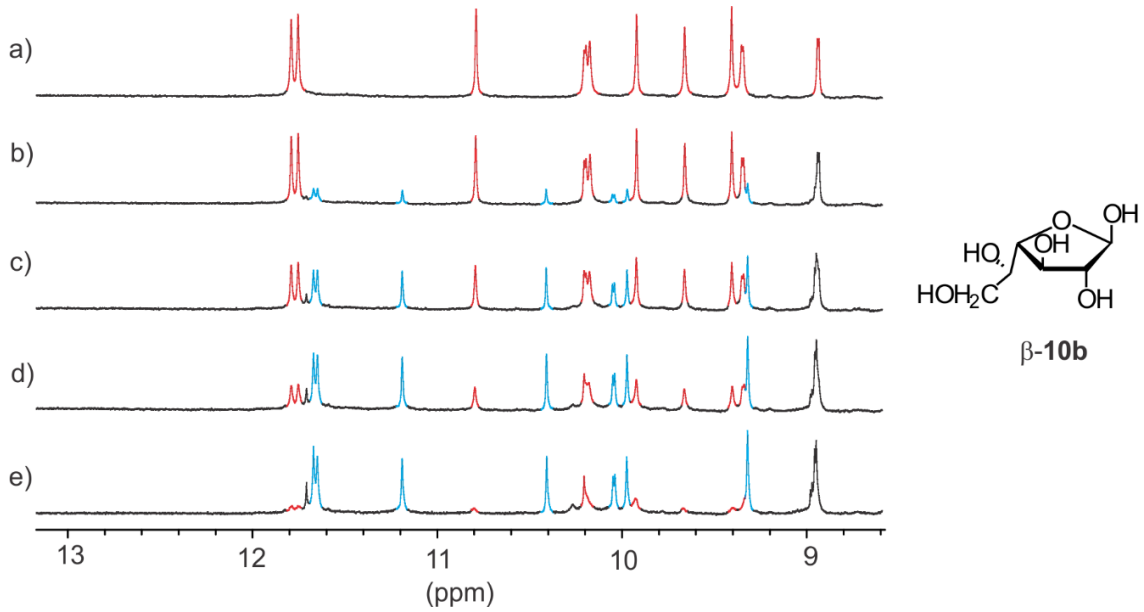

Supplementary Figure S25. Part of the ^{1}H NMR spectrum (800 MHz) at 298K of capsule **2** (0.5 mM) in $CDCl_3$/d6-DMSO (80:20) in the presence of: (a) 0 equiv.; (b) 0.25 equiv.; (c) 0.75 equiv.; (d) 1.5 equiv.; (e) 5 equiv. of *D*-galactose. Signals of the empty host and of the host–guest complex (**2**⊃β-*D*-galactofuranose) peaks are marked with red and blue colors, respectively. *K*a = 3150 L mol^{-1}.

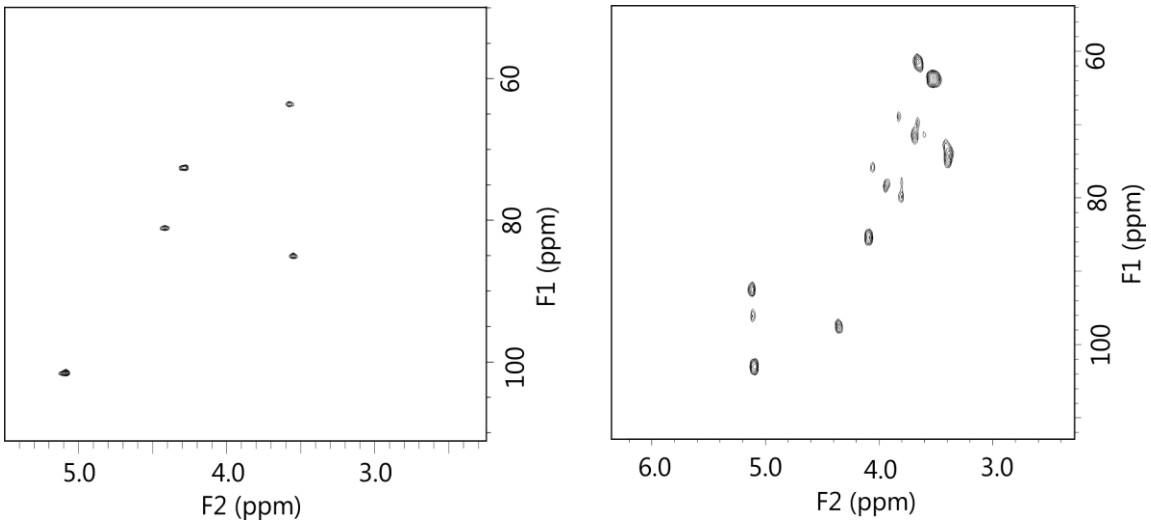

Supplementary Figure S26. (a) Part of the ^{1}H-^{13}C HSQC NMR spectrum (700 MHz) at 298K of capsule **2** (1 mM) in $CDCl_3$/d_6-DMSO (95:5) in the presence of 1 equiv. of *D*-[$^{13}C_6$]galactose **10**. (b) As a reference, part of the ^{1}H-^{13}C HSQC NMR spectrum (700 MHz) at 298K of *D*-[$^{13}C_6$]galactose (2 mM) alone in $CDCl_3$/d_6-DMSO (80:20) after 12 hours of incubation. β-**10a**: 23%; α-**10a**: 11%; β-**10b**: 41%; α-**10b**: 25%. The assignment of the ^{13}C signals to the corresponding carbohydrate tautomer was based on dihedral angle values between CH and OH groups derived from ^{3}J-coupling constants, on bidimensionnal NMR experiments (COSY, TOCSY, HSQC), and on comparisons with literature data about assignments in other solvents.

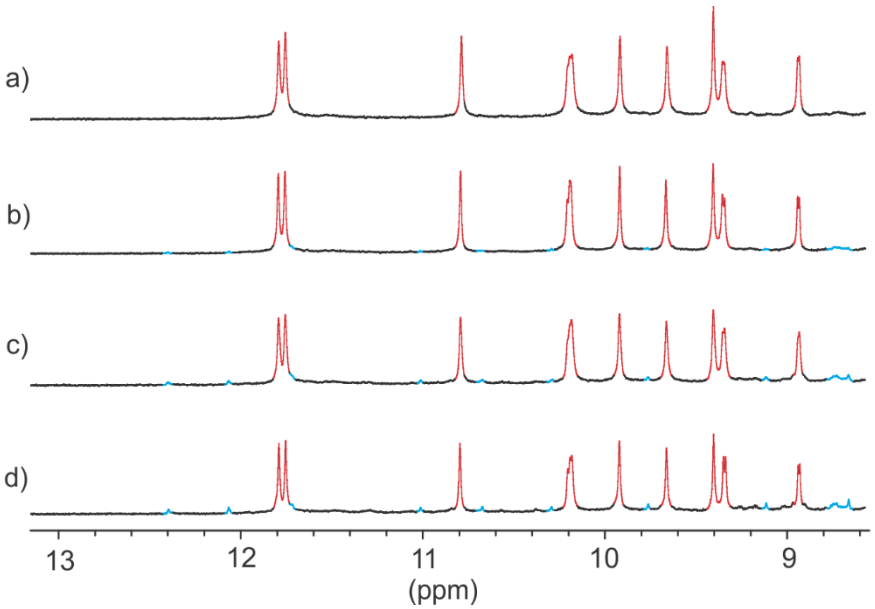

Supplementary Figure S27. Part of the ^{1}H NMR spectrum (800 MHz) at 298K of capsule **2** (0.5 mM) in $CDCl_3$/d6-DMSO (80:20) in the presence of: (a) 0 equiv.; (b) 2 equiv.; (c) 12 equiv.; (d) 24 equiv. of *D*-*N*-acetylglucosamine **11**. Signals of the empty host and of the host–guest complex (**2**⊃β-*D*-*N*-acetylglucosamine) peaks are marked with red and blue colors, respectively. *K*a < 10 L mol^{-1}.

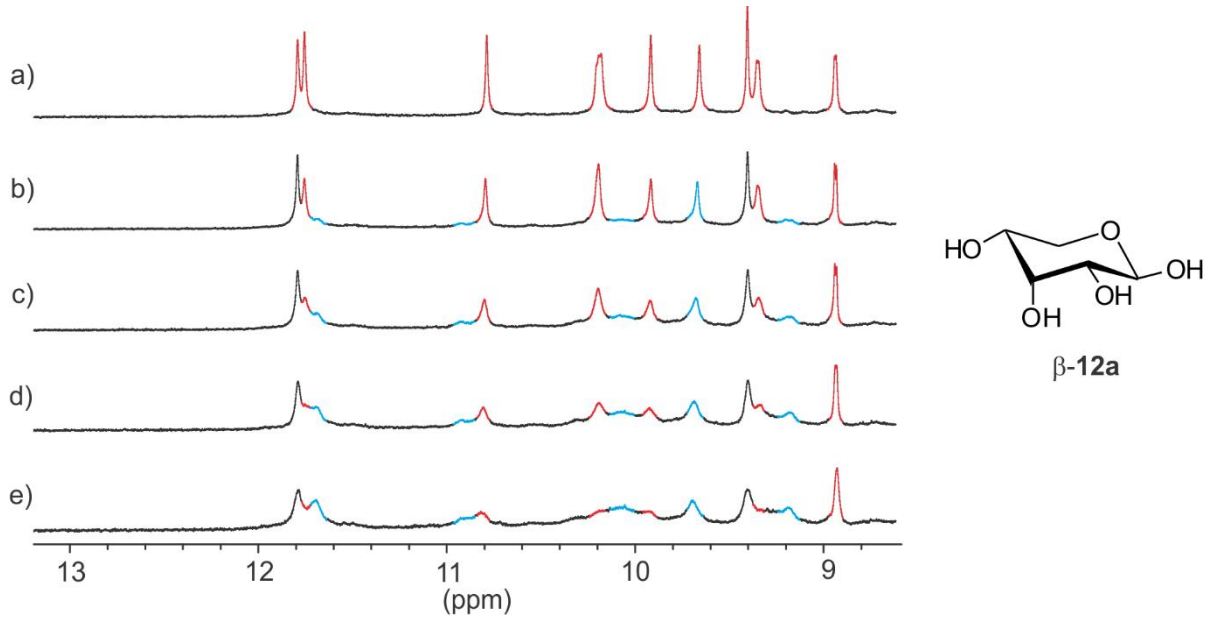

Supplementary Figure S28. Part of the ^{1}H NMR spectrum (800 MHz) at 298K of capsule **2** (0.5 mM) in $CDCl_3/d_6$-DMSO (80:20) in the presence of: (a) 0 equiv.; (b) 2 equiv.; (c) 6 equiv.; (d) 12 equiv.; (e) 24 equiv. of *D*-ribose. Signals of the empty host and of the host–guest complex peaks are marked with red and blue colors, respectively. *K*a ~ L mol^{-1}.

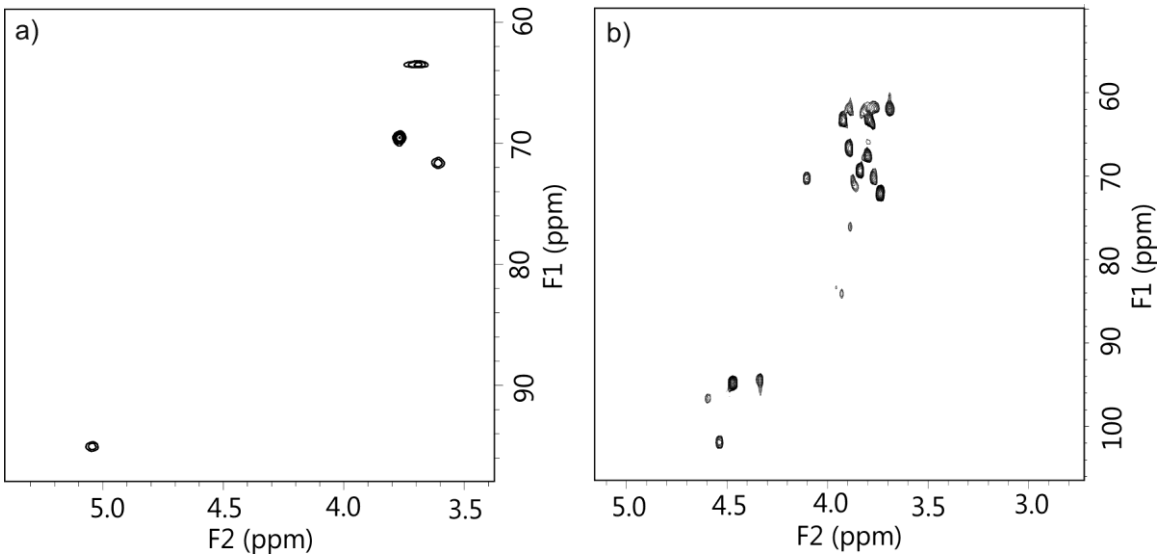

Supplementary Figure S29. (a) Part of the ^{1}H-^{13}C HSQC NMR spectrum (700 MHz) at 298K of capsule **2** (1 mM) in $CDCl_3/d_6$-DMSO (95:5) in the presence of 1 equiv. of *D*-[$^{13}C_5$]ribose **12**. (b) As a reference, part of the ^{1}H-^{13}C HSQC NMR spectrum (700 MHz) at 298K of *D*-[$^{13}C_5$]ribose **12** (2 mM) alone in $CDCl_3/d_6$-DMSO (80:20) after 12 hours of incubation. β-**12a**: 77%; α-**12a**: 8%; β-**12b**: 12%; α-**12b**: 3%. The assignment of the ^{13}C signals to the corresponding carbohydrate tautomer was based on dihedral angle values between CH and OH groups derived from ^{3}J-coupling constants, on bidimensionnal NMR experiments (COSY, TOCSY, HSQC), and on comparisons with literature data about assignments in other solvents.

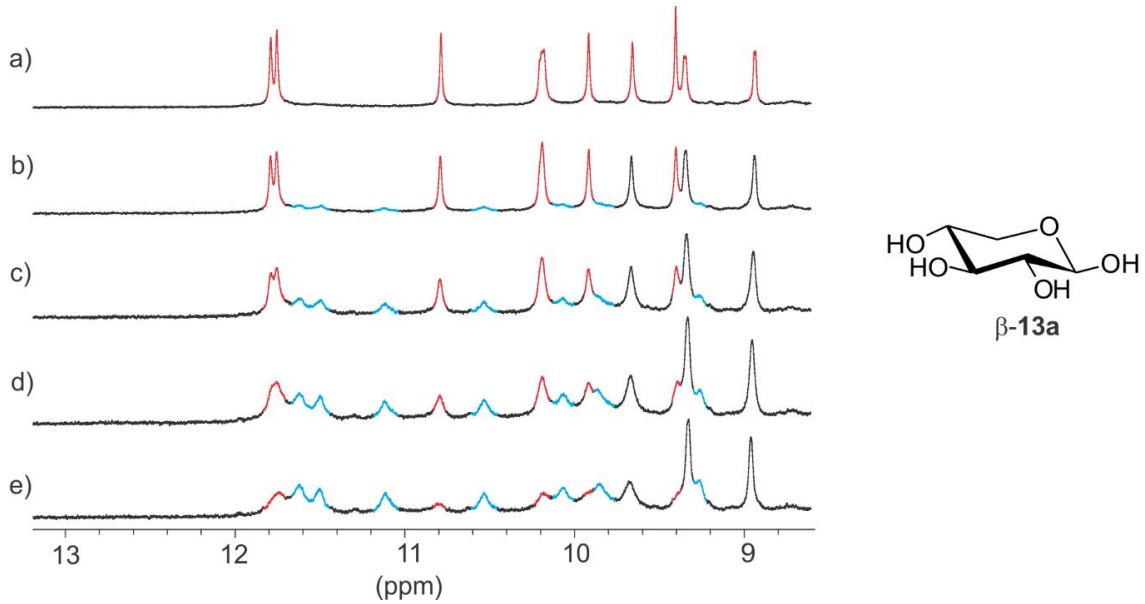

Supplementary Figure S30. Part of the ^{1}H NMR spectrum (800 MHz) at 298K of capsule **2** (0.5 mM) in $CDCl_3$/d_6-DMSO (80:20) in the presence of: (a) 0 equiv.; (b) 2 equiv.; (c) 6 equiv.; (d) 12 equiv.; (e) 24 equiv. of *D*-xylose. Signals of the empty host and of the host–guest complex (**2**⊃β-*D*-xylopyranose) peaks are marked with red and blue colors, respectively. *K*a = 300 L mol^{-1}.

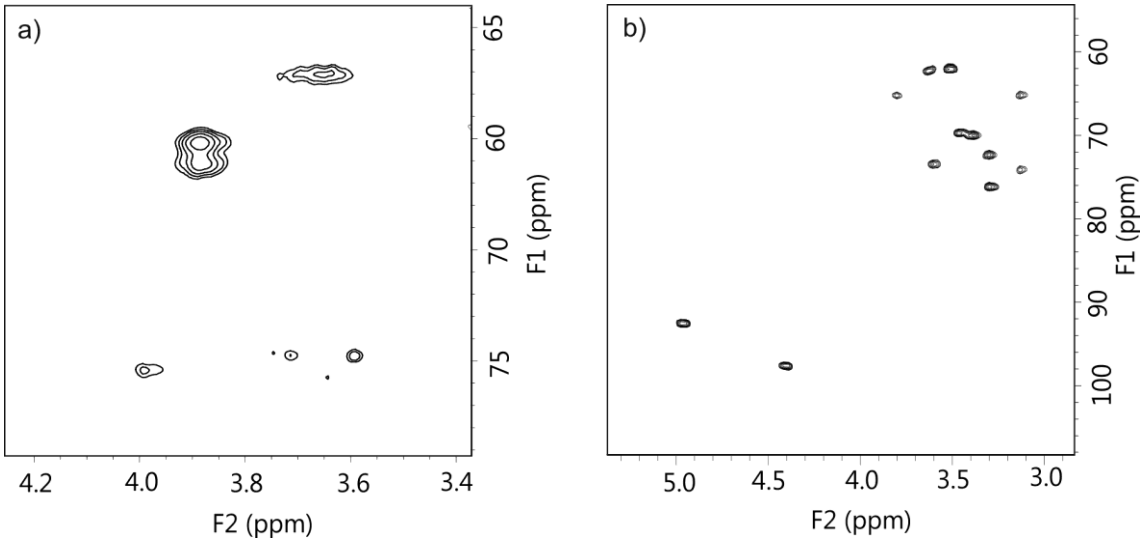

Supplementary Figure S31. (a) Part of the ^{1}H-^{13}C HSQC NMR spectrum (700 MHz) at 298K of capsule **2** (1 mM) in $CDCl_3$/d_6-DMSO (95:5) in the presence of 1 equiv. of *D*-[$^{13}C_5$]xylose **13**. (b) As a reference, part of the ^{1}H-^{13}C HSQC NMR spectrum (700 MHz) at 298K of *D*-[$^{13}C_5$]xylose **13** (2 mM) alone in $CDCl_3$/d_6-DMSO (80:20) after 12 hours of incubation. β-**13a**: 43%; α-**13a**: 57%. The assignment of the 13C signals to the corresponding carbohydrate tautomer was based on dihedral angle values between CH and OH groups derived from ^{3}J-coupling constants, on bidimensionnal NMR experiments (COSY, TOCSY, HSQC), and on comparisons with literature data about assignments in other solvents.

Titrations with capsule **4**

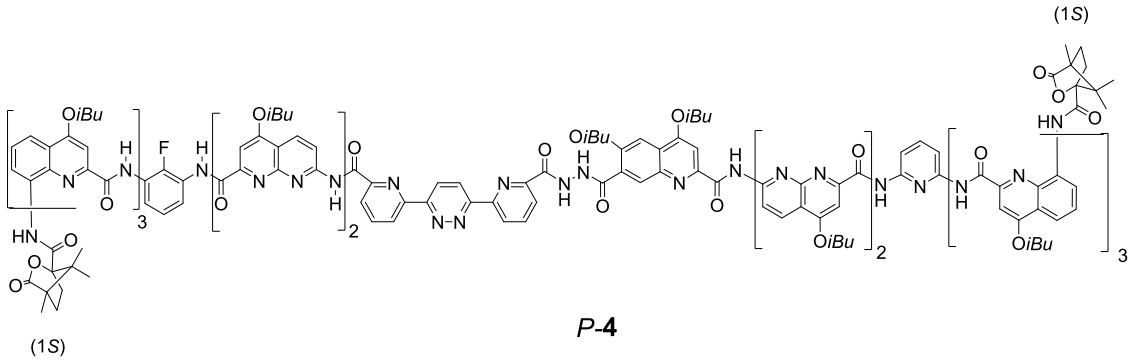

P-**4**

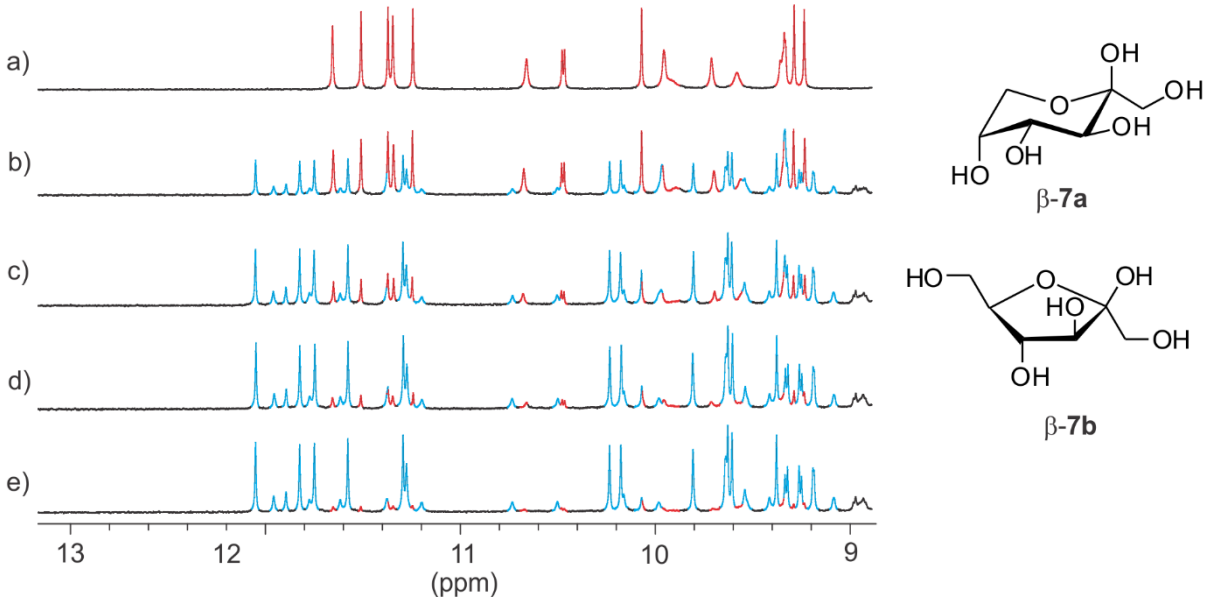

Supplementary Figure S32. Part of the ^{1}H NMR spectrum (800 MHz) at 298K of capsule **4** (0.5 mM) in $CDCl_3$/d_6-DMSO (80:20) in the presence of: (a) 0 equiv.; (b) 0.5 equiv.; (c) 1 equiv.; (d) 3 equiv.; (e) 5 equiv. of *D*-fructose. Signals of the empty host and of the host–guest complex (**4**⊃β-*D*-fructopyranose; **4**⊃β-*D*-fructofuranose) peaks are marked with red and blue colors, respectively. *K*a = 33000 L mol^{-1}.

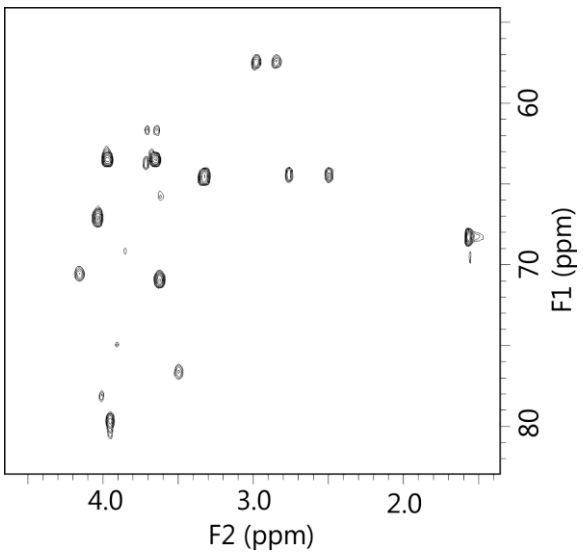

Supplementary Figure S33. Part of the ^{1}H-^{13}C HSQC NMR spectrum (700 MHz) at 298K of capsule **4** (1 mM) in $CDCl_3$/d_6-DMSO (95:5) in the presence of 1 equiv. of *D*-[$^{13}C_6$]fructose **7**. The assignment of the 13C signals to the corresponding carbohydrate tautomer was based on dihedral angle values between CH and OH groups derived from ^{3}J-coupling constants, on bidimensionnal NMR experiments (COSY, TOCSY, HSQC), and on comparisons with literature data about assignments in other solvents.

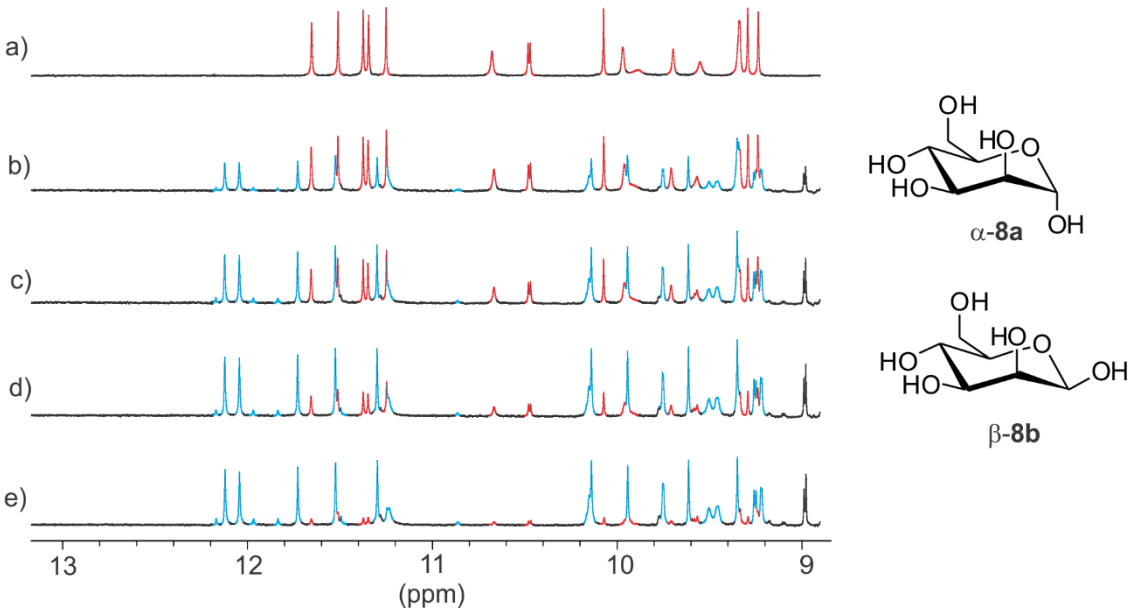

Supplementary Figure S34. Part of the ^{1}H NMR spectrum (800 MHz) at 298K of capsule **4** (0.5 mM) in $CDCl_3/d_6$-DMSO (80:20) in the presence of: (a) 0 equiv.; (b) 1 equiv.; (c) 2 equiv.; (d) 4 equiv.; (e) 12 equiv. of *D*-mannose. Signals of the empty host and of the host–guest complex (**4**⊃α-*D*-mannopyranose) peaks are marked with red and blue colors, respectively. *K*a = 1600 L mol^{-1}.

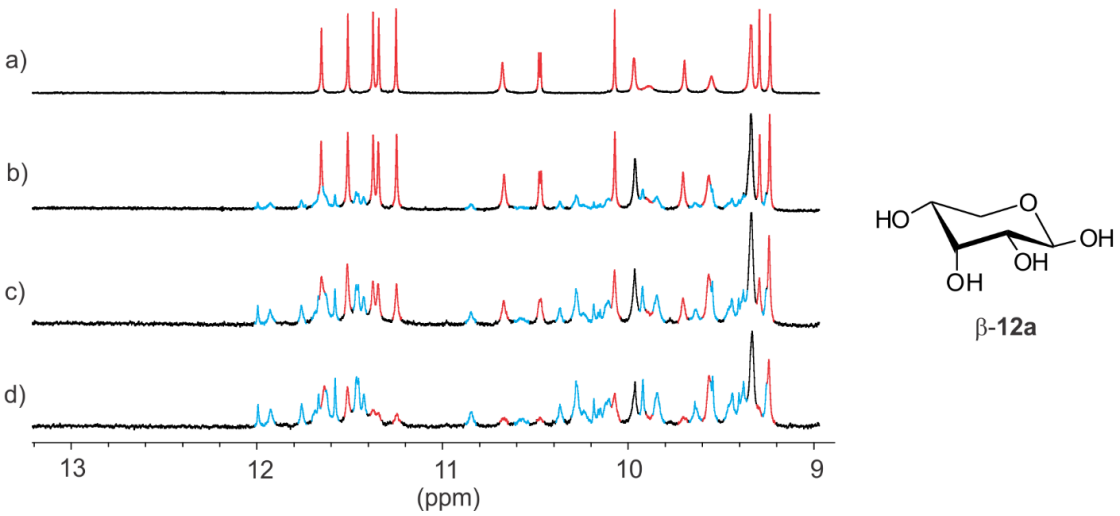

Supplementary Figure S35. Part of the ^{1}H NMR spectrum (800 MHz) at 298K of capsule **4** (0.5 mM) in $CDCl_3/d_6$-DMSO (80:20) in the presence of: (a) 0 equiv.; (b) 10 equiv.; (c) 30 equiv.; (d) 90 equiv. of *D*-ribose. Signals of the empty host and of the host–guest complex peaks are marked with red and blue colors, respectively. *K*a = 40 L mol^{-1}.

Titrations with capsule **6**

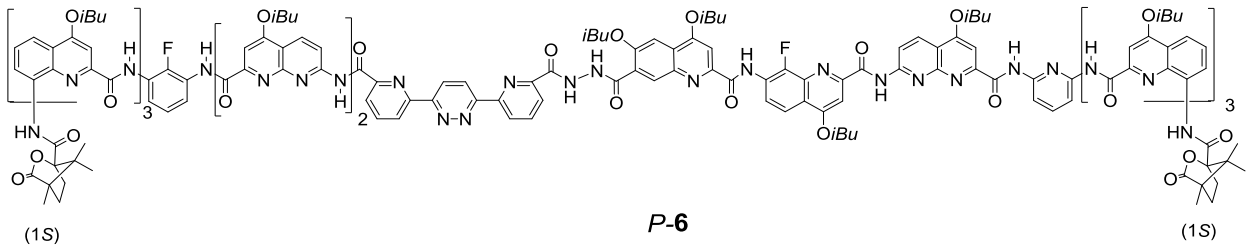

P-**6**

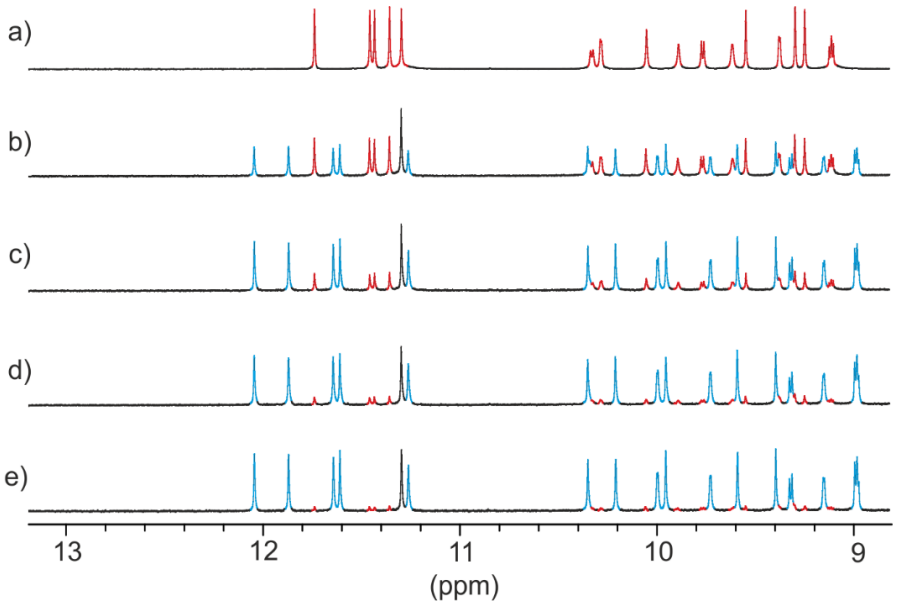

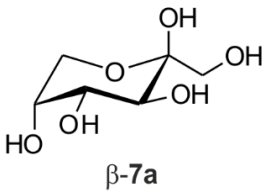

β-**7a**

Supplementary Figure S36. Part of the ^{1}H NMR spectrum (800 MHz) at 298K of capsule **6** (0.5 mM) in $CDCl_3/d_6$-DMSO (80:20) in the presence of: (a) 0 equiv.; (b) 0.5 equiv.; (c) 1 equiv.; (d) 1.5 equiv.; (e) 2.5 equiv. of *D*-fructose. Signals of the empty host and of the host–guest complex (**6**⊃β-*D*-fructopyranose) peaks are marked with red and blue colors, respectively. *K*a = 27500 L mol^{-1}.

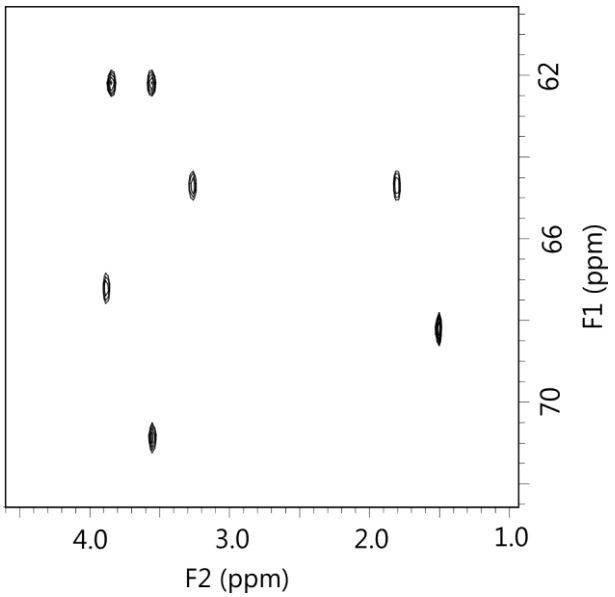

Supplementary Figure S37. Part of the ^{1}H-^{13}C HSQC NMR spectrum (700 MHz) at 298K of capsule **6** (1 mM) in $CDCl_3/d_6$-DMSO (95:5) in the presence of 1 equiv. of *D*-[$^{13}C_6$]fructose **7**. The assignment of the 13C signals to the corresponding carbohydrate tautomer was based on dihedral angle values between CH and OH groups derived from ^{3}J-coupling constants, on bidimensionnal NMR experiments (COSY, TOCSY, HSQC), and on comparisons with literature data about assignments in other solvents.

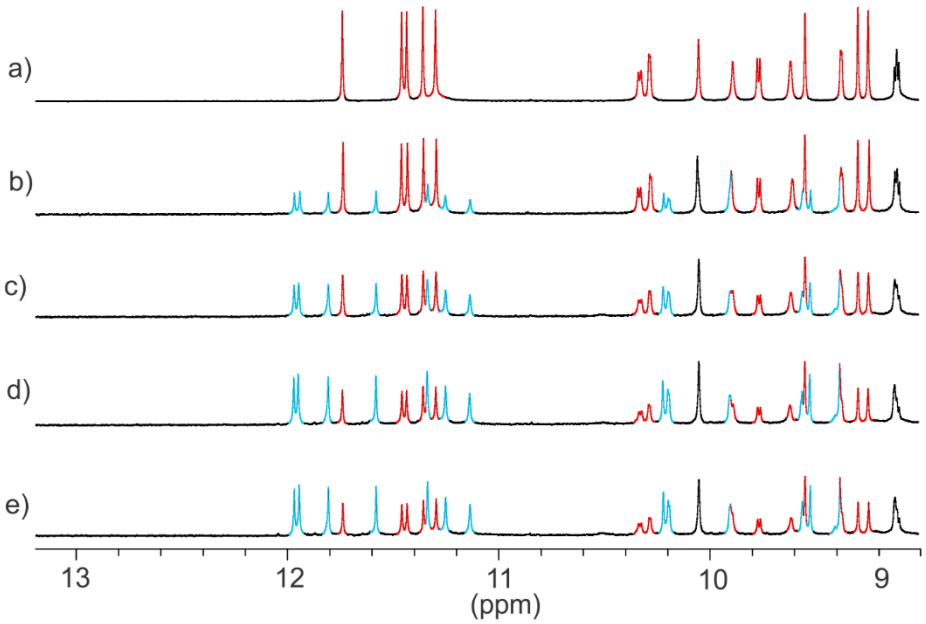

Supplementary Figure S38. Part of the ^{1}H NMR spectrum (800 MHz) at 298K of capsule **6** (0.5 mM) in $CDCl_3$/d_6-DMSO (80:20) in the presence of: (a) 0 equiv.; (b) 5 equiv.; (c) 10 equiv.; (d) 15 equiv.; (e) 20 equiv. of *D*-mannose **8**. Signals of the empty host and of the host–guest complex (**6**⊃α-*D*-mannopyranose) peaks are marked with red and blue colors, respectively. *K*a = 150 L mol^{-1}.

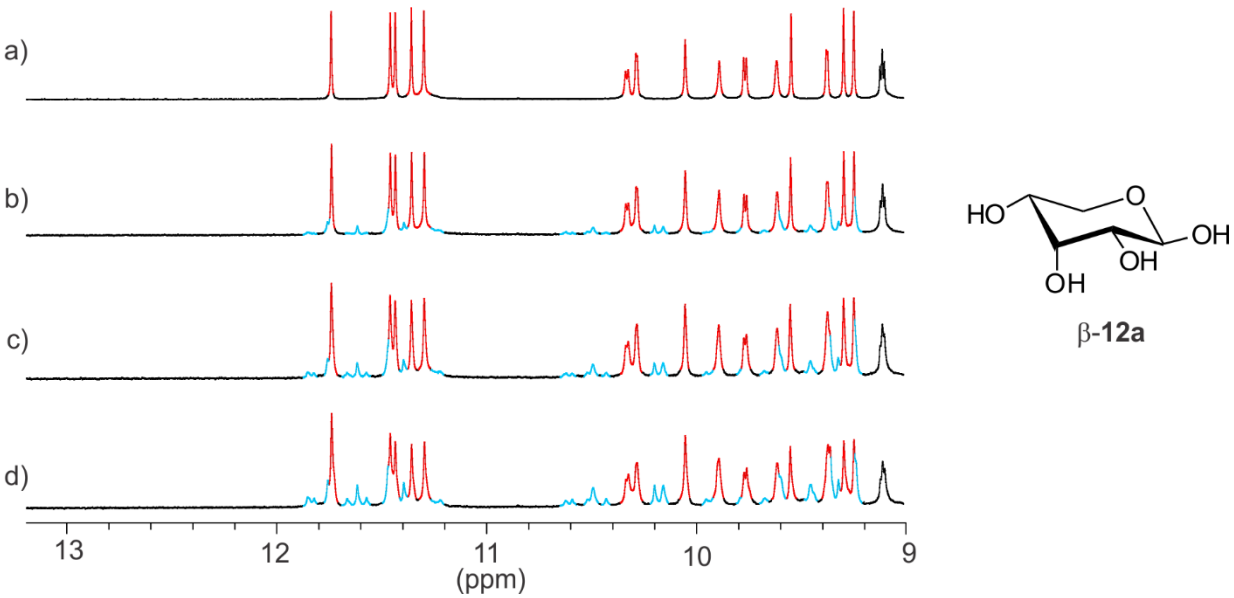

Supplementary Figure S39. Part of the ^{1}H NMR spectrum (800 MHz) at 298K of capsule **6** (0.5 mM) in $CDCl_3$/d_6-DMSO (80:20) in the presence of: (a) 0 equiv.; (b) 10 equiv.; (c) 30 equiv.; (d) 90 equiv. of *D*-ribose **12**. Signals of the empty host and of the host–guest complex peaks are marked with red and blue color, respectively. *K*a = 30 L mol^{-1}.

4.4 Determination of d.e. values, time and temperature dependence of NMR spectra

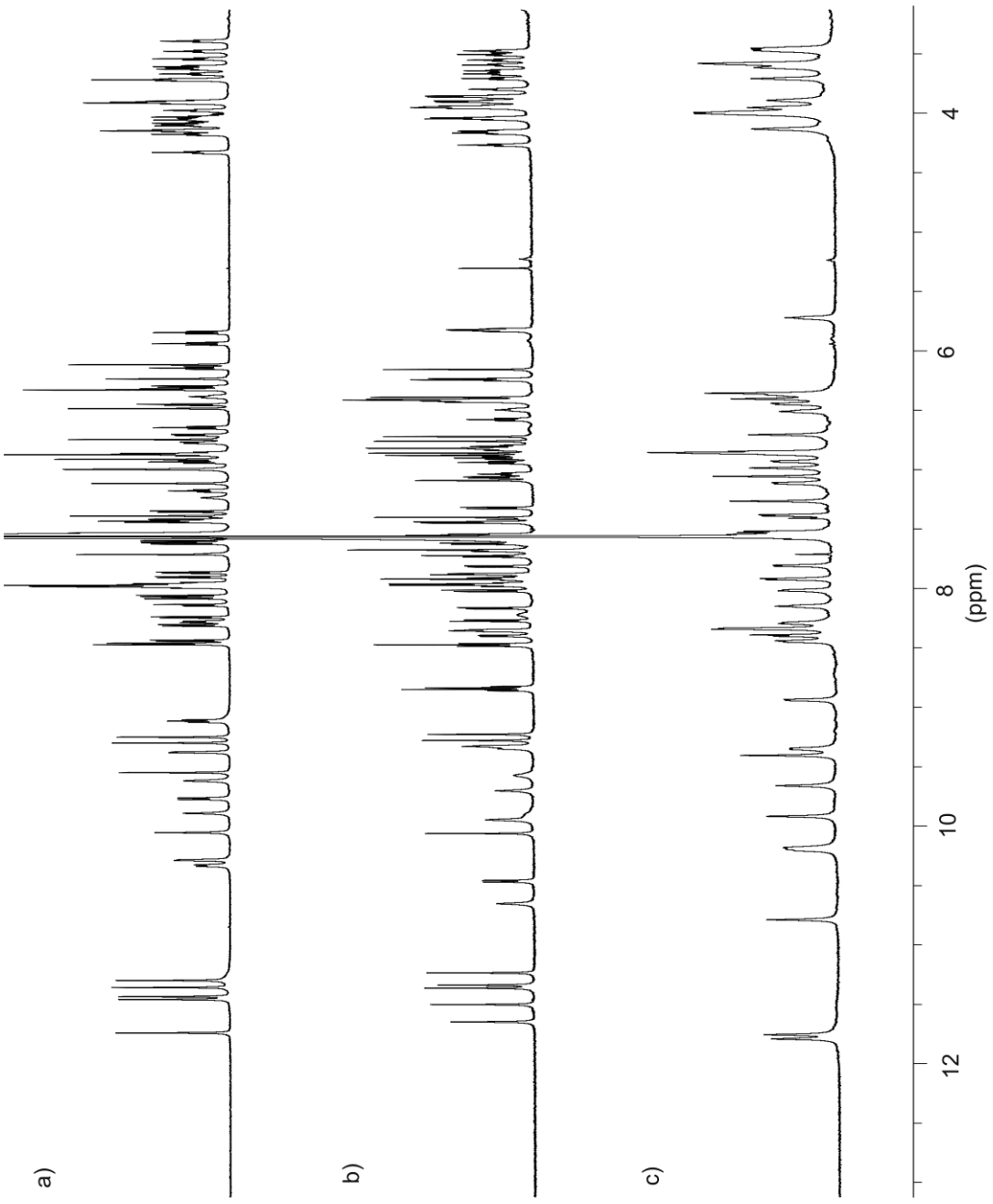

Supplementary Figure S40. ^{1}H NMR spectra in $CDCl_3/d_6$-DMSO (80:20) at 700 MHz of: (a) capsule **6**; (b) capsule **4** and (c) capsule **2**. The number of aromatic amide signals (12 – 8.5 ppm) denotes the symmetry of the receptor. In (c) the C_2 symmetrical receptor **2** displays 8 aromatic amide peaks (+ 1 extra signal for the aliphatic-aromatic amide of the chiral camphanamide) whereas (b) and (c) which lack any symmetry shows 14 amide signals (+ 2 signals for camphanamide).

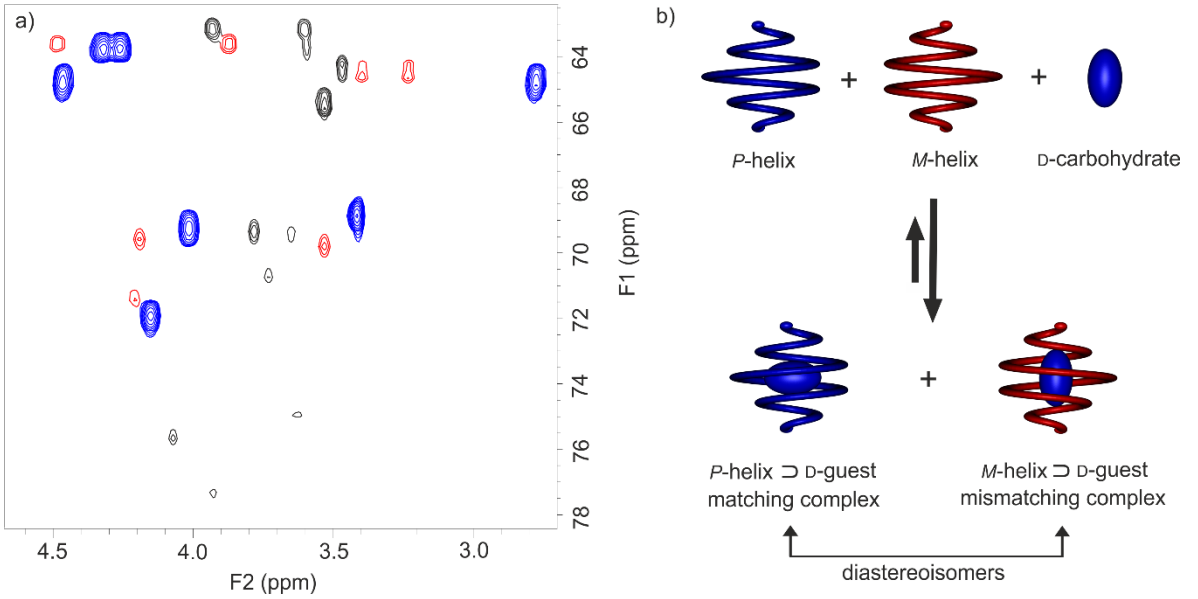

Supplementary Figure S41. Determination of d.e. (diastereomeric excess). a) Part of the ^{1}H-^{13}C HSQC NMR spectrum (700 MHz) at 298K of capsule **1** (4 mM) in $CDCl_3$/d_6-DMSO (80:20) in the presence of 1 equiv. of D-[$^{13}C_6$]fructose **7**. b) Equilibria involved in host-guest complex formation. NMR Signals of *P*-**1**⊃β-**7a** (matching complex), *M*-**1**⊃β-**7a** (mismatching complex) and free **7a** are denoted in blue, red and black, respectively. The assignment of the ^{13}C signals of the corresponding carbohydrate tautomer was based on dihedral angle values between CH and OH groups derived from ^{3}J-coupling constants, on bidimensionnal NMR experiments (COSY, TOCSY, HSQC), and on comparisons with literature data about assignments in other solvents. The assignment of *P* helix handedness to the major species (*P*-**1**⊃β-**7a**) was inferred from the sign of the CD band at 360 nm (see Figure S2) and crystallographic studies (Figure S52). The assignment of *M* helix handedness to the minor species (*M*-**1**⊃β-**7a**), and not to a complex between *P*-**1** and another tautomer of **7a**, was confirmed by the fact that this species completely disappears when capsule **2** (which is exclusively *P*) and β-**7a** are mixed. The proportions between *P* and *M* helices as measured in the HSQC spectrum were used to calibrate the CD experiments performed under the same conditions (Fig. S2). The proportions between *P* and *M* helices for other host-guest complexes with **1** could thus be calculated directly from CD intensity. In the case of **7a**, the diastereomeric excess (*d.e.*) was calculated through the integration of the cross-peak volumes and was found to be 72%. The *d.e.* is described here as ([*P* complex] – [*M* complex]) / ([*P* complex] + [*M* complex]).

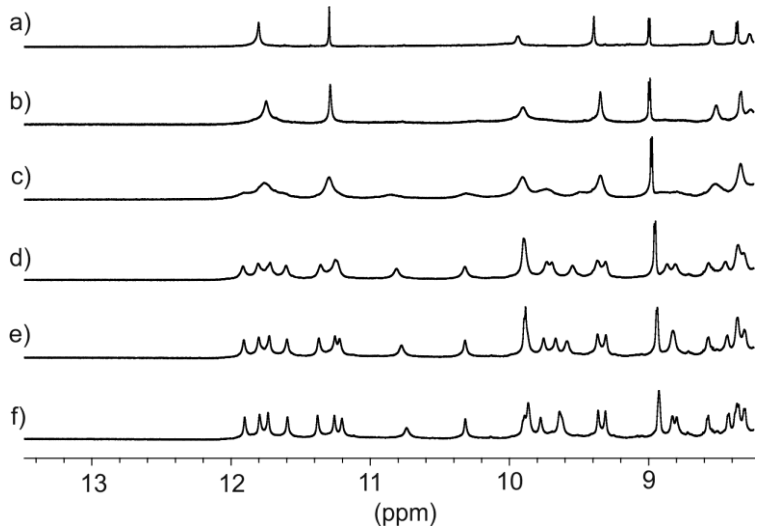

Supplementary Figure S42. ^{1}H NMR spectra (700 MHz) in $CDCl_3/CD_3OH$ (90/10) of **2**⊃α-**8a** recorded at: (a) 298K; (b) 283K; (c) 273K; (d) 263K; (e) 256K and (f) 250K. The multiplicity of signals are the same for **2**⊃α-**8a** as for the empty host **2** showing that the host-guest complex retains an average C_2 symmetry as the guest tumbles rapidly in the cavity at 298K. Upon cooling, signals of the host broaden and split into two sets when tumbling of the guest becomes slow in (f) at 250K.

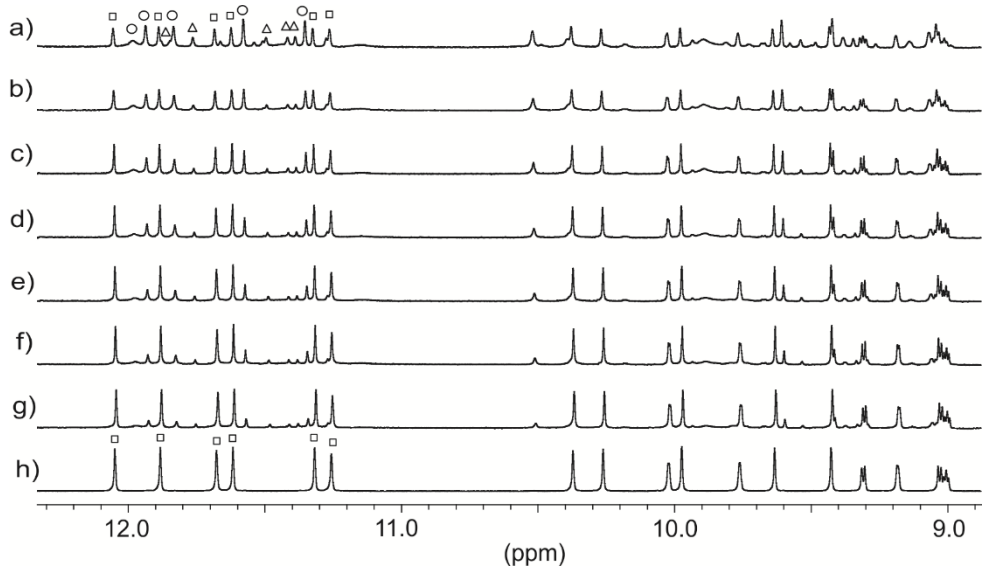

Supplementary Figure S43. ^{1}H NMR spectra (800 MHz, 313K) of **6** (1 mM) and **7** (1 mM) in $CDCl_3/d_6$-DMSO (95:5) at: (a) 5 min.; (b) 4.3 hours; (c) 7.5 hours, (d) 10.8 hours; (e) 14 hours; (f) 17 hours; (g) 22.3 hours; (h) 72 hours after the addition of the sugar. The final spectrum (h) correspond to **6**⊃β–**7a.** Signals of **6**⊃β–**7a** are denoted with squares whereas those of the complexes of with fructofuranose anomers **6**⊃**7b** are denoted with circles and triangles. The acquired spectra revealed the expected coexistence of the three major tautomers in the cavity (β-**7a**; β-**7b**; α-**7b**) 5 minutes after the addition of fructose (a). Upon equilibrating over three days (h) only one tautomer remains in the cavity β-**7a**.

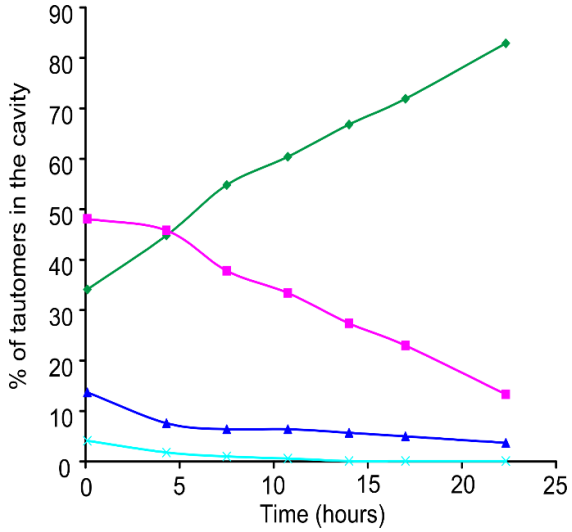

Supplementary Figure S44. . Time trace of the isomerisation *D*-fructose in capsule **6** ([**6**⊃**7**] = 1 mM) in $CDCl_3$/d_6-DMSO (95:5) monitored by ^{1}H NMR at 313K. β-*D*-fructopyranose β–**7a**, α-*D*-fructopyranose α–**7a**, β-*D*-fructofuranose β–**7b** and α–*D*-fructofuranose α–**7b** are denoted in green, light blue, magenta and blue, respectively.

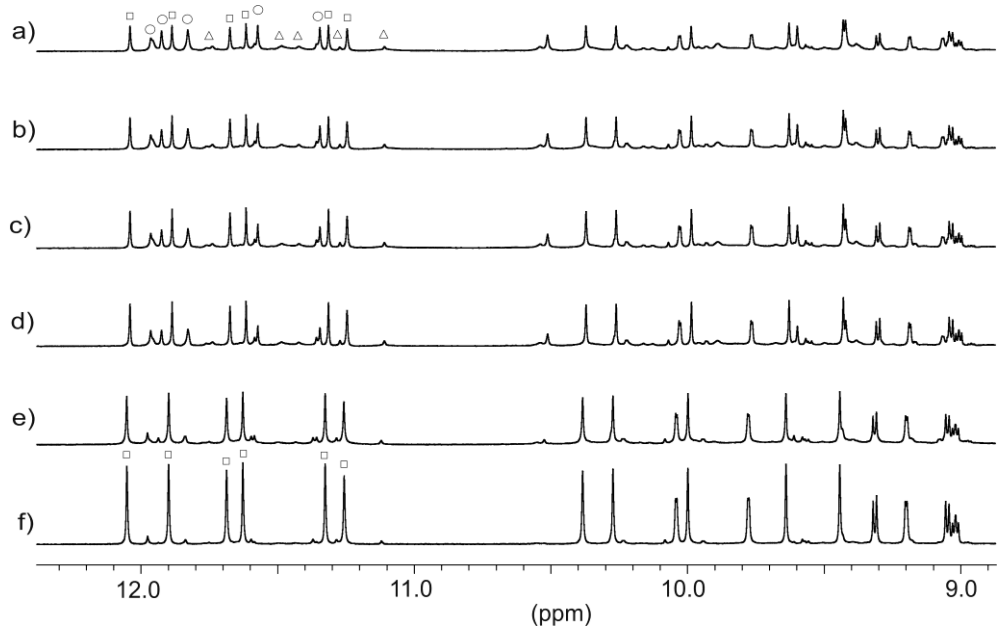

Supplementary Figure S45. ^{1}H NMR spectra (700 MHz, 318K) of **6** (1 mM) and a mixture of sugars **7**, **8**, **9**, **10**, **12** and **13** (1 mM each) in $CDCl_3$/d_6-DMSO (95:5) at: (a) 15 min.; (b) 45 min.; (c) 75 min., (d) 105 min.; (e) 5 hours; (f) 23 hours after the addition of the sugars. The final spectrum (f) correspond almost exclusively to **6**⊃β–**7a.** Signals of **6**⊃β–**7a** are denoted with squares whereas those of the complexes of with fructofuranose anomers **6**⊃**7b** are denoted with circles and triangles, respectively.

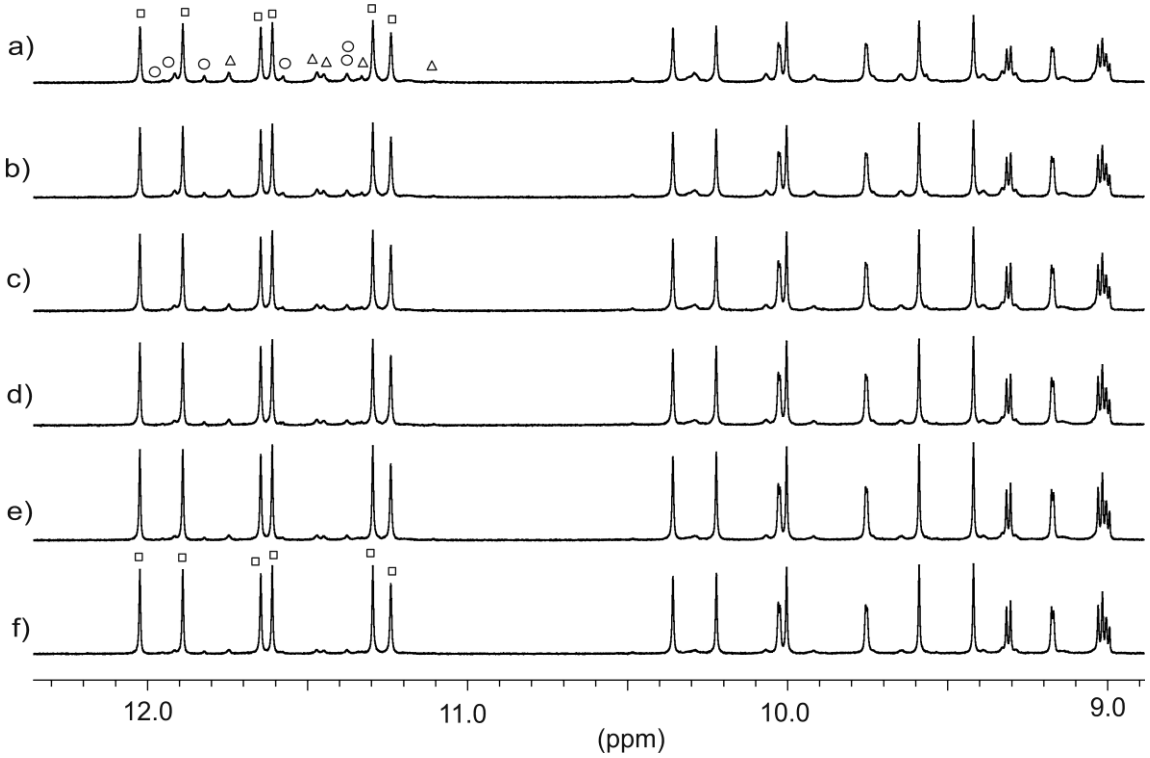

Supplementary Figure S46. ^{1}H NMR spectra (700 MHz, 318K) of **6** (1 mM) and a mixture of sugars **7**, **8**, **9**, **10**, **12** and **13** (3 mM each) in $CDCl_3/d_6$-DMSO (95:5): (a) 15 min.; (b) 45 min.; (c) 75 min., (d) 105 min.; (e) 3 hours; (f) 4 hours after the addition of the sugars. The final spectrum (f) correspond almost exclusively to **6**⊃β–**7a.** Signals of **6**⊃β–**7a** are denoted with squares whereas those of the complexes of with fructofuranose anomers **6**⊃**7b** are denoted with circles and triangles, respectively. The faster equilibration time is due to the higher concentration used in this experiment.

5. NMR structure assignment

5.1 Labelling of complex **6** ($Q_3PNQ^FHpyr\text{-}pyz\text{-}pyr\text{-}N_2FQ_3$)⊃**7a** (β-*D*-fructopyranose)

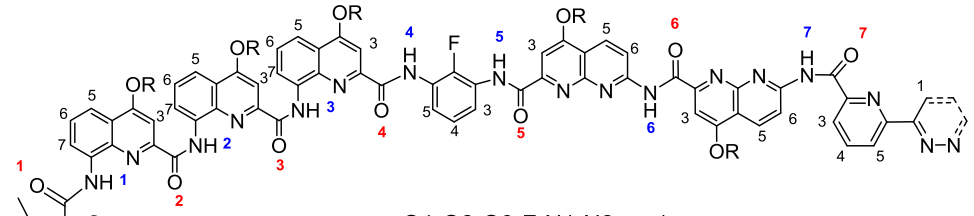

Q1-Q2-Q3-F-N1-N2-pyr1-pyz---

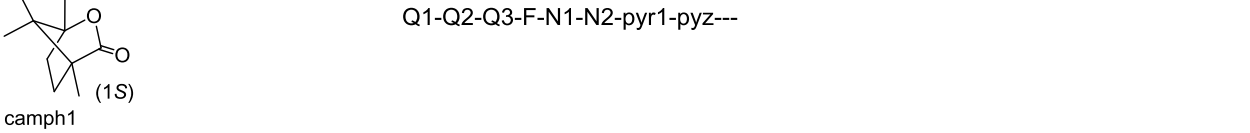

camph1

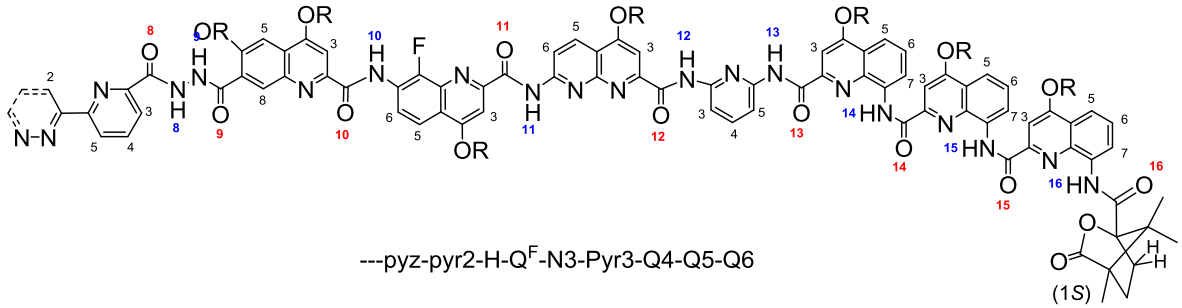

---pyz-pyr2-H-Q^F-N3-Pyr3-Q4-Q5-Q6

camph2

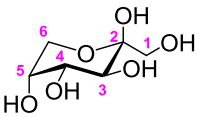

7a (β-D-fructopyranose)

Supplementary Table S2. Full assignment of the ^{1}H chemical shifts of **6⊃7a** (β-*D*-fructopyranose) in $CDCl_3$/d_6-DMSO (95:5) at 298K (800MHz). The five side chain resonances (*H*-C, two diastereotopic H_2-C, and two methyl H_3) are listed in order for each capsule monomer.

	^{1}H (ppm)		^{1}H (ppm)		^{1}H (ppm)
Q1-H7	8.08	**N3-H3**	7.70	**camph1**	1.44
Q1-H6	6.77	**N3-H5**	8.57	**camph1**	1.71
Q1-H5	7.59	**N3-H6**	8.66	**camph2**	1.30
Q1-H3	6.73	**Pyr3-H3**	6.89	**camph2**	1.58
Q2-H7	7.92	**Pyr3-H4**	6.41	**fruHO-1**	5.62
Q2-H6	5.82	**Pyr3-H5**	6.50	**fruHO-2**	5.10
Q2-H5	6.46	**Q4-H7**	7.54	**fruHO-3**	4.47
Q2-H3	7.16	**Q4-H6**	6.89	**fruHO-4**	5.07
Q3-H7	7.51	**Q4-H5**	7.53	**fruHO-5**	4.18
Q3-H6	6.92	**Q4-H3**	5.91	**fruH1a**	3.29
Q3-H5	7.62	**Q5-H7**	7.86	**fruH1b**	1.82
Q3-H3	5.97	**Q5-H6**	5.74	**fruH3**	3.90
F-H5	7.41	**Q5-H5**	6.84	**fruH4**	3.57
F-H4	6.74	**Q5-H3**	7.09	**fruH5**	1.52
F-H3	7.38	**Q6-H7**	8.09	**fruH6a**	3.86
N1-H3	6.49	**Q6-H6**	6.67	**fruH6b**	3.56
N1-H5	7.90	**Q6-H5**	7.61	**C*H*-O*iBu* Q1**	2.22, 3.64, 3.90, 1.04, 1.04
N1-H6	7.33	**Q6-H3**	6.41	**C*H*-O*iBu* Q2**	1.25, 2.89, 2.98, 0.03, 0.44
N2-H3	7.22	**NH-1**	9.42	**C*H*-O*iBu* Q3**	2.33, 3.58, 3.87, 1.20, 1.20
N2-H5	7.54	**NH-2**	11.63	**C*H*-O*iBu* N1**	2.36, 3.66, 3.78, 1.21, 1.27
N2-H6	8.09	**NH-3**	11.34	**C*H*-O*iBu* N2**	2.36, 3.92, 4.30, 1.26, 1.33
Pyr1-H3	8.47	**NH-4**	9.19	**C*H*-O*iBu* H - 2**	2.50, 4.02, 4.14, 1.35, 1.40
Pyr1-H4	8.04	**NH-5**	9.75	**C*H*-O*iBu* H - 1**	2.44, 4.10, 4.16, 1.25, 1.25
Pyr1-H5	8.59	**NH-6**	11.70	**C*H*-O*iBu* Qf**	2.45, 4.25, 4.42, 1.21, 1.27
Pyz-1	7.85	**NH-7**	10.27	**C*H*-O*iBu* N3**	2.43, 4.18, 4.29, 1.28, 1.28
Pyz-2	8.61	**NH-8**	9.01	**C*H*-O*iBu* Q4**	2.25, 3.40, 3.62, 1.14, 1.39
Pyr2-H3	7.92	**NH-9**	9.34	**C*H*-O*iBu* Q5**	0.87, 3.14, 3.23, -0.16, 0.45
Pyr2-H4	7.87	**NH-10**	10.01	**C*H*-O*iBu* Q6**	2.00, 3.41, 3.47, 0.90, 0.90
Pyr2-H5	8.46	**NH-11**	9.94		
H-H3	7.53	**NH-12**	10.38		
H-H5	7.45	**NH-13**	11.30		
H-H8	8.16	**NH-14**	11.89		
Q^F-H3	7.94	**NH-15**	12.09		
Q^F -H5	8.26	**NH-16**	9.65		
Q^F -H6	9.01				

Supplementary Table S3. Full assignment of the hydrogen-bound ^{15}N chemical shifts of **6⊃7a** (β-*D*-fructopyranose) in $CDCl_3$/d_6-DMSO (95:5) at 298K (800MHz).

	^{15}N (ppm)		^{15}N (ppm)		^{15}N (ppm)
NH-1	119.54	**NH-7**	131.85	**NH-13**	131.68
NH-2	118.48	**NH-8**	128.75	**NH-14**	120.65
NH-3	116.09	**NH-9**	136.83	**NH-15**	119.67
NH-4	107.26	**NH-10**	108.95	**NH-16**	120.30
NH-5	111.18	**NH-11**	131.94		
NH-6	134.86	**NH-12**	133.75		

Supplementary Table S4. ^{13}C chemical shift assignment of **6⊃7a** (β-*D*-fructopyranose) in $CDCl_3$/d_6-DMSO (95:5) at 298K (800MHz).

	^{13}C (ppm)		^{13}C (ppm)		^{13}C (ppm)
Q1-C7	114.81	**N2-C6**	114.42	**Pyr3-C5**	107.06
Q1-C6	125.94	**Pyr1-C3**	123.09	**Q4-C7**	114.97
Q1-C5	114.50	**Pyr1-C4**	135.72	**Q4-C6**	124.34
Q1-C3	97.76	**Pyr1-C5**	123.72	**Q4-C5**	115.43
Q2-C7	114.24	**Pyz-C1**	122.54	**Q4-C3**	96.56
Q2-C6	124.09	**Pyz-C2**	124.42	**Q5-C7**	114.35
Q2-C5	113.79	**Pyr2-C3**	120.98	**Q5-C6**	124.45
Q2-C3	99.11	**Pyr2-C4**	136.52	**Q5-C5**	112.93
Q3-C7	114.65	**Pyr2-C5**	122.77	**Q5-C3**	98.21
Q3-C6	124.81	**H-C3**	96.74	**Q6-C7**	114.81
Q3-C5	115.28	**H-C5**	99.47	**Q6-C6**	124.02
Q3-C3	96.31	**H-C8**	134.59	**Q6-C5**	115.28
F-C5	112.78	**Q^F-C3**	96.75	**Q6-C3**	96.61
F-C4	121.86	**Q^F-C5**	117.15	**fru-C1**	64.91
F-C3	112.15	**Q^F-C6**	118.37	**fru-C3**	67.49
N1-C3	95.40	**N3-C3**	98.51	**fru-C4**	70.87
N1-C5	132.34	**N3-C5**	132.43	**fru-C5**	68.27
N1-C6	111.24	**N3-C6**	112.79	**fru-C6**	62.48
N2-C3	96.18	**Pyr3-C3**	107.34		
N2-C5	129.79	**Pyr3-C4**	137.82		

Supplementary Table S5. NMR statistics for the ensemble of twenty structures of **6⊃7a** (β-*D*-fructopyranose)

NMR distance restraints	
Total	**311**
Capsule-capsule	199
Fructose-fructose	35
Capsule-fructose	77
Structure statistics (mean and standard deviation)	
Violations	
Distance Restraints (Å)[a]	0.070 ± 0.03
Energy (kJ/mol)	78 ± 6
Minimization Energies (kJ/mol)[b]	
Total	**2903 ± 8**
Stretch	270 ± 1
Bend	947 ± 7
Torsion	140 ± 11
Improper Torsion	3.5 ± 0.1
VDW	2328 ± 3
Electrostatic	-617 ± 2
Cross Terms	25.3 ± 0.4
Solvation	-271 ± 1
Average pairwise rmsd (Å)	
All atoms	0.06 ± 0.04

[a] No violation greater than 0.45 Å.
[b] Final energies from minimization by using MMFFs (Maestro v. 6.5.007)

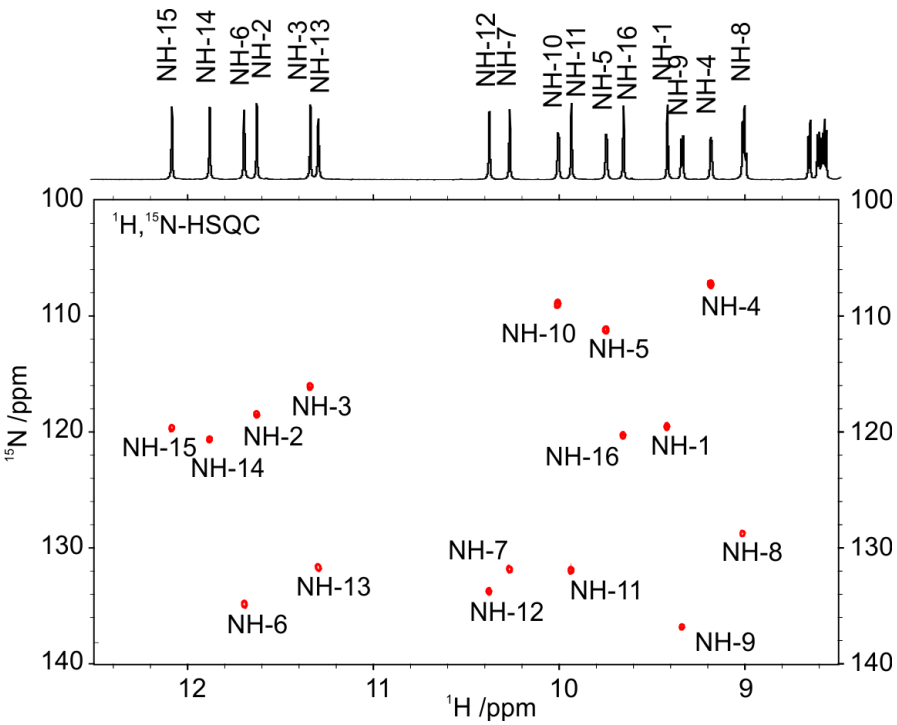

Supplementary Figure S47. Part of the 800 MHz ^{1}H/^{15}N HSQC plot of **6⊃7a** 2 mM in $CDCl_3$/d_6-DMSO (95:5) at 298 K, showing cross-peaks between directly bonded hydrogen and nitrogen. The horizontal scale is that of proton resonances and the vertical scale is that of nitrogen resonances.

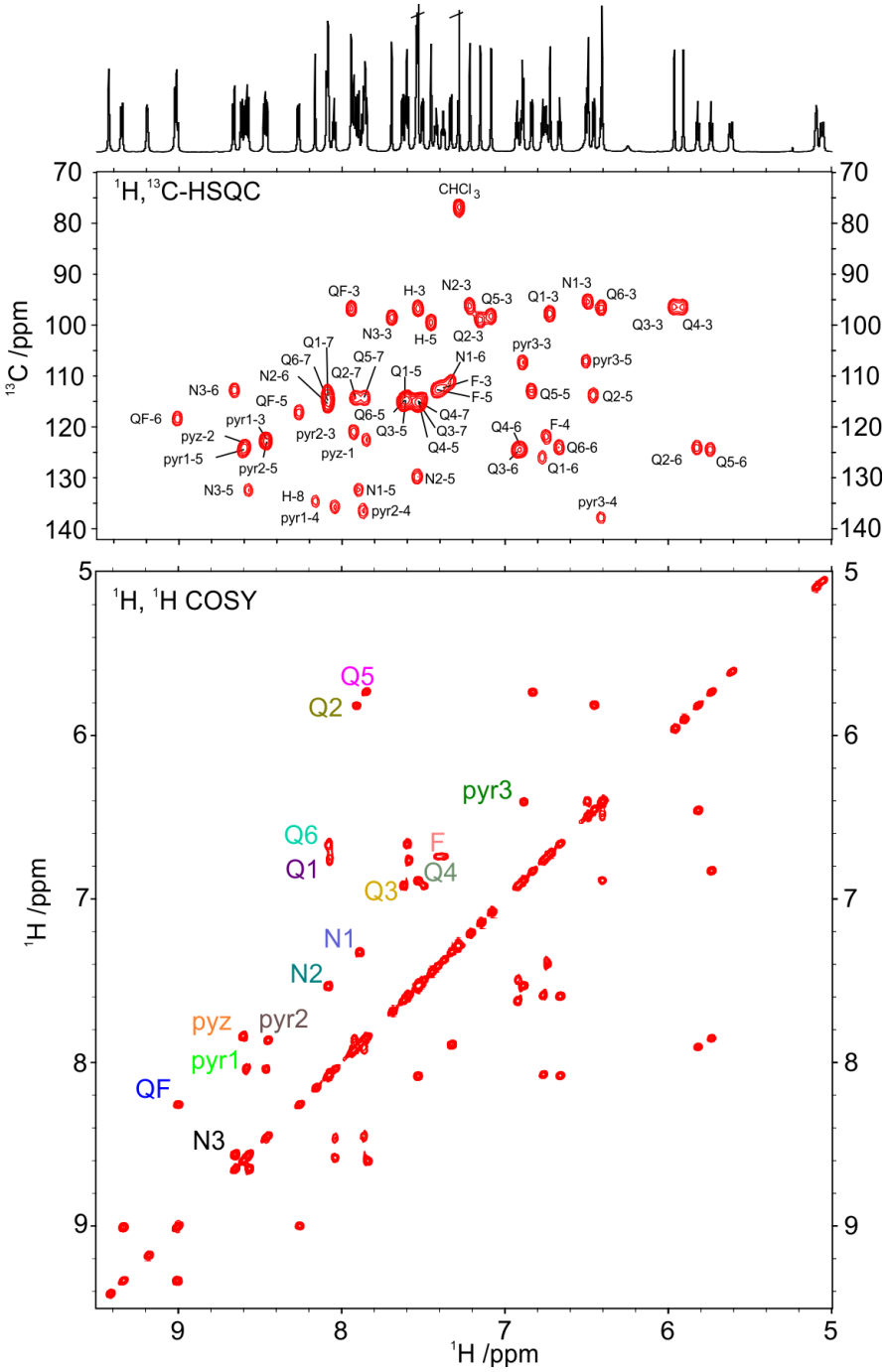

Supplementary Figure S48. Part of the 800 MHz of **6⊃7a** 2 mM in $CDCl_3$/DMSO (95:5) at 298 K of: **Top**. $^{1}H/^{13}C$ HSQC plot of **6⊃7a**, showing cross-peaks between directly bonded hydrogen and carbon. The horizontal scale is that of proton resonances and the vertical scale is that of carbon resonances; **Bottom**. COSY plot of **6⊃7a** showing the different spin systems of the aromatic rings. The horizontal and vertical scales are for proton resonances.

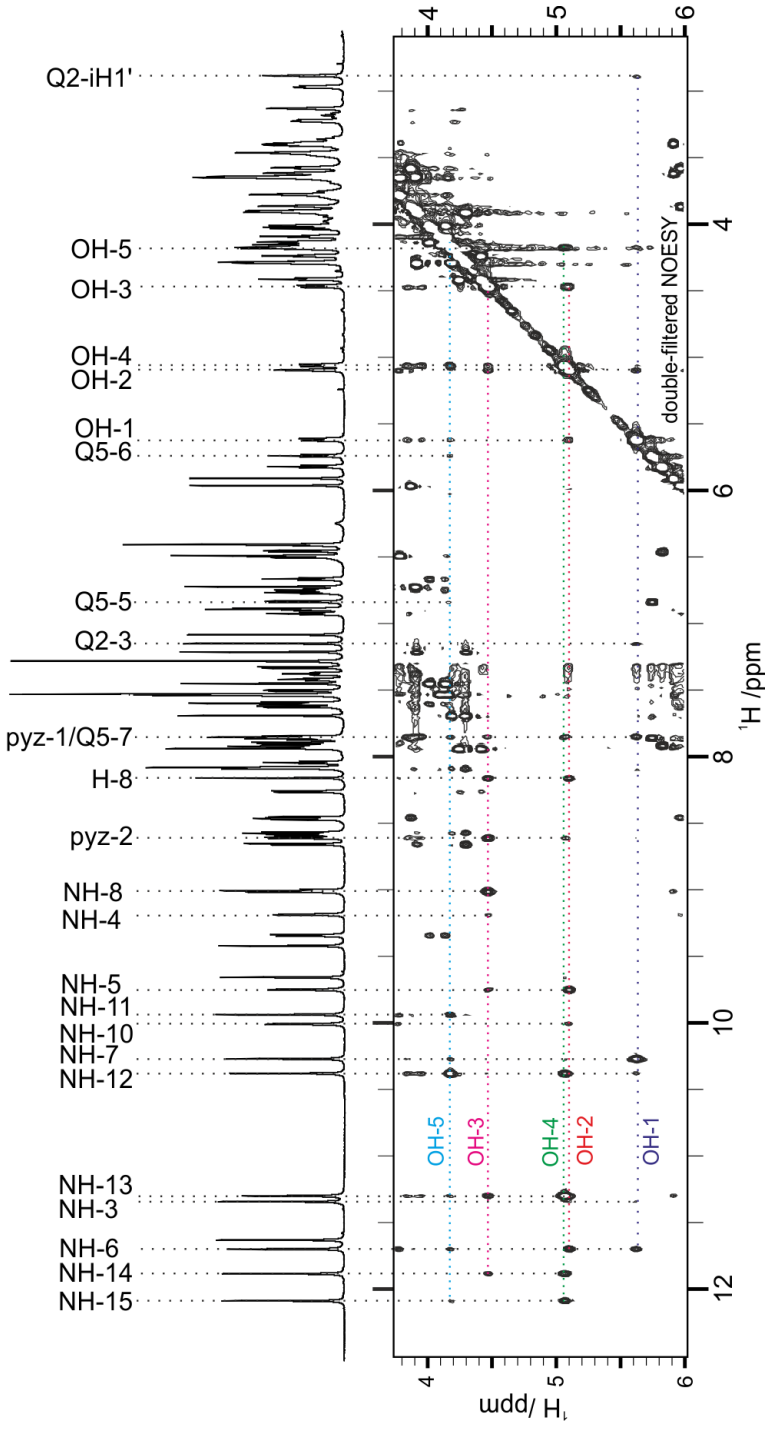

Supplementary Figure S49. Expansion of the ^{1}H-^{1}H double filtered NOESY spectrum recorded with 150 ms mixing time of **6⊃7a** 2 mM in $CDCl_3$/DMSO (95:5) at 298 K showing dipolar couplings between the capsule and the hydroxyls of the sugar.

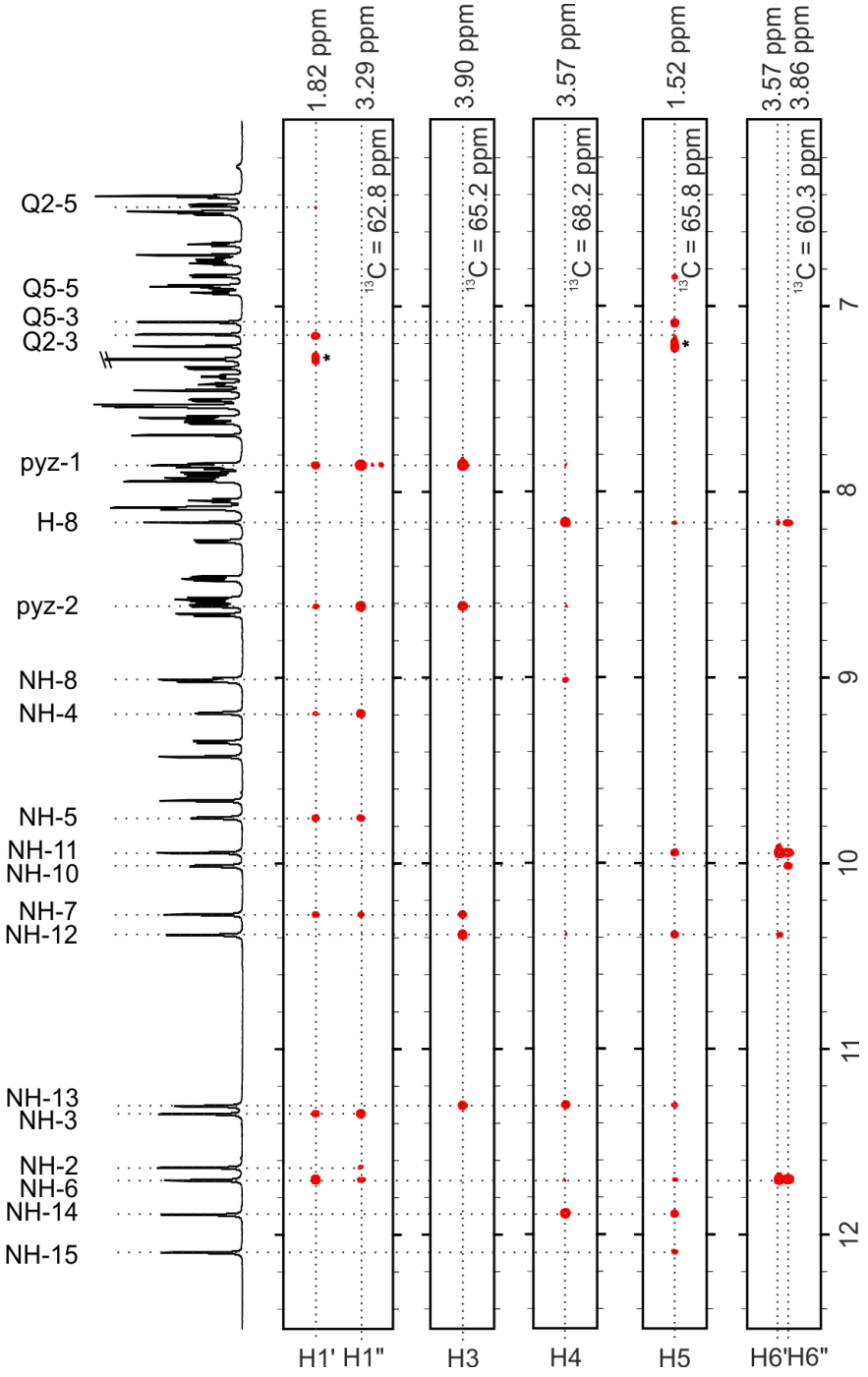

Supplementary Figure S50. Expansion of the ^{1}H-^{1}H 3D NOESY edited spectra recorded with 150 ms mixing time of **6⊃7a** 2 mM in $CDCl_3$/d_6-DMSO (95:5) at 298 K showing nOe contacts between the capsule and the C*H* of the ^{13}C labelled guest.

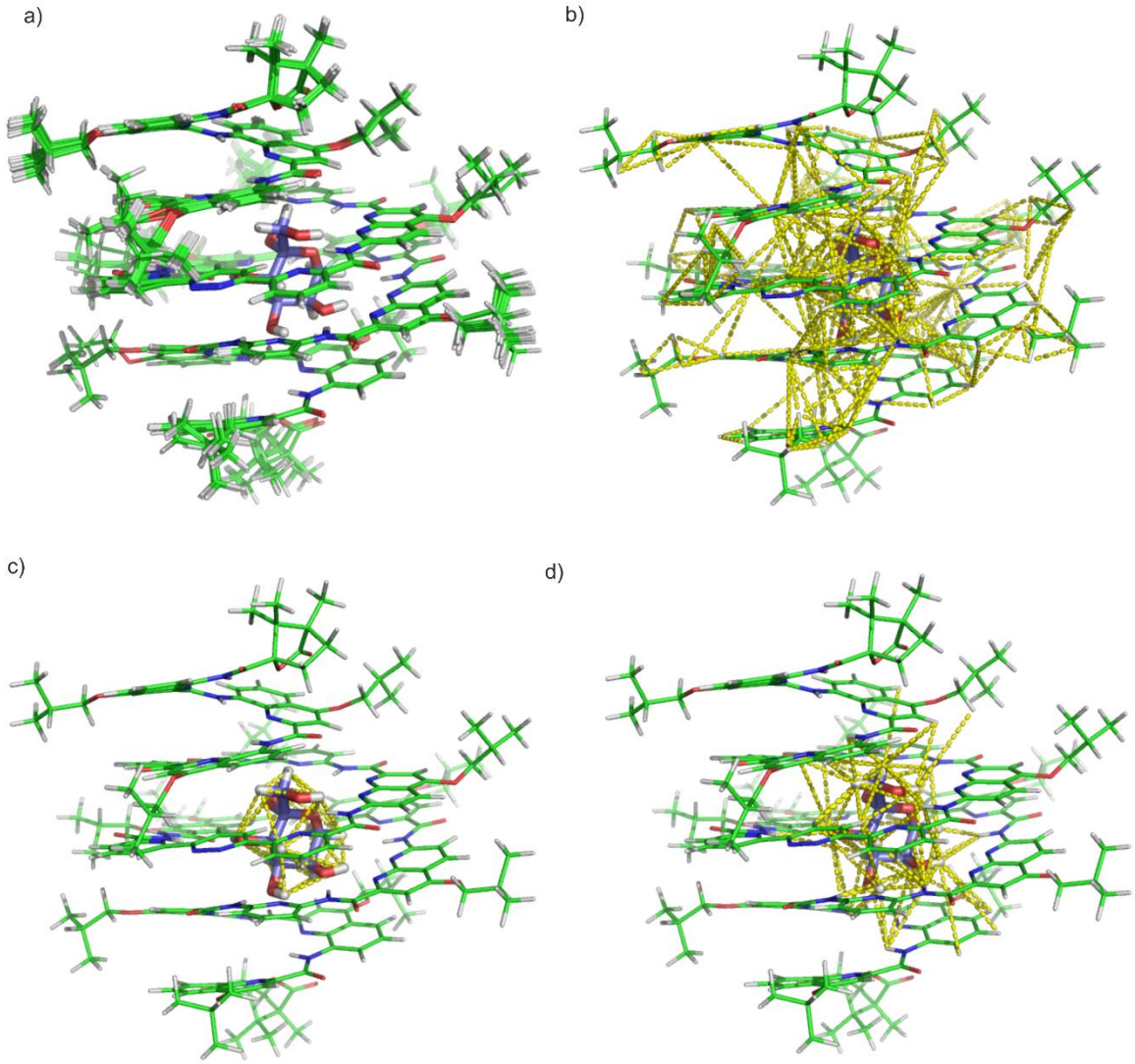

Supplementary Figure S51. Distance restraints used to calculate the ensemble of 20 structures for **6⊃7a**. (a) ensemble of 20 structures. (b) Dotted yellow lines indicate the complete set of 311 distance restraints mapped onto a representative structure from the ensemble. (c) Location of the 35 intramolecular fructose restraints that confirm the β-*D*-pyranose conformation of the encapsulated fructose. (d) Location of the 77 intermolecular capsule-fructose restraints used to position the fructose within the capsule.

6. Solid state X-Ray Crystallography

6.1 X-Ray crystallographic data for host-guest complex **1**⊃β-**7a**

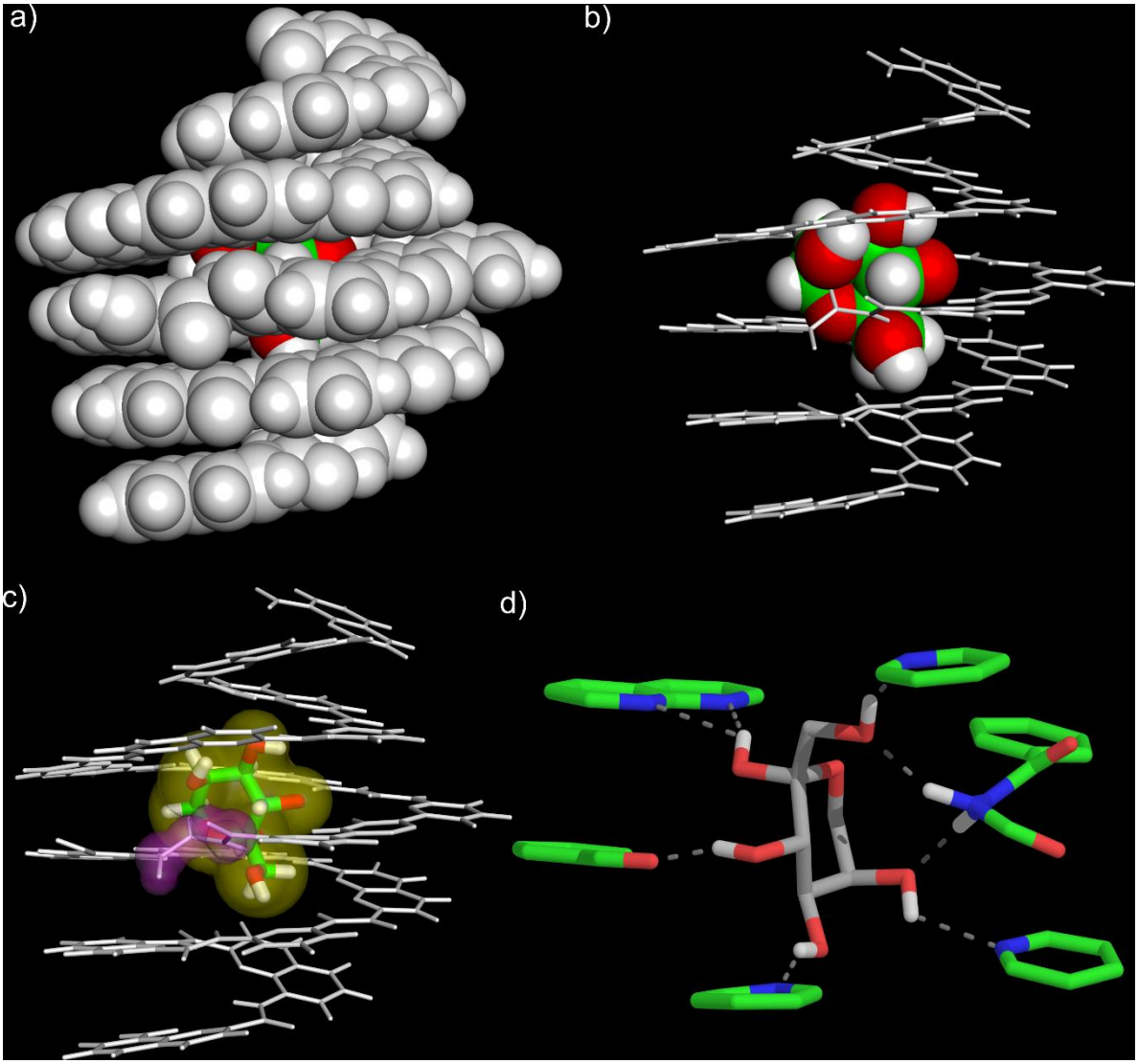

Supplementary Figure S52. Side view of the crystal structures of **1**⊃β-**7a** in: (a) CPK representation and (b) tube and CPK representation for the helix and the guest, respectively. (c) Side view of the same complex in tube representation. Volume of the guest is shown as a yellow transparent isosurface. The *gauche* conformation of one hydrazide bond is highlighted in purple. (d) View of the same complex showing the array of hydrogen bonds. The eight hydrogen bonds are shown as grey dashes. Isobutyl side chains and solvent molecules have been removed for clarity.

Supplementary Table S6: Crystal data and structure refinement for host-guest complex **1**⊃β-**7a**

Formula	C411 H417 N81 O80
M	7771.28
Crystal system	triclinic
Space group	P 1
a/Å	17.018(3)
b/Å	19.782(4)
c/Å	33.512(7)
α/°	81.76(3)
β/°	88.25(3)
γ/°	82.41(3)
U/Å³	11067(4)
T /K	100
Z	1
ρ/g cm⁻¹	1.166
size (mm)	0.1x0.05x0.01
λ/ Å	0.8
μ/mm⁻¹	0.107
Total reflections	62554
Unique data	35952
R_{int}	0.2310
parameters/restraints	4626/9954
R1, wR2	0.1217/0.2979
goodness of fit	1.135
CCDC #	999559

6.2 X-Ray crystallographic data for host-guest complex **1**⊃α-**8a**

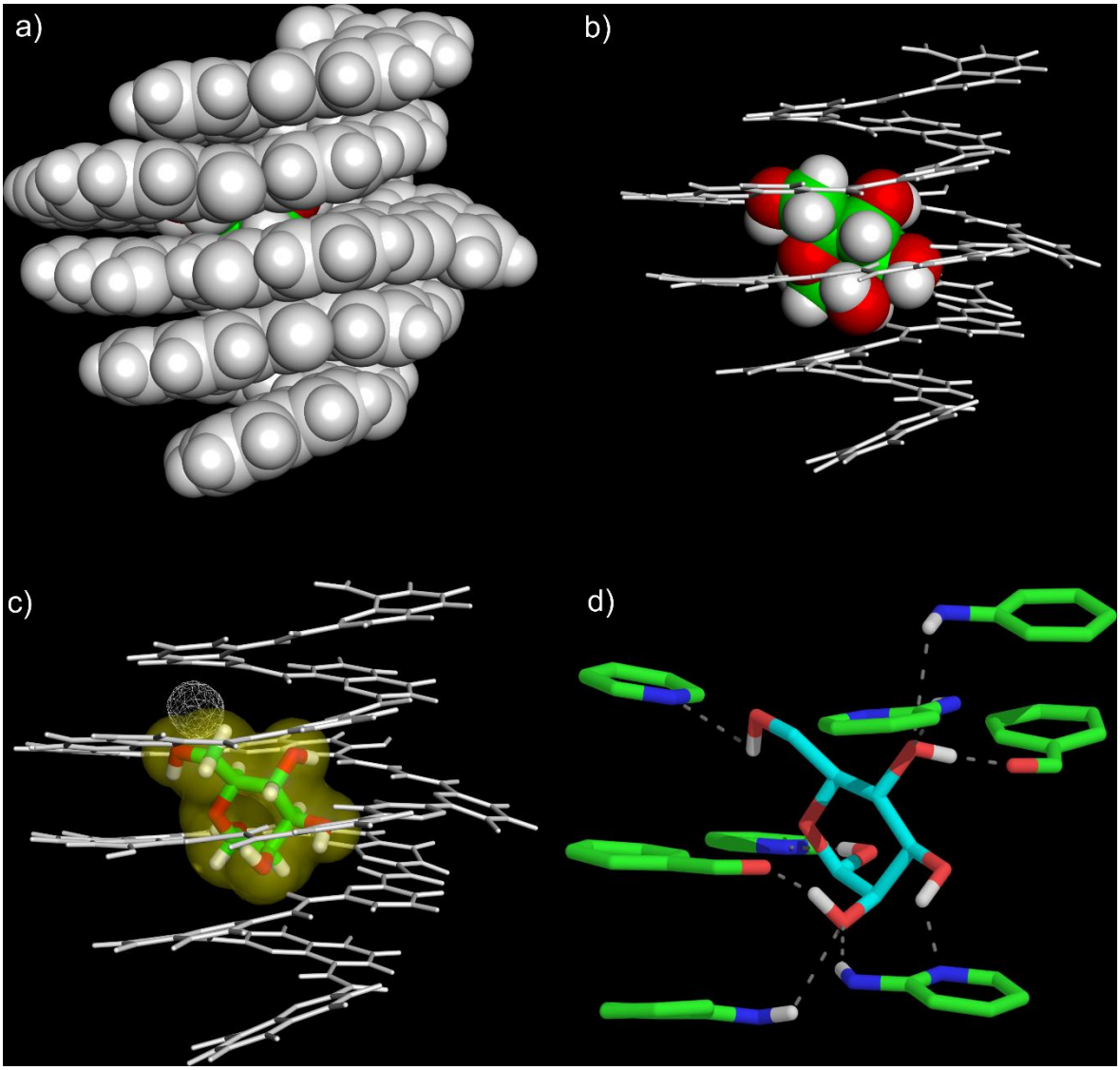

Supplementary Figure S53. Side view of the crystal structures of **1**⊃α-**8a** in: (a) CPK representation and (b) tube and CPK representation for the helix and the guest, respectively. (c) Side view of the same complex in tube representation. Volume of the guest is shown as a yellow transparent isosurface. A void in the complex is shown as white triangle mesh. (d) Top view of the same complex showing the array of hydrogen bonds. The ten hydrogen bonds are shown as grey dashes. Isobutyl side chains and solvent molecules have been removed for clarity.

Supplementary Table S7: Crystal data and structure refinement for host-guest complex **1**⊃α-**8a**

Formula	C206 H210 N40 O40
M	3886.13
Crystal system	monoclinic
Space group	P 2_1/c
a/Å	24.4430(6)
b/Å	21.3714(5)
c/Å	46.5745(10)
α/°	90.0000
β/°	101.9260(10)
γ/°	90.0000
U/Å³	23804.5(10)
T /K	100(2)
Z	4
ρ/g cm⁻¹	1.084
size (mm)	0.2x0.1x0.01
λ/ Å	1.54178
μ/mm⁻¹	0.634
Total reflections	119248
Unique data	39610
R_{int}	0.0400
parameters/restraints	2533/124
R1, wR2	0.1677, 0.4601
goodness of fit	1.482
CCDC #	999560

6.3 X-Ray crystallographic data for host-guest complex **1**⊃β-**9a**

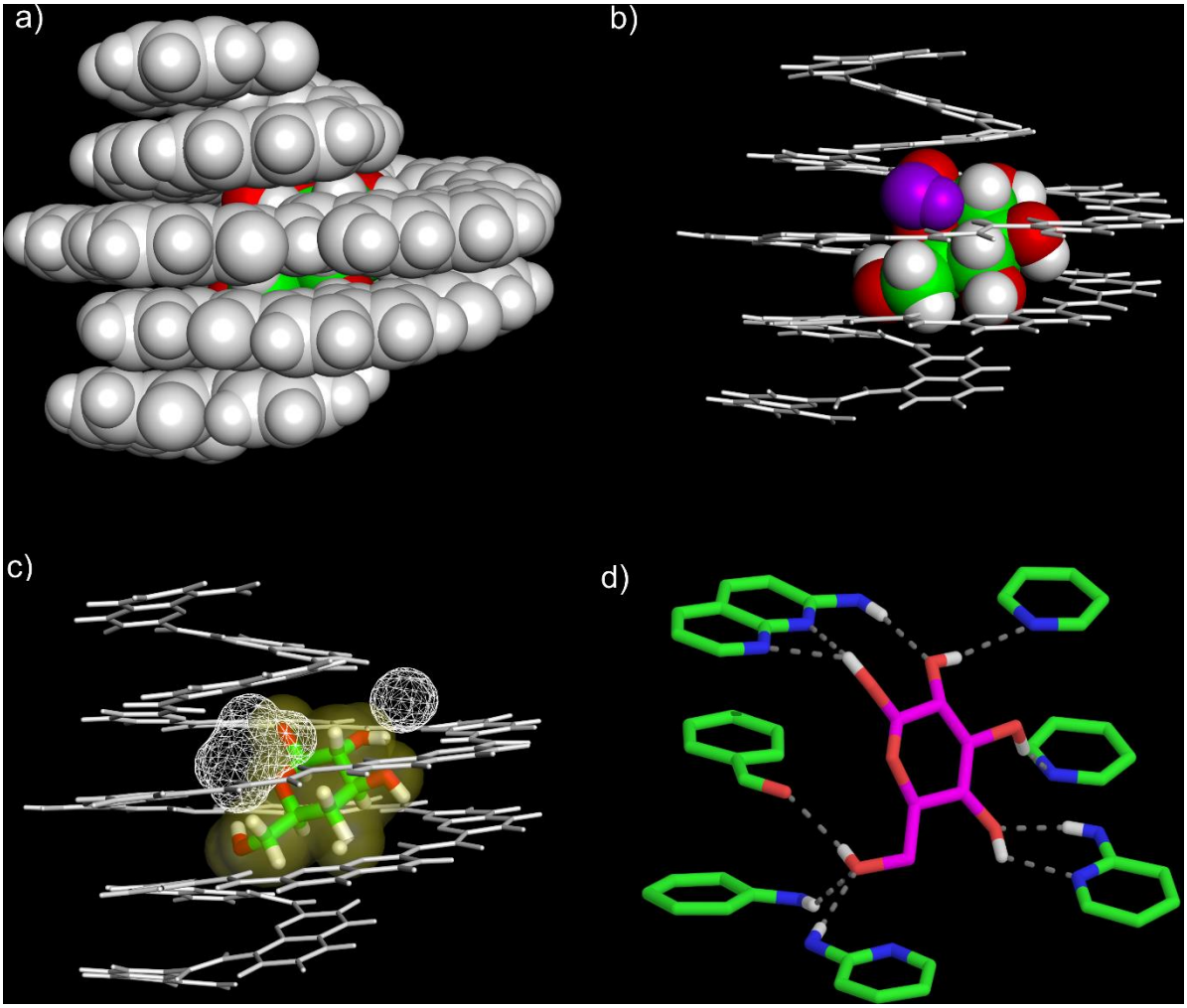

Supplementary Figure S54. Side view of the crystal structures of **1**⊃β-**9a** in: (a) CPK representation and (b) tube and CPK representation for the helix and the guest, respectively. An included water molecule is highlighted in purple. (c) Side view of the same complex in tube representation. Volume of the guest is shown as a yellow transparent isosurface. Two voids in the complex are shown as white triangle mesh. (d) View of the same complex showing the array of hydrogen bonds. The ten hydrogen bonds are shown as grey dashes. Isobutyl side chains and included solvent molecules have been removed for clarity.

Supplementary Table S8: Crystal data and structure refinement for host-guest complex **1**⊃β-**9a**

Formula	C825 H841 N160 O165
M	7818.78
Crystal system	triclinic
Space group	P -1
a/Å	29.180(6)
b/Å	31.720(6)
c/Å	32.140(6)
α/°	69.39(3)
β/°	73.89(3)
γ/°	68.09(3)
U/Å³	25466(12)
T /K	100(2)
Z	2
ρ/g cm⁻¹	1.020
size (mm)	0.05x0.05x0.05
λ/ Å	0.78
μ/mm⁻¹	0.089
Total reflections	305056
Unique data	44096
R_{int}	0.0339
parameters/restraints	5158/192
R1, wR2	0.1380, 0.4015
goodness of fit	1.706
CCDC #	999617

6.4 X-Ray crystallographic data for host-guest complex **1**⊃α-**13a**

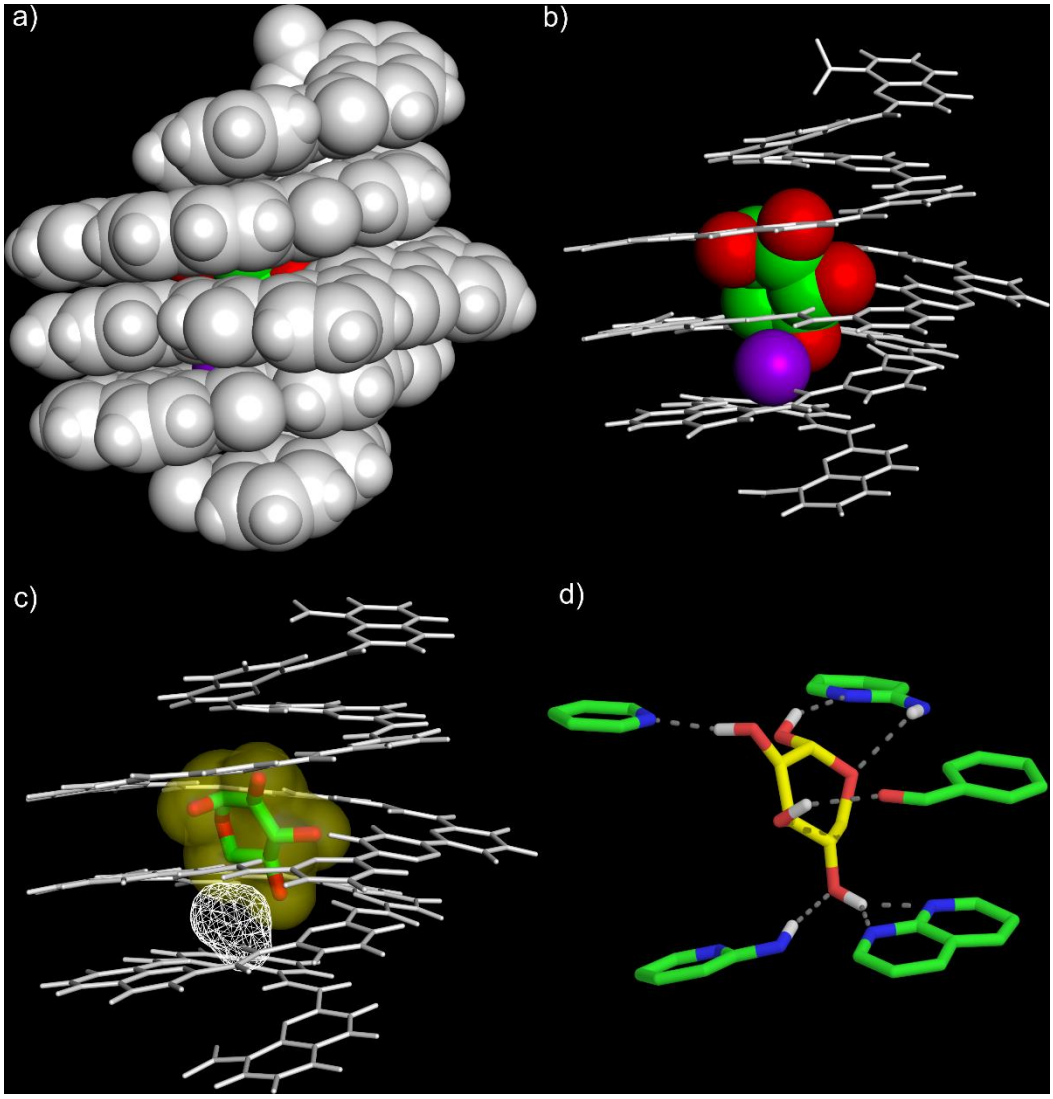

Supplementary Figure S55. Side view of the crystal structures of **1**⊃α-**13a** in: (a) CPK representation and (b) tube and CPK representation for the helix and the guest, respectively. An included water molecule is highlighted in purple. (c) Side view of the same complex in tube representation. Hydrogens of the guest are not visible due to a greater agitation of the guest within the cavity. Hydrogen of hydroxyl groups were thus placed using molecular modelling (see methods). Estimated volume of the guest with hydrogen in theoretical position (not represented) is shown as a yellow transparent isosurface. A void in the complex is shown as white triangle mesh. (d) View of the same complex showing the array of hydrogen bonds. Isobutyl side chains and included solvent molecules have been removed for clarity.

Supplementary Table S9: Crystal data and structure refinement for host-guest complex **1**⊃α-**13a**

Formula	C205 H206 N40 O45
M	3950.09
Crystal system	triclinic
Space group	P -1
a/Å	20.683
b/Å	24.67620(10)
c/Å	25.9639(19)
α/°	117.362(3)
β/°	93.860(8)
γ/°	103.065(6)
U/Å³	11237.3(9)
T /K	100(2)
Z	2
ρ/g cm⁻¹	1.167
size (mm)	0.05x0.05x0.01
λ/ Å	1.54178
μ/mm⁻¹	0.697
Total reflections	158611
Unique data	39576
R_{int}	0.0470
parameters/restraints	2538/55
R1, wR2	0.1719, 0.4644
goodness of fit	1.350
CCDC #	999616

6.5 X-Ray crystallographic data for host-guest complex **3**⊃β-**7a**

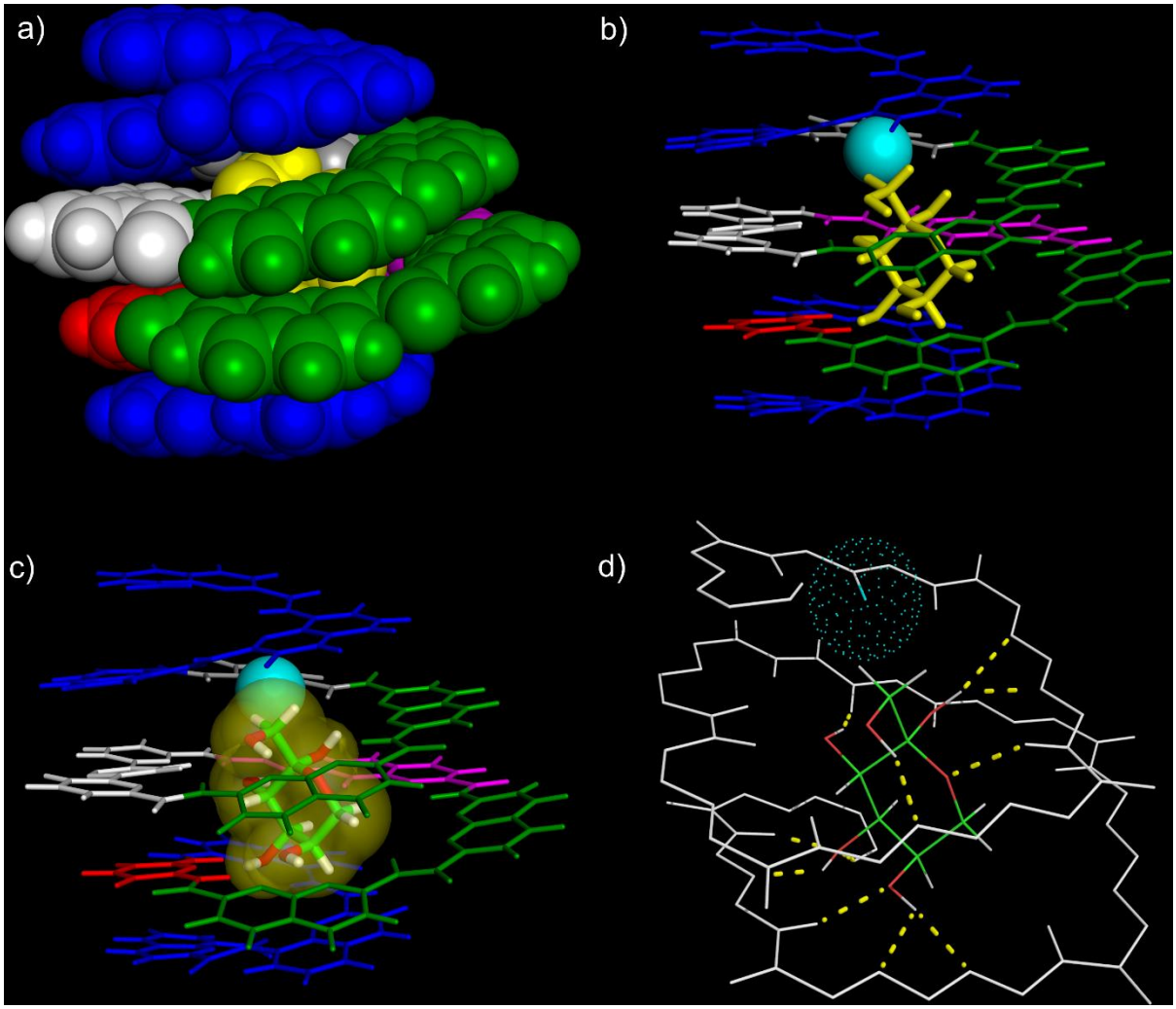

Supplementary Figure S56. Side view of the crystal structures of **3**⊃β-**7a** in: (a) CPK representation and (b) tube and CPK representation for the helix and the guest, respectively. Monomer are color coded as in Figure 1 of the manuscript. A fluorine atom is shown in CPK (cyan). (c) Side view of the same complex in tube representation. Volume of the guest is shown as a yellow transparent isosurface. (d) View of the same complex showing the array of hydrogen bonds. Only the inner rim of the capsule in white tube representation is shown. The eleven hydrogen bonds are shown as yellow dashes. Isobutyl side chains and included solvent molecules have been removed for clarity.

Supplementary Table S10: Crystal data and structure refinement for host-guest complex **3**⊃β-**7a**

Formula	C188 H186 Cl0 F N36 O36
M	3544.72
Crystal system	triclinic
Space group	P -1
a/Å	17.5372(14)
b/Å	19.8099(16)
c/Å	33.578(3)
α/°	105.041(3)
β/°	90.103(2)
γ/°	108.356(3)
U/Å^3	10648.0(16)
T /K	100(2)
Z	2
ρ/g cm^{-1}	1.106
size (mm)	0.1x0.1x0.05
λ/ Å	1.54178
μ/mm^{-1}	0.652
Total reflections	50396
Unique data	20804
R_{int}	0.0632
parameters/restraints	2351/28
R1, wR2	0.1538, 0.3813
goodness of fit	1.437
CCDC #	999615

6.6 X-Ray crystallographic data for host-guest complex **5**⊃β-**7a**

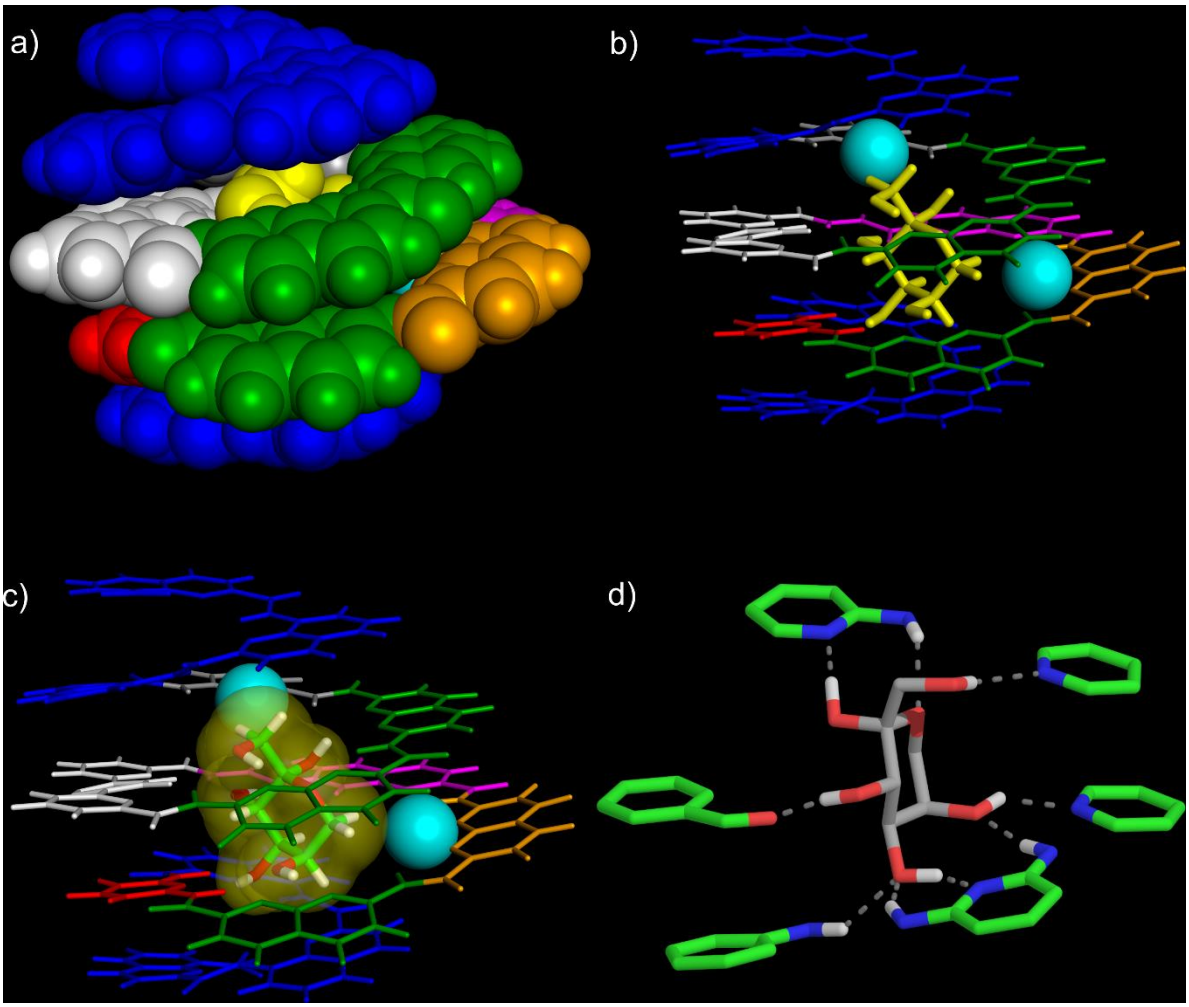

Supplementary Figure S57. Side view of the crystal structures of **5**⊃β-**7a** in: (a) CPK representation and (b) tube and CPK representation for the helix and the guest, respectively. Monomer are color coded as in Figure 1 of the manuscript. Two fluorine atoms are shown in CPK (CPK). (c) Side view of the same complex in tube representation. Volume of the guest is shown as a yellow transparent isosurface. (d) View of the same complex showing the array of hydrogen bonds. The eleven hydrogen bonds are shown as grey dashes. Isobutyl side chains and solvent molecules have been removed for clarity.

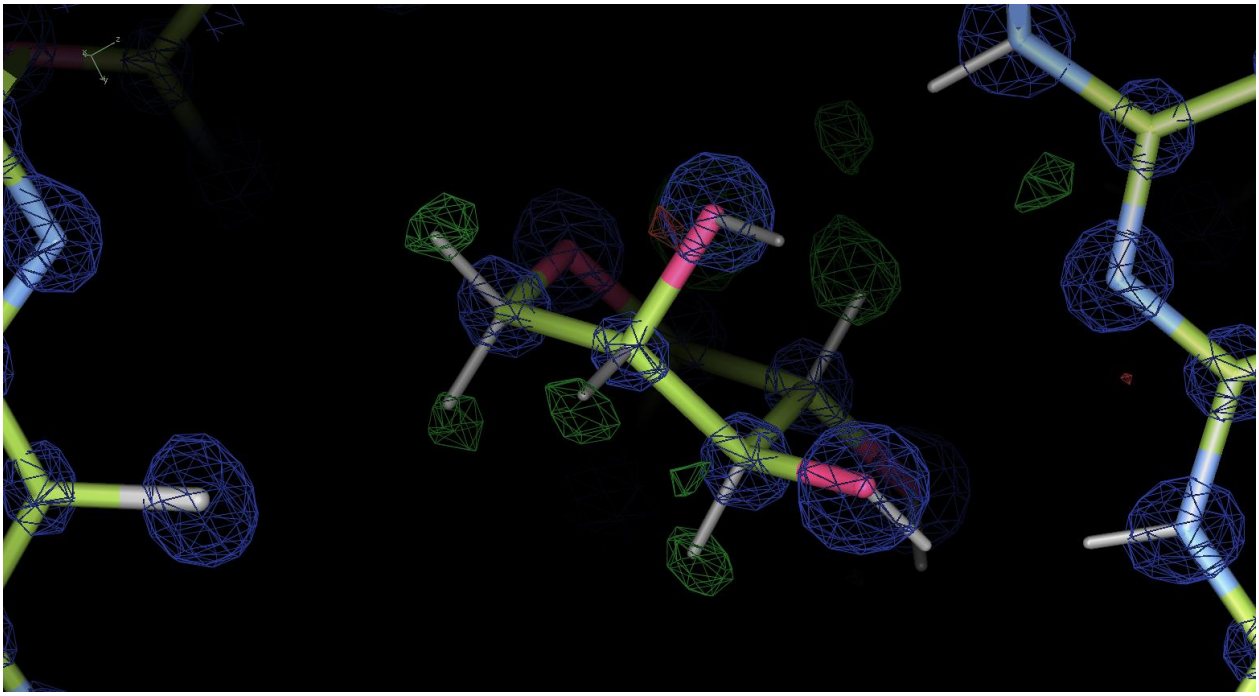

Supplementary Figure S58. A section of 2Fo − Fc (blue) and difference Fo − Fc (green) electron density maps contoured at the 3.0 and 1.5σ level showing the overall quality of the model and the position of some hydrogen atoms of the guest molecule in the complex **5**⊃β-**7a**. The Fo − Fc correspond to an "omit map" in which the Fc are calculated on a model that does not contain the H atoms of the sugar.

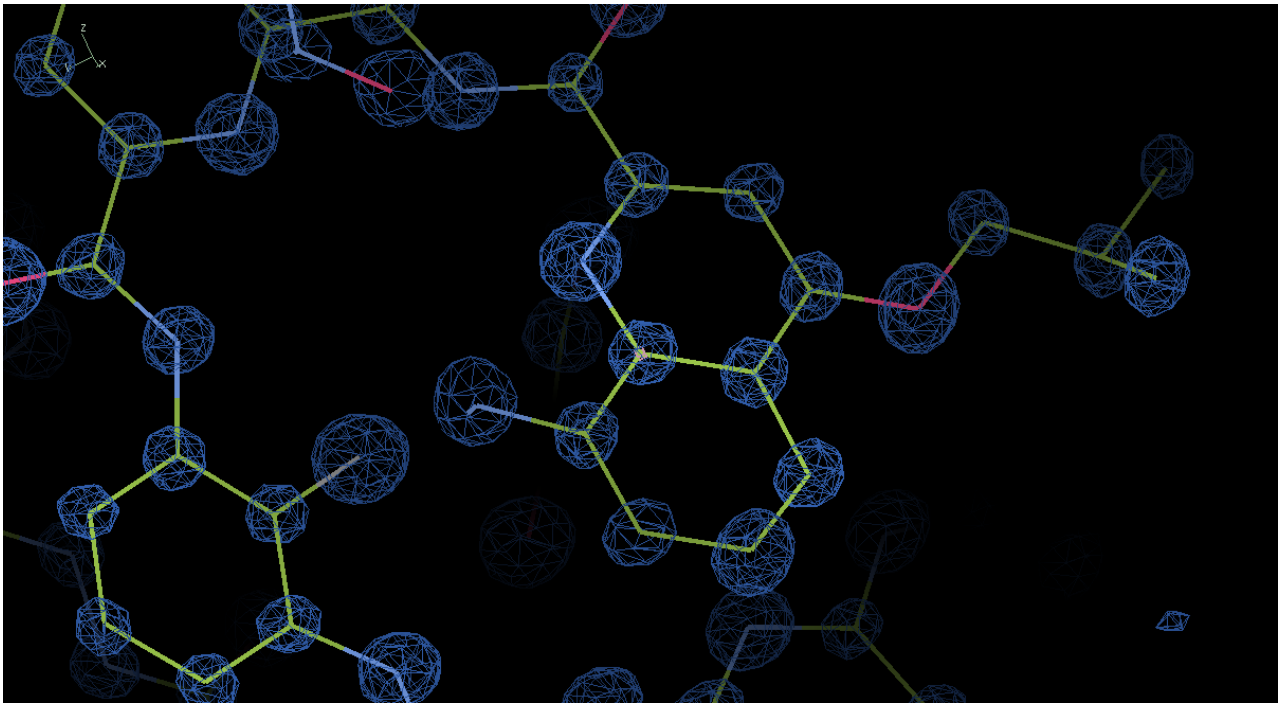

Supplementary Figure S59. Section of $2F_o - F_c$ (blue) electron density maps contoured at the 2.5σ level superimposed to the foldamer main chain showing the high quality of the refined structure of the complex **5**⊃β-**7a**.

Supplementary Table S11: Crystal data and structure refinement for host-guest complex **5**⊃β-**7a**

Formula	C191 H189 Cl6 F2 N35 O36
M	3801.48
Crystal system	triclinic
Space group	P -1
a/Å	17.554(4)
b/Å	19.747(4)
c/Å	33.398(7)
α/°	74.98(3)
β/°	89.62(3)
γ/°	71.99(3)
U/Å³	10600(4)
T /K	100(2)
Z	2
ρ/g cm⁻¹	1.191
size (mm)	0.05x0.05x0.01
λ/ Å	0.85043
μ/mm⁻¹	0.249
Total reflections	41958
Unique data	28320
R_{int}	0.0379
parameters/restraints	2432/1
R1, wR2	0.1265, 0.3559
goodness of fit	1.527
CCDC #	999614

6.7 Determination of the internal volume of the capsules

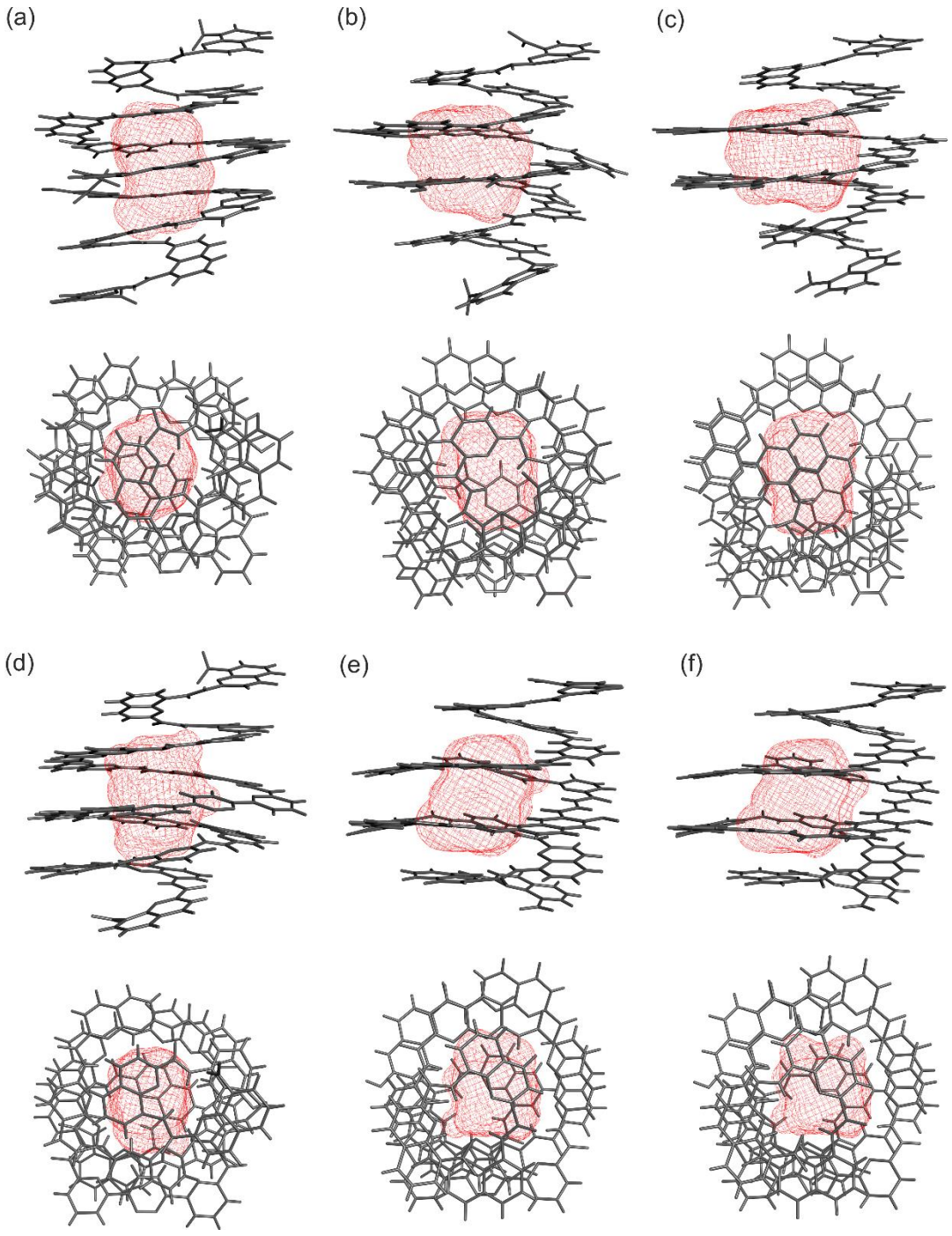

Supplementary Figure S60. Tube representations (light grey) of the side and top views of the solid-state structures of: (a) *P*-**1**⊃β-D-**7a**; (b) *P*-**1**⊃α-L-**8a**; (c) *P*-**1**⊃β-D-**9a**; (d) *P*-**1**⊃α-L-**13a**; (e) *P*-**3**⊃β-D-**7a**; (f) *P*-**5**⊃β-D-**7a**. Volumes of cavities are obtained using SURFNET (see methods) after the removal of carbohydrates and shown as red isosurfaces (quad mesh). Isobutoxy groups and solvent molecules are not shown for clarity.

Supplementary Table S12. Volumes of capsules and their selected guest, and packing coefficients as calculated with SURFNET[11].

	Host – Guest Complex					
	1⊃β-7a	**1⊃α-8a**	**1⊃β-9a**	**1⊃α-13a**	**3⊃β-7a**	**5⊃β-7a**
Cavity volume (Å^3)	202	236	245	195	201	196
Guest volume (Å^3)	128.8	129.2	128.0	107.4	128.2	128.2
Packing coefficient (%)	63.8	54.7	52.2	55.1	63.8	65.4

6.8 Hydrogen bond patterns

Supplementary Table S13. Hydrogen bond donors and acceptors of the inner wall of capsules **1**, **3** and **5** involved in the formation of complexes with the carbohydrates.

Type of Hydrogen Bond (capsule·····sugar)	**Host – Guest Complex**					
	1⊃β-7a	**1⊃α-8a**	**1⊃β-9a**[a]	**1⊃α-13a**[a]	**3⊃β-7a**	**5⊃β-7a**
H bond donor: N*H*·····O*H*	2	5	4	5	3	3
H bond donor: N*H*·····O	0	0	0	0	1	1
H bond acceptor: N·····H*O*	5	3	5	2	6	6
H bond acceptor: C=O·····H*O*	1	2	1	1	1	1
Total	**8**	**10**	**10**	**8**	**11**	**11**

[a]A water molecule is also included in the complex giving two hydrogen bonds to the inner wall of the capsule and a single hydrogen bond to the endocyclic oxygen of the carbohydrate.

Supplementary Table S14. Full details of hydrogen bond networks for **1**⊃β-**7a**, **1**⊃α-**8a**, **1**⊃β-**9a**, **1**⊃α-**13a**,**3**⊃β-**7a** and **5**⊃**β-7a** host-guest complexes. Atom numbers are those of the cif files.

Molecule-H	Element(Atom-H)	Molecule-A	Element(Atom-A)	Distance (< 2.6 Å)	DHA angle (>90°)	HAB angle (>60°)
β-**7a**	H809	**1**	N205	2.48	156.9	143.3
β-**7a**	H809	**1**	N199	2.36	132.0	101.0
β-**7a**	H803	**1**	N258	2.21	123.2	135.7
1	H426	β-**7a**	O803	2.17	165.4	102.4
1	H55	β-**7a**	O811	2.17	142.8	97.1
β-**7a**	H805	**1**	N268	2.13	151.5	131.7
β-**7a**	H807	**1**	O19	2.04	144.7	160.1
β-**7a**	H811	**1**	N183	1.99	149.1	125.3

Molecule-H	Element(Atom-H)	Molecule-A	Element(Atom-A)	Distance (< 2.6 Å)	DHA angle (>90°)	HAB angle (>60°)
1	H24	α-**8a**	O6M	2.48	123.8	112.4
1	H36	α-**8a**	O6M	2.48	162.1	85.7
α-**8a**	H7M1	**1**	N58	2.46	131.5	91.6
1	H148	α-**8a**	O4M	2.40	164.2	92.9
α-**8a**	H7M1	**1**	N60	2.36	159.3	146.8
1	H129	α-**8a**	O2M	2.36	165.3	89.1
1	H43	α-**8a**	O5M	2.33	135.0	70.8
α-**8a**	H5M1	**1**	N38	2.20	144.3	105.5
α-**8a**	H6M1	**1**	O16	2.02	156.4	145.2
α-**8a**	H4M	**1**	O19	1.77	166.2	168.3

Molecule-H	Element(Atom-H)	Molecule-A	Element(Atom-A)	Distance (< 2.6 Å)	DHA angle (>90°)	HAB angle (>60°)
1	H477	β-**9a**	O977	2.51	145.3	123.2
β-**9a**	H921	**1**	N10	2.49	170.9	92.9
1	H486	β-**9a**	O920	2.36	146.5	81.8
1	H527	β-**9a**	O921	2.35	169.8	145.1
1	H479	β-**9a**	O977	2.30	148.3	115.0
β-**9a**	H92	**1**	N526	2.27	147.8	86.9
β-**9a**	H92	**1**	N5	2.09	148.6	96.1
β-**9a**	H920	**1**	N485	2.05	140.5	117.7
β-**9a**	H977	**1**	O71	1.94	152.6	160.5
β-**9a**	H43	**1**	N28	1.89	173.8	117.4

Molecule-H	Element(Atom-H)	Molecule-A	Element(Atom-A)	Distance (<2.6 Å)	DHA angle (>90°)	HAB angle (>60°)
α-**13a**	H4X	**1**	O19	2.45	155.8	163.8
1	H29	α-**13a**	O2X	2.43	165.7	82.1
1	H32	α-**13a**	O3X	2.39	163.4	79.5
α-**13a**	H5X	**1**	N705	2.39	143.4	86.1
α-**13a**	H2X	**1**	N27	2.35	164.5	87.5
α-**13a**	H5X	**1**	N11	2.30	152.2	91.2
α-**13a**	H3X	**1**	N602	2.30	138.1	97.6
α-**13a**	H2X	**1**	N28	2.30	131.6	144.9

Molecule-H	Element(Atom-H)	Molecule-A	Element(Atom-A)	Distance (<2.6 Å)	DHA angle (>90°)	HAB angle (>60°)
β-**7a**	H925	**3**	N27	2.46	130.2	152.7
3	H923	β-**7a**	O3F	2.43	138.8	108.8
3	H806	β-**7a**	O2F	2.36	171.8	152.5
3	H914	β-**7a**	O1F	2.30	149.3	98.0
β-**7a**	H925	**3**	N913	2.19	156.5	98.5
β-**7a**	H500	**3**	N601	2.16	168.0	153.4
β-**7a**	H500	**3**	N600	2.15	121.3	156.0
β-**7a**	H34	**3**	N30	2.14	153.7	119.0
3	H508	β-**7a**	O3F	2.10	154.8	132.7
β-**7a**	H33	**3**	N807	1.96	140.6	117.0
β-**7a**	H21A	**3**	O36	1.58	161.2	167.0

Molecule-H	Element(Atom-H)	Molecule-A	Element(Atom-A)	Distance (<2.6 Å)	DHA angle (>90°)	HAB angle (>60°)
β-**7a**	H18	**5**	N505	2.47	128.4	148.7
5	H40	β-**7a**	O14	2.36	150.2	95.8
5	H515	β-**7a**	O15	2.33	147.9	106.8
5	H512	β-**7a**	O32	2.28	170.4	153.3
β-**7a**	H32	**5**	N10	2.26	165.4	155.2
β-**7a**	H18	**5**	N25	2.25	151.0	142.4
β-**7a**	H26	**5**	N24	2.20	156.5	119.9
β-**7a**	H32	**5**	N511	2.10	124.1	148.7
β-**7a**	H15	**5**	N513	2.06	138.3	128.6
5	H3	β-**7a**	O15	2.04	156.6	132.9
β-**7a**	H19	**5**	O509	1.59	162.4	162.5

6.9 Structural comparison of D-fructopyranose vs. D-mannopyranose

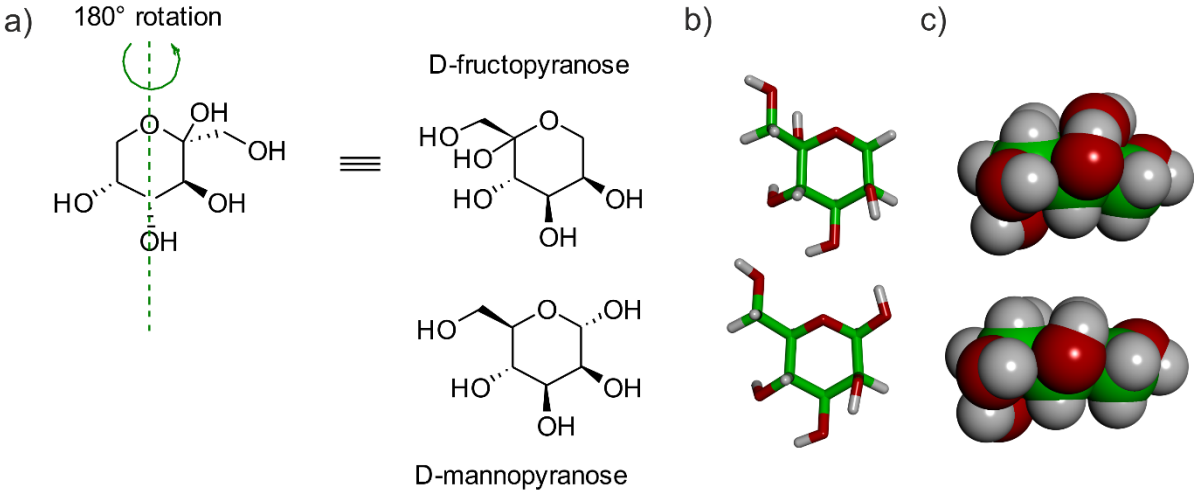

Supplementary Figure S61. a) Structures of D-fructopyranose and D-mannopyranose. D-fructopyranose can be seen as a 1-deoxy-5-hydroxy analogue of D-mannopyranose. b) Top view of the tube representation D-fructopyranose and D-mannopyranose. c) Side view the CPK representation of D-fructopyranose and D-mannopyranose.

7. References

References of the supplementary material

S1. Kabsch, W. *Acta Cryst* **D66**, 125 (2010).

S2. Palatinus, L., Chapuis, G. *Appl. Crystallogr.* **40**, 786 (2007).

S3. Farrugia, L. J. *J. Appl. Crystallogr.* **32**,837 (1999).

S4. Sheldrick, G. M. *Acta Cryst.* **A64**, 112 (2008).

S5. Spek, A. L. SQUEEZE *J. Appl. Cryst* **36**, 7 (2003).

S6. Ferrand, Y. *et al. J. Am. Chem. Soc.* **134**, 11282 (2012).

S7. Ferrand, Y. *et al. Angew. Chem. Int. Ed.* **49**, 1778 (2010).

S8. Gan, Q. *et al. Angew. Chem. Int. Ed.*, **47**, 1715 (2008).

S9. Jiang, H., Léger, J.-M., Huc, I. *J. Am. Chem. Soc.*, **125**, 3448 (2003).

S10. Lautrette, G. *et al. Angew. Chem. Int. Ed.* **52**, 11517 (2013).

S11. Laskowski, R.A. *J. Mol. Graph.* **13**, 323 (1995).

References with full author list of the main text

2. Appella, D. H., Christianson, L. A., Klein, D. A., Powell, D. R., Huang, X., Barchi Jr., J. J., Gellman, S. H. Residue-based control of helix shape in β-peptide oligomers. *Nature* **387**, 381–384 (1997).

7. Zhu, J., Parra, R. D., Zeng, H., Skrzypczak-Jankun, E., Zeng, X. C., Gong, B. New class of folding oligomers: crescent oligoamides. *J. Am. Chem. Soc.* **122**, 4219–4220 (2000).

16. Ferrand, Y., Klein, E., Barwell, N. P., Crump, M. P., Jiménez-Barbero, J., Vicent, C., Boons, G.-J., Ingale, S., Davis, A. P. A synthetic lectin for *O*-linked β-*N*-acetylglucosamine *Angew. Chem. Int. Ed.* **48**, 1775–1779 (2009).

27. Ardá, A., Venturi, C., Nativi, C., Francesconi, O., Gabrielli, G., Cañada, F. J., Jiménez-Barbero, J., Roelens, S. A chiral pyrrolic tripodal receptor enantioselectively recognizes β-mannose and β-mannosides. *Chem. Eur. J.* **16**, 414–418 (2010).

29. Hou, J.-L., Shao, X.-B., Chen, G.-J., Zhou, Y.-X., Jiang, X.-K., Li, Z.-T. Hydrogen bonded oligohydrazide foldamers and their recognition for saccharides. *J. Am. Chem. Soc.* **126**, 12386–12394 (2004).

31. Bao, C., Kauffmann, B., Gan, Q., Srinivas, K., Jiang, H., Huc, I. Converting sequences of aromatic amino acid monomers into functional three-dimensional structures: second-generation helical capsules. *Angew. Chem. Int. Ed.* **47**, 4153–4156 (2008).

36. Ferrand, Y., Chandramouli, N., Kendhale, A. M., Aube, C., Kauffmann, B., Grélard, A., Laguerre, M., Dubreuil, D., Huc, I. Long-range effects on the capture and release of a chiral guest by a helical molecular capsule. *J. Am. Chem. Soc.* **134**, 11282–11288 (2012).

39. Cocinero, E. J., Lesarri, A., Écija, P., Cimas, A., Davis, B. G., Basterretxea, F. J., Fernández, J. A., Castaño, F. Free fructose is conformationally locked. *J. Am. Chem. Soc.* **135**, 2845–2852 (2013).

41. Pentelute, B. L., Gates, Z. P., Tereshko, V., Dashnau, J. L., Vanderkooi, J. M., Kossiakoff, A. A., Kent, S. B. H. X-ray structure of snow flea antifreeze protein determined by racemic crystallization of synthetic protein enantiomers. *J. Am. Chem. Soc.* **130**, 9695–9701 (2008).

42. Lautrette, G., Kauffmann, B., Ferrand, Y., Aube, C., Chandramouli, N., Dubreuil, D., Huc, I. Structure elucidation of host-guest complexes of tartaric and malic acid by quasi-racemic crystallography. *Angew. Chem. Int. Ed.* **52**, 11517–11520 (2013).

43. Çarcabal, P., Jockusch, R. A., Hünig, I., Snoek, L. C., Kroemer, R. T., Davis, B. G., Gamblin, D. P., Compagnon, I., Oomens, J., Simons, J. P. Hydrogen bonding and cooperativity in isolated and hydrated sugars: mannose, galactose, glucose, and lactose. *J. Am. Chem. Soc.* **127**, 11414–11425 (2005).

45. Doores, K. J., Fulton, Z., Hong, V., Patel, M. K., Scanlan, C. N., Wormald, M. R., Finn, M. G., Burton, D. R., Wilson, I. A., Davis, B. G. A nonself sugar mimic of the HIV glycan shield shows enhanced antigenicity. *Proc. Natl. Acad. Sci. U.S.A.* **107**, 17107–117112 (2010).

48. Singleton, M. L., Castellucci, N., Massip, S., Kauffmann, B., Ferrand, Y., Huc, I. Synthesis of 1,8-diazaanthracenes as building blocks for internally functionalized aromatic oligoamide foldamers. *J. Org. Chem.* **79**, 2115–2122 (2014).

8. ^{1}H NMR and ^{13}C NMR spectra of new synthetic compounds.

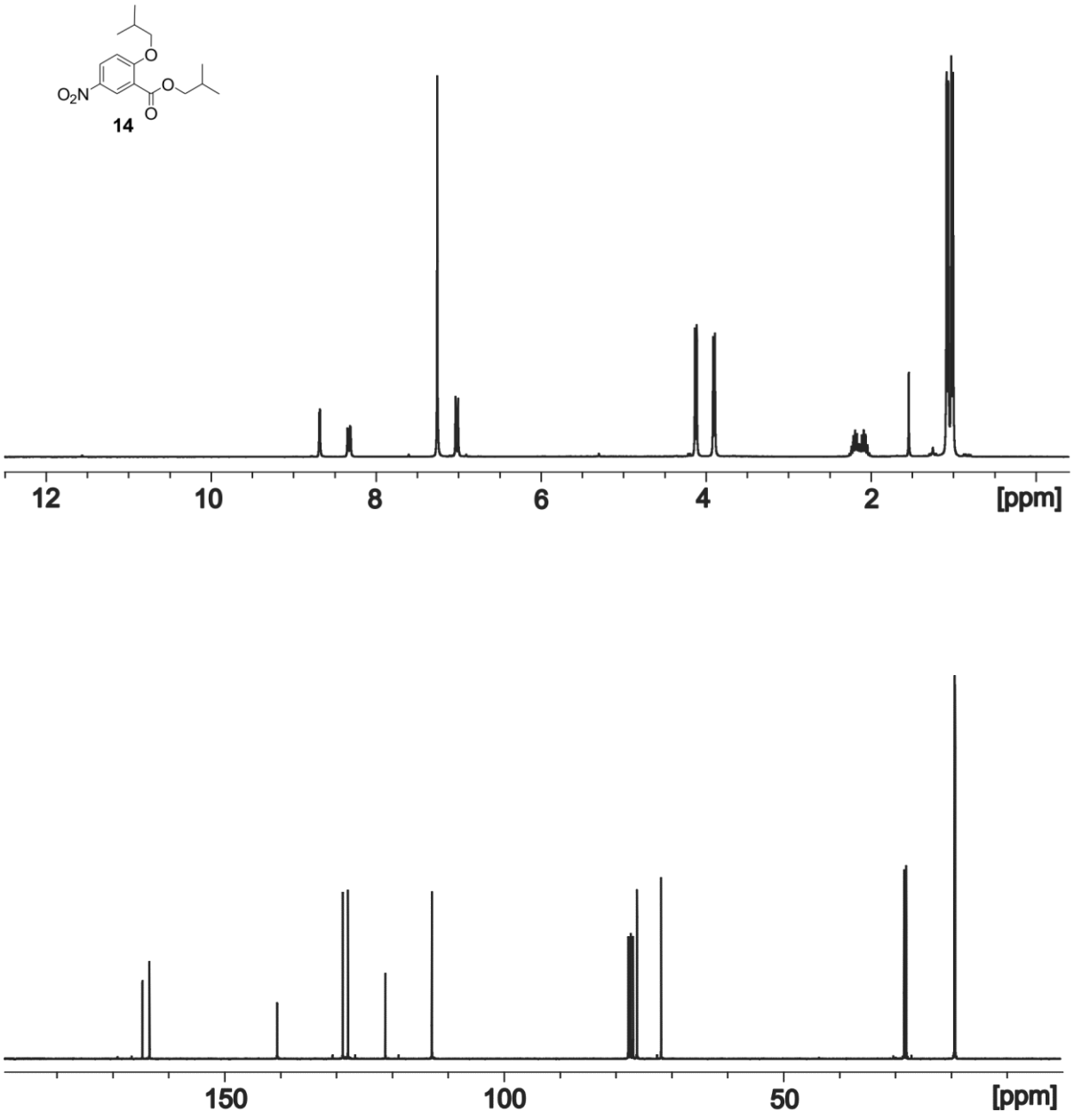

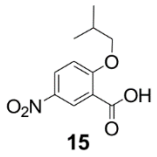

15

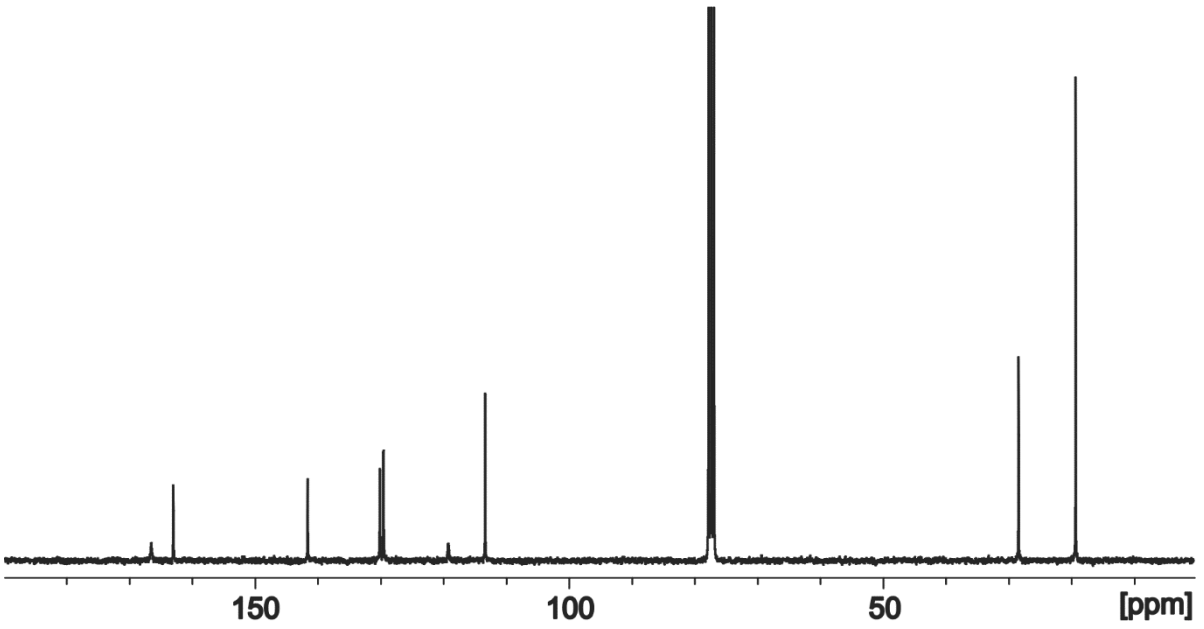

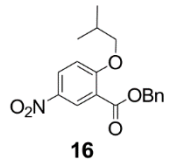

16

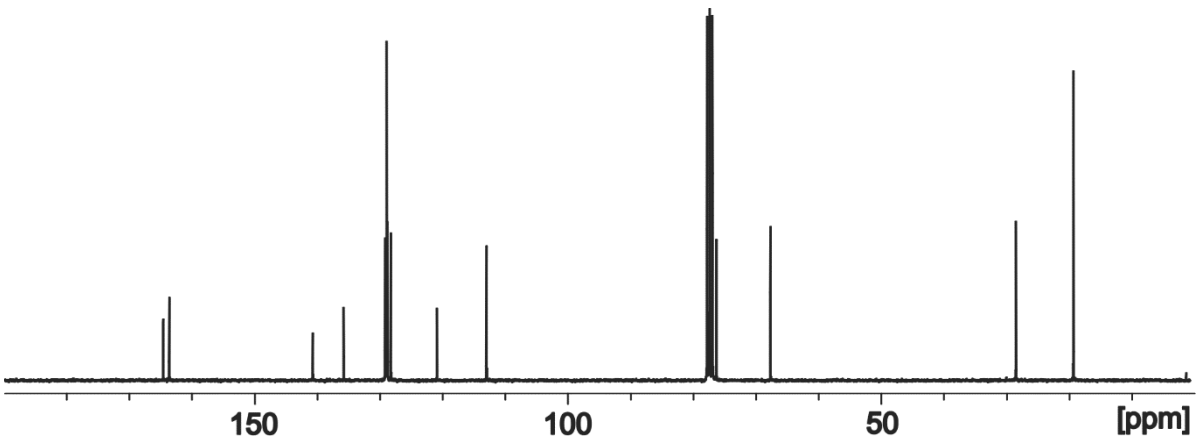

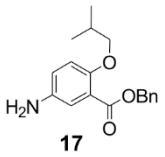

17

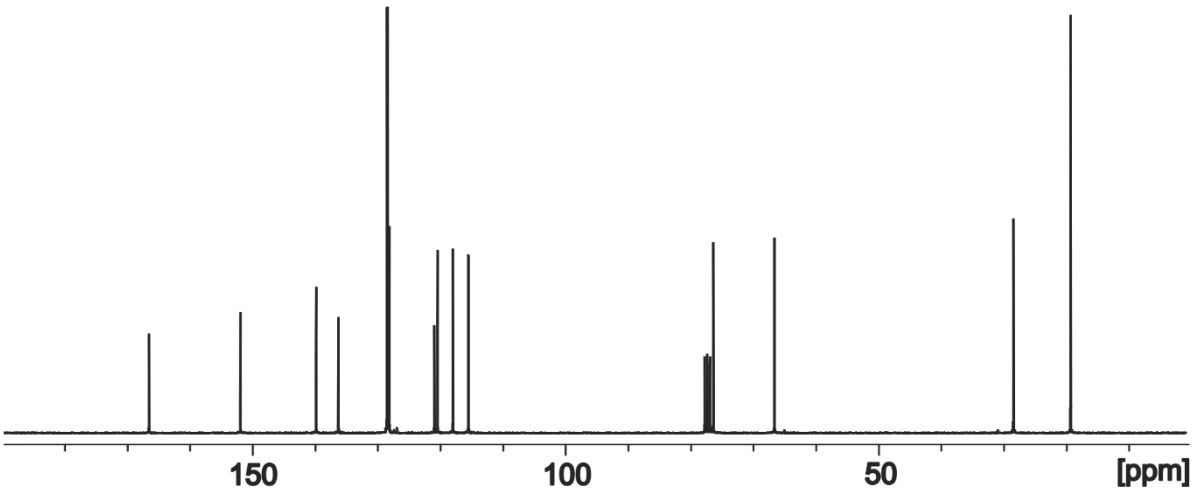

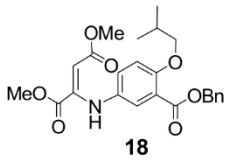

18

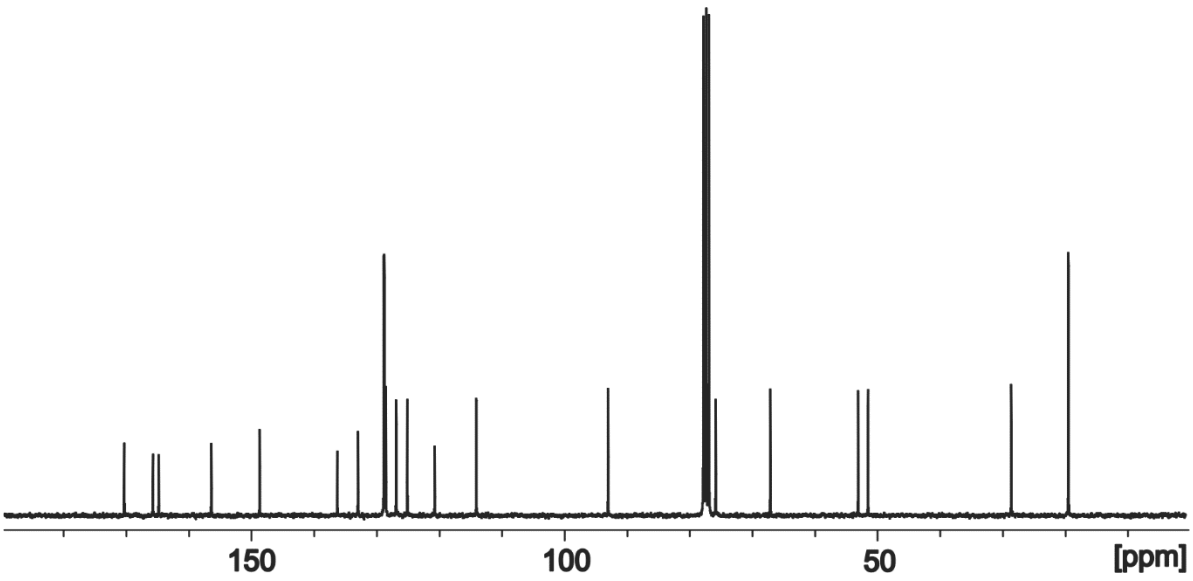

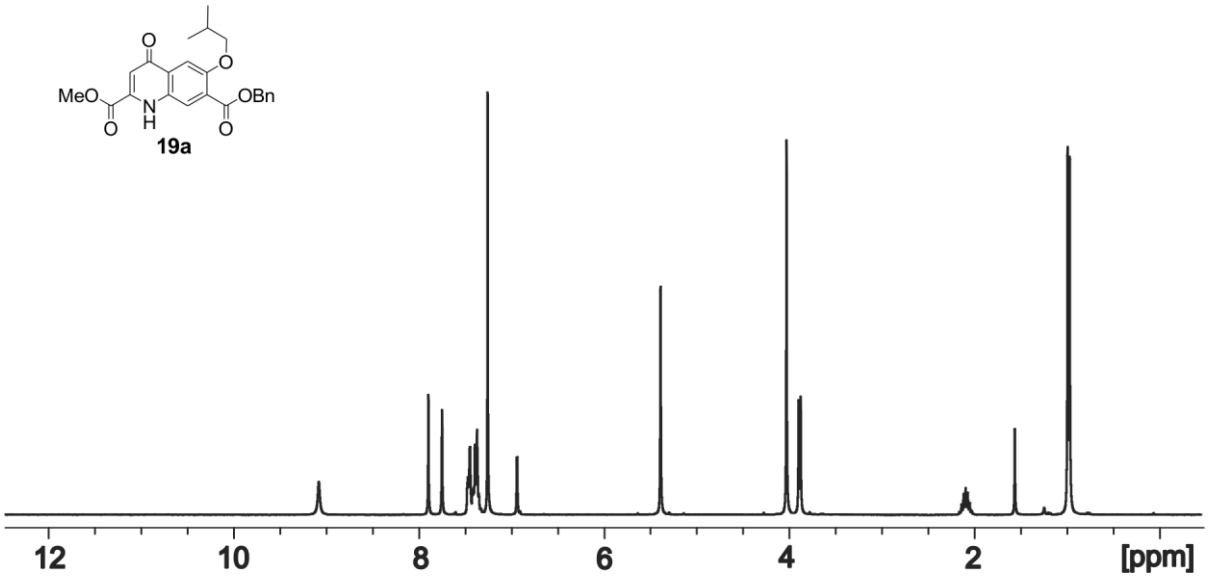

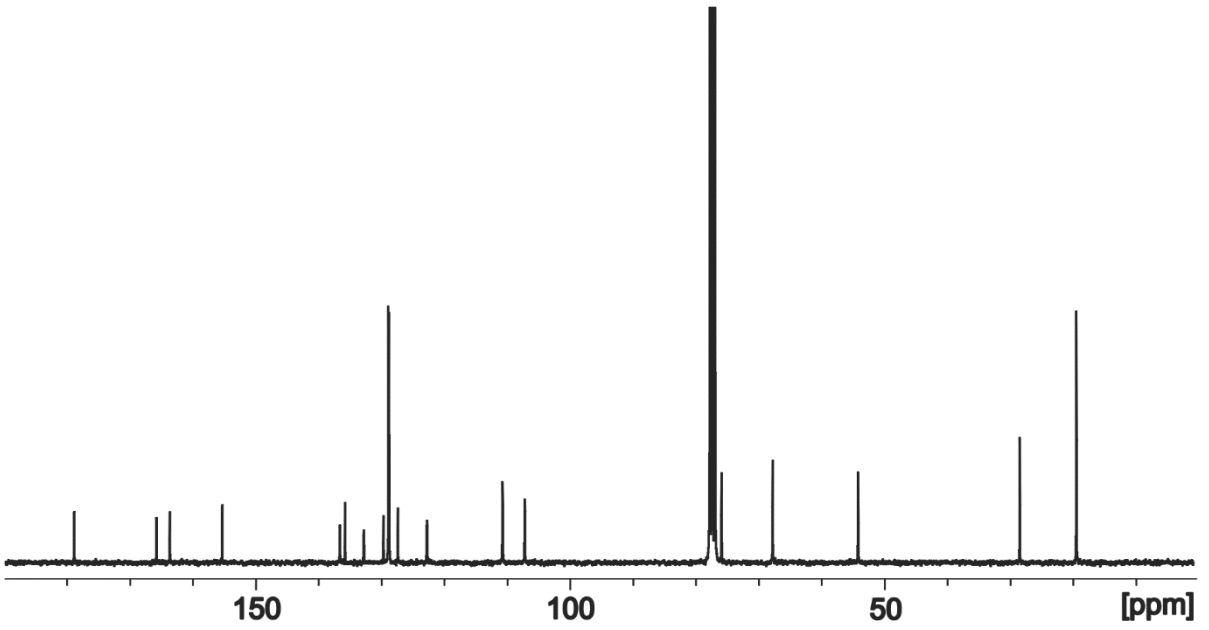

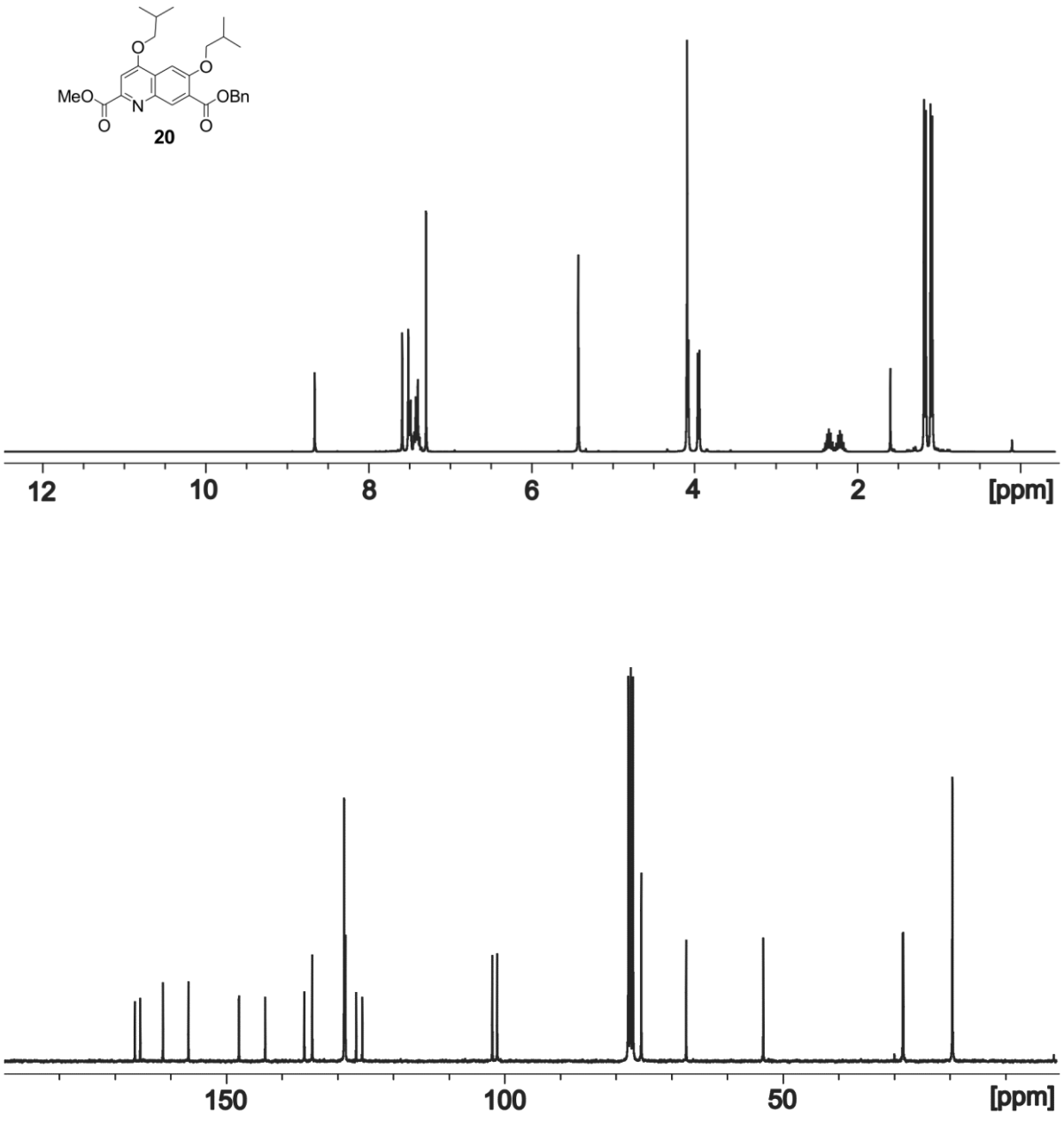

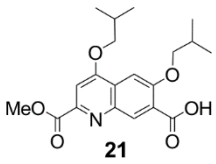

21

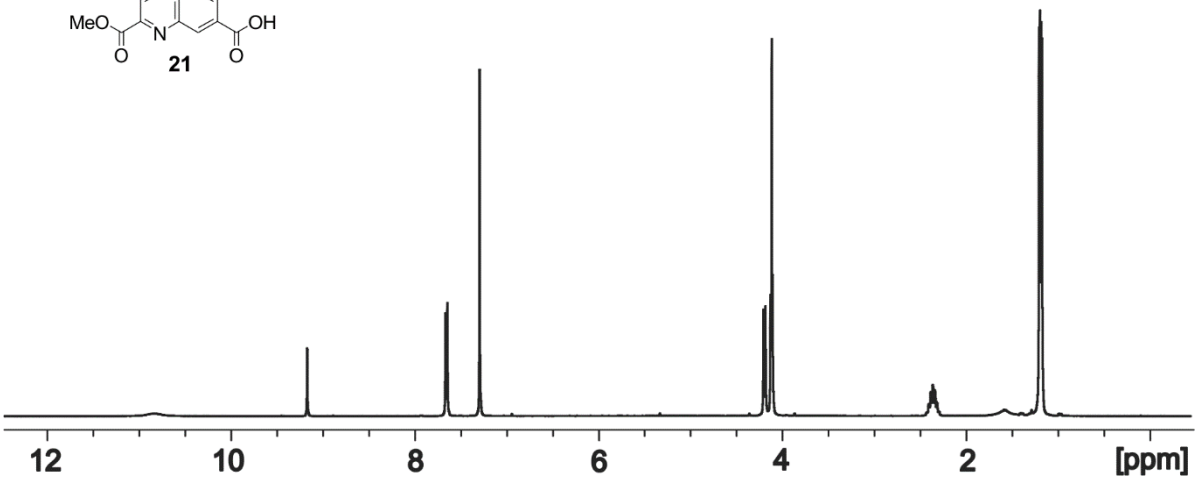

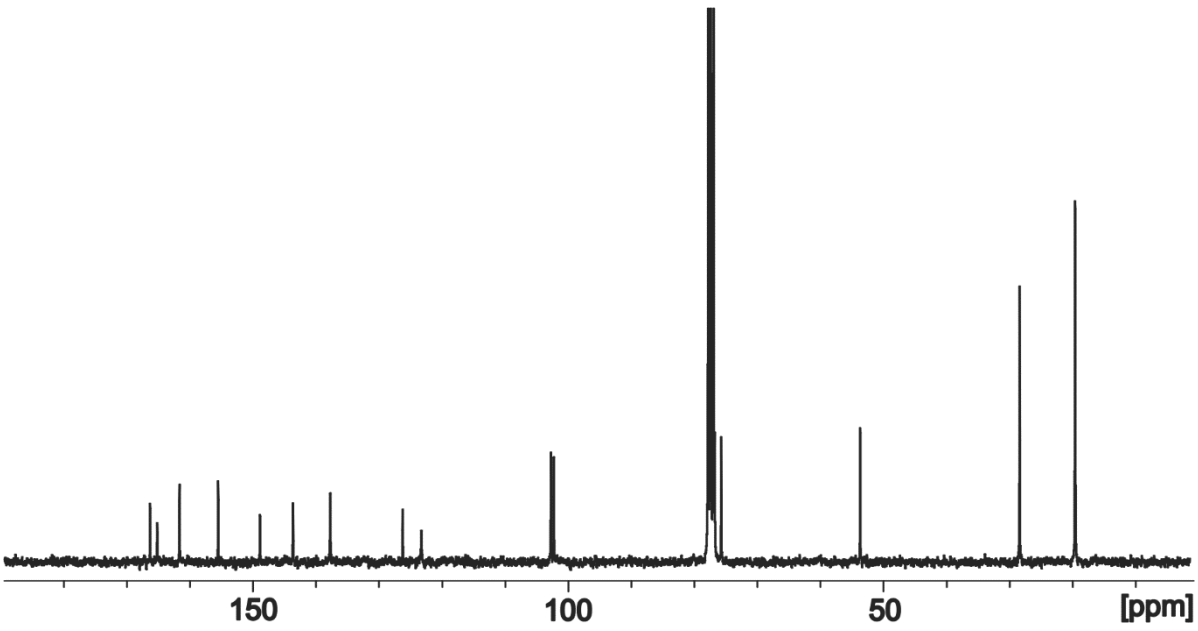

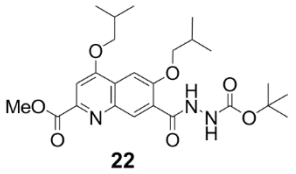

22

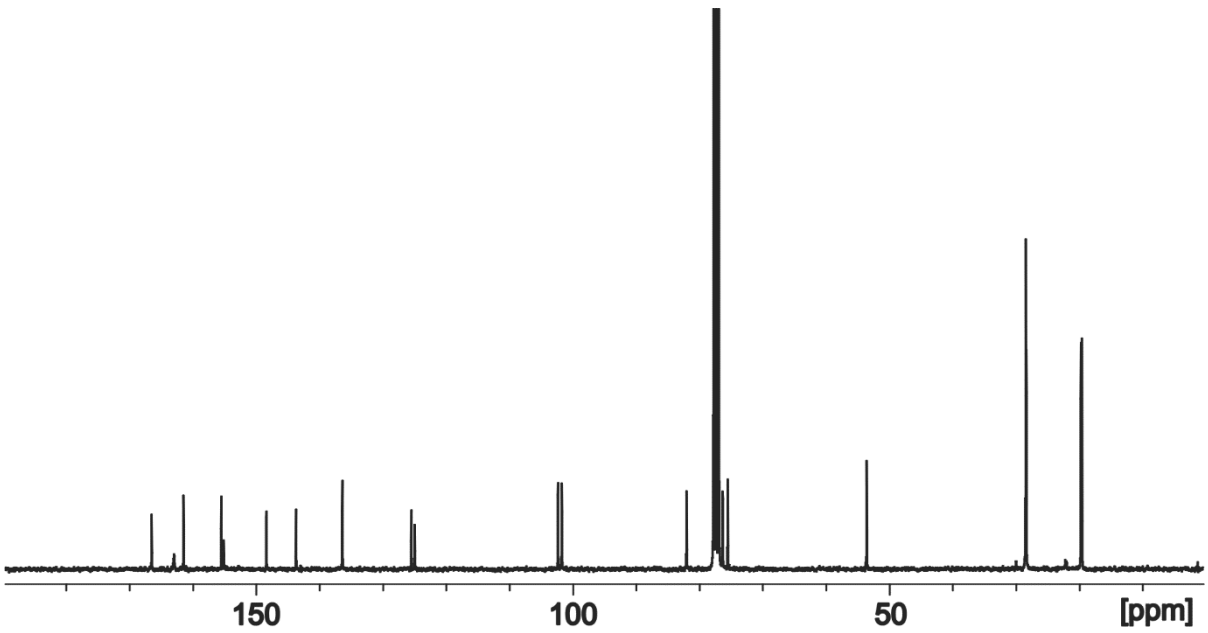

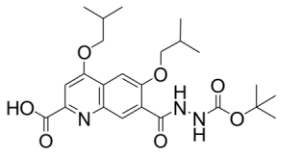

23

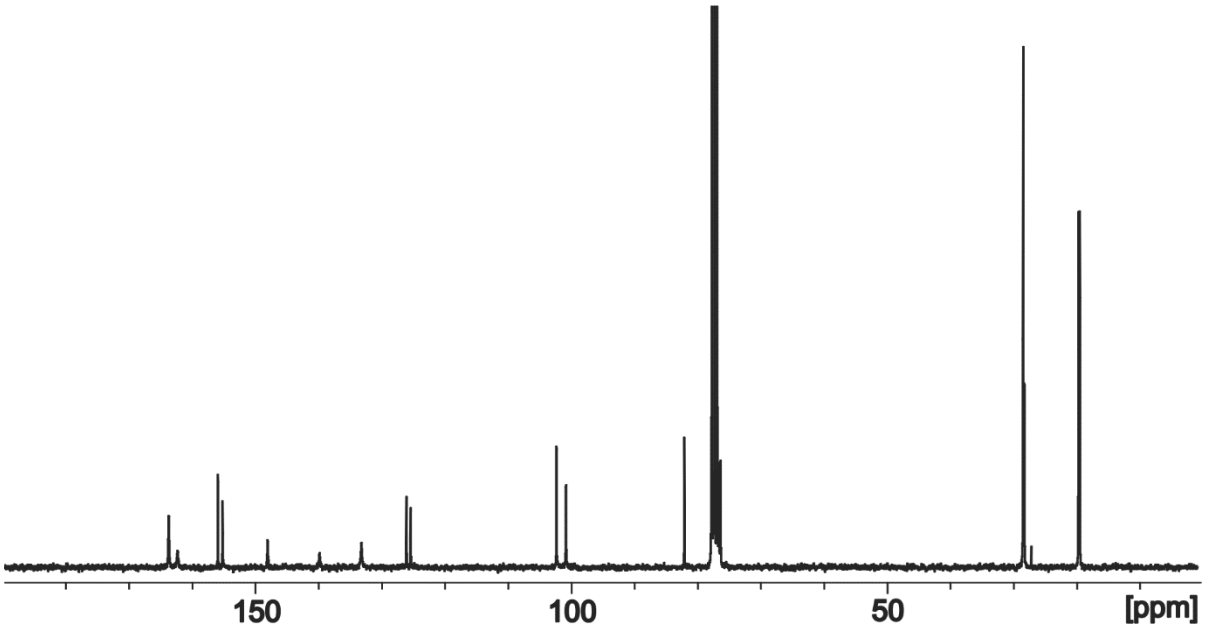

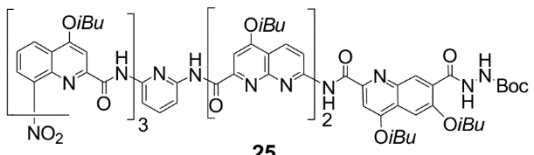

25

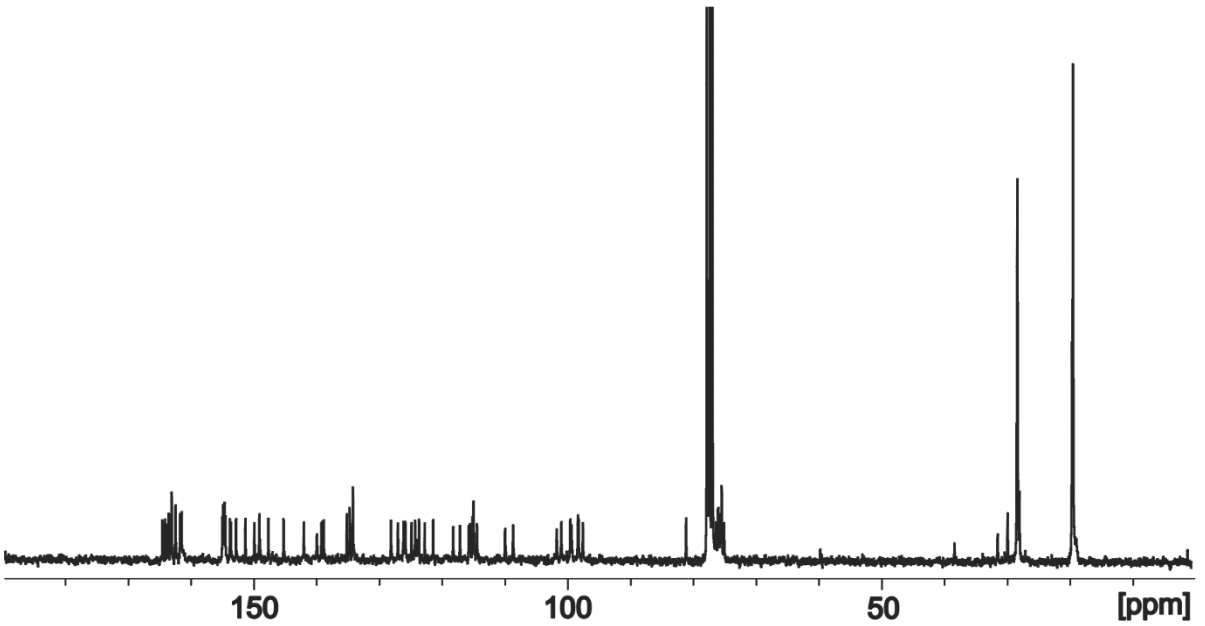

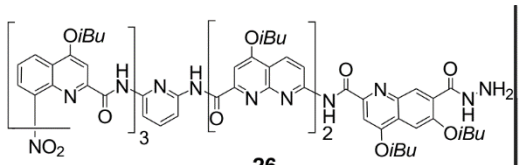

26

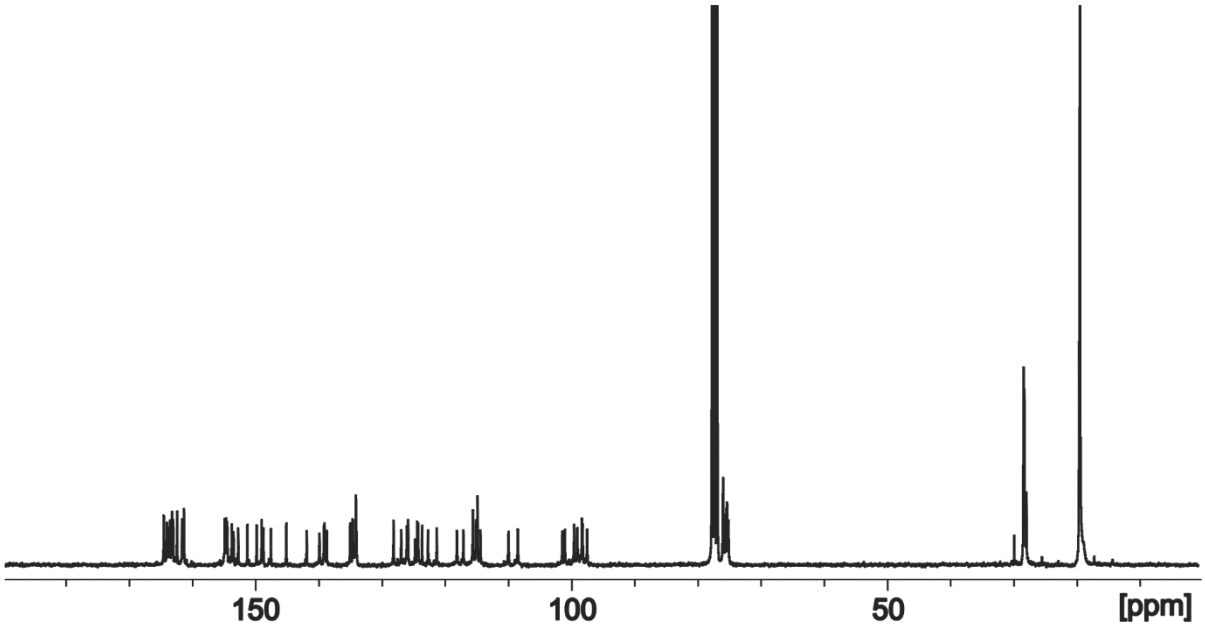

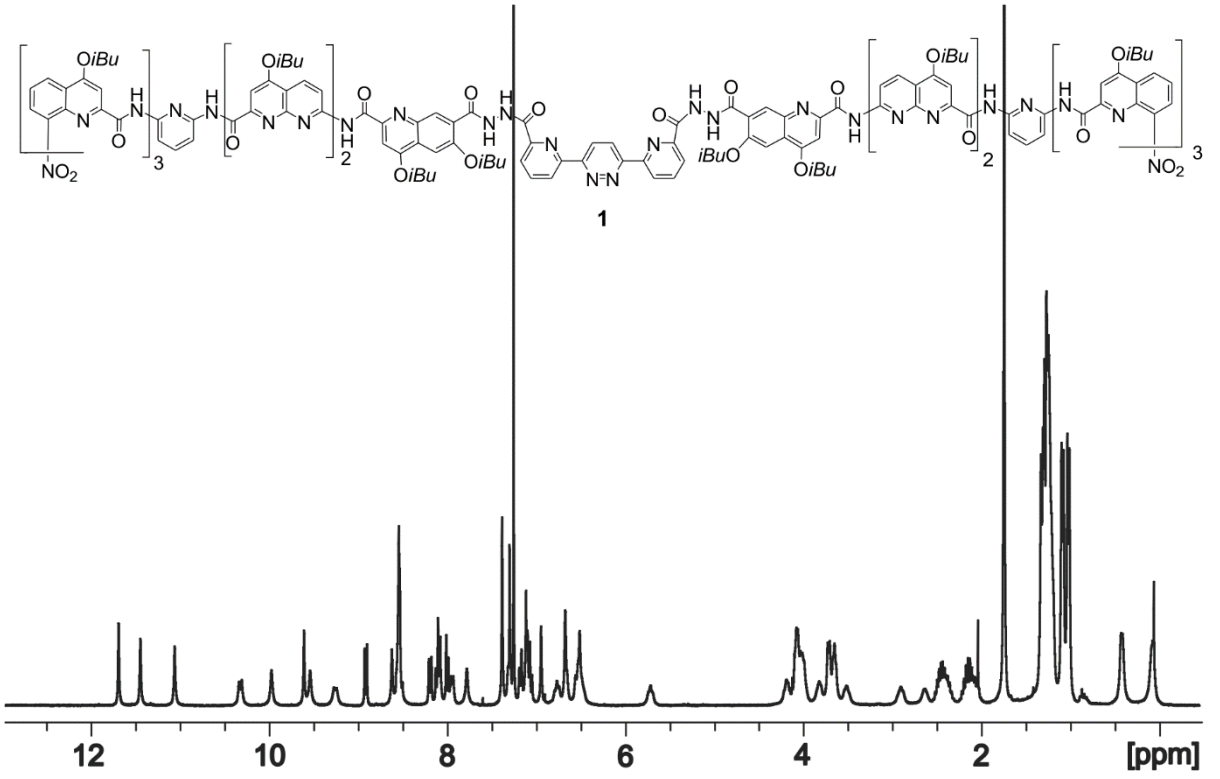

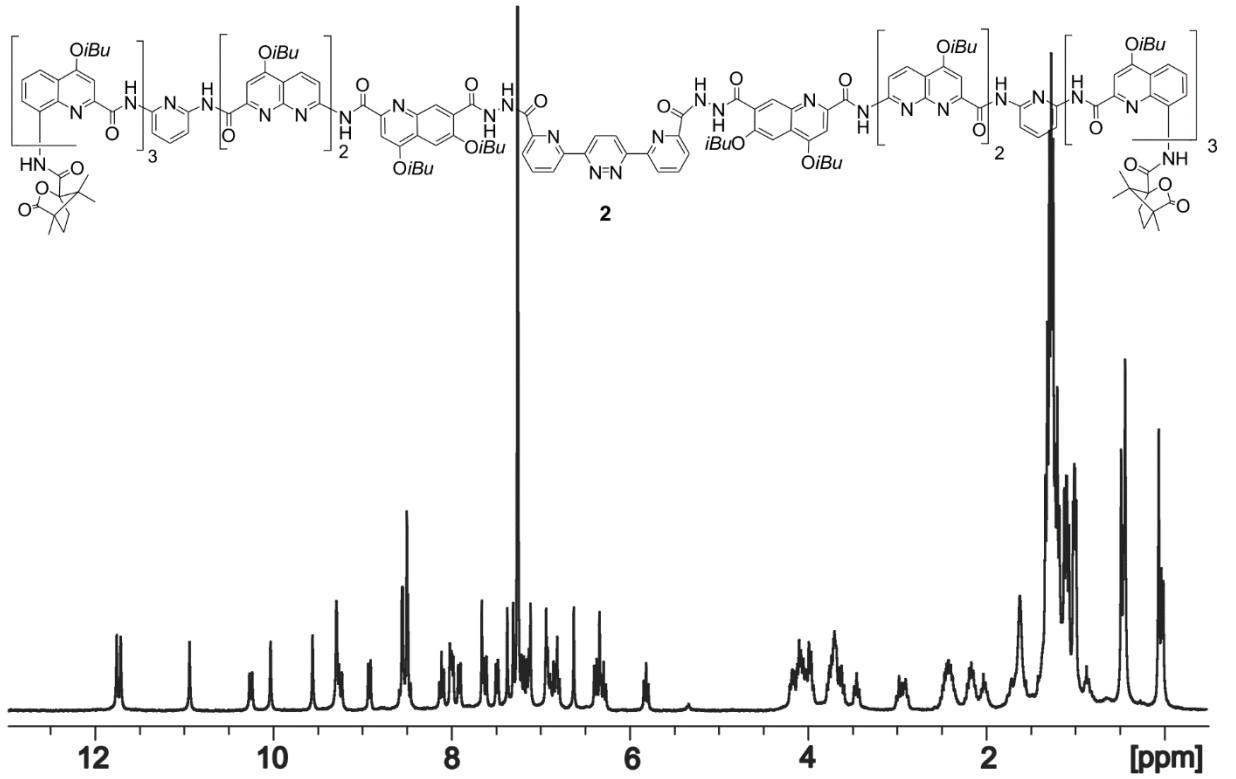

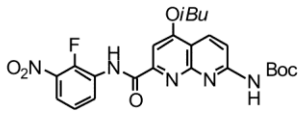

31

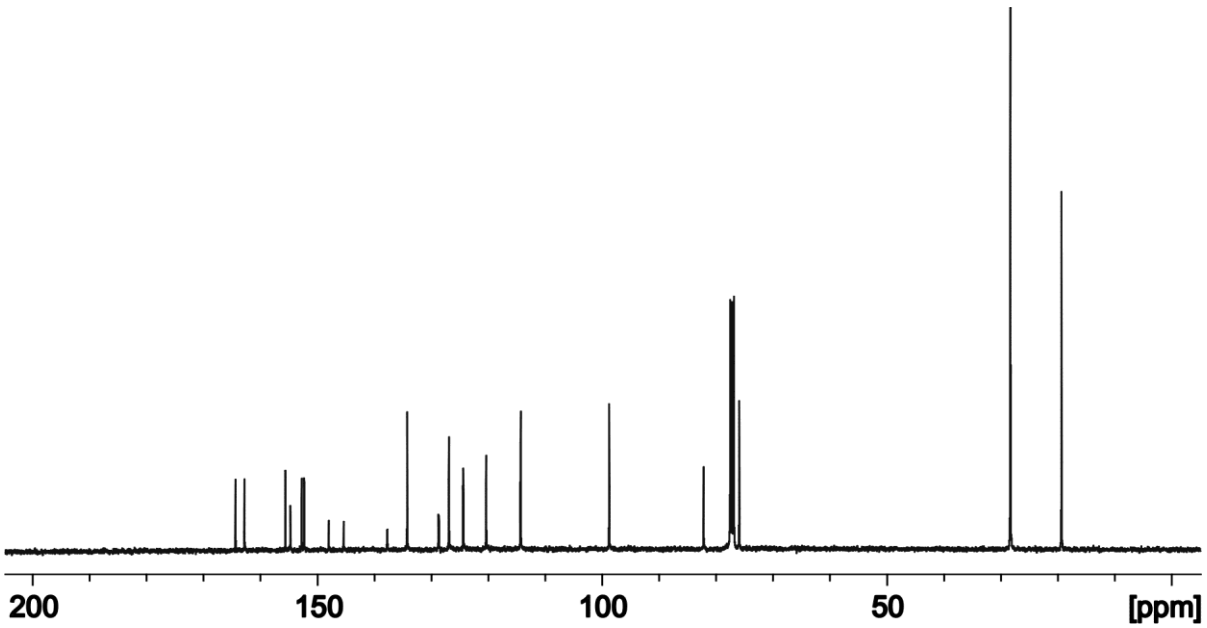

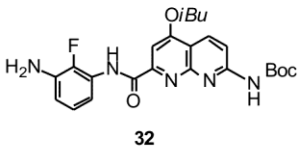

32

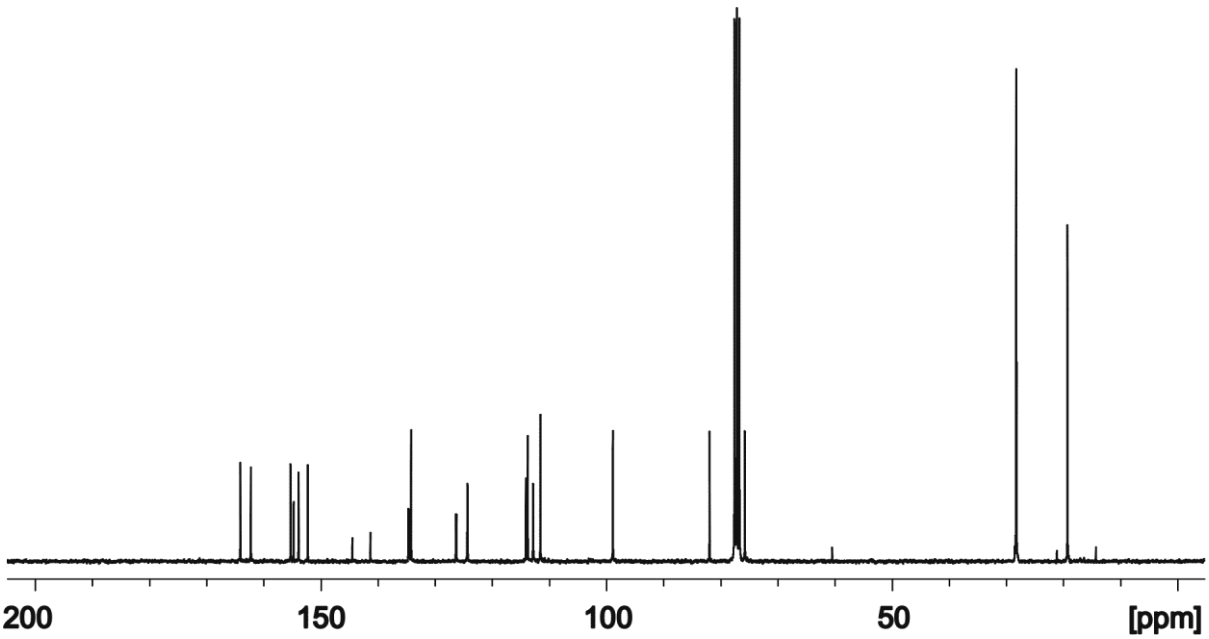

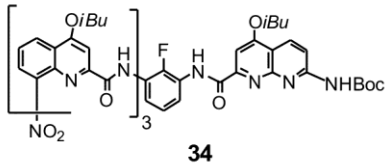

34

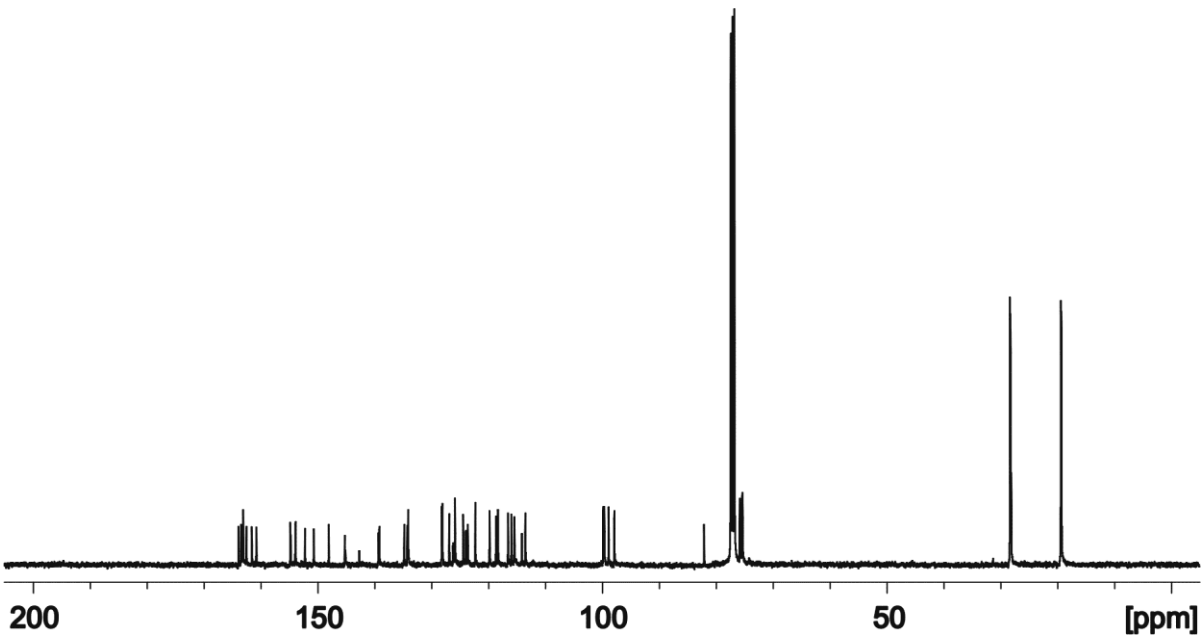

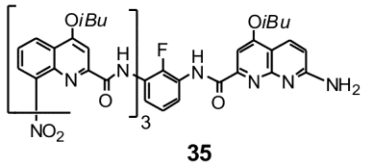

35

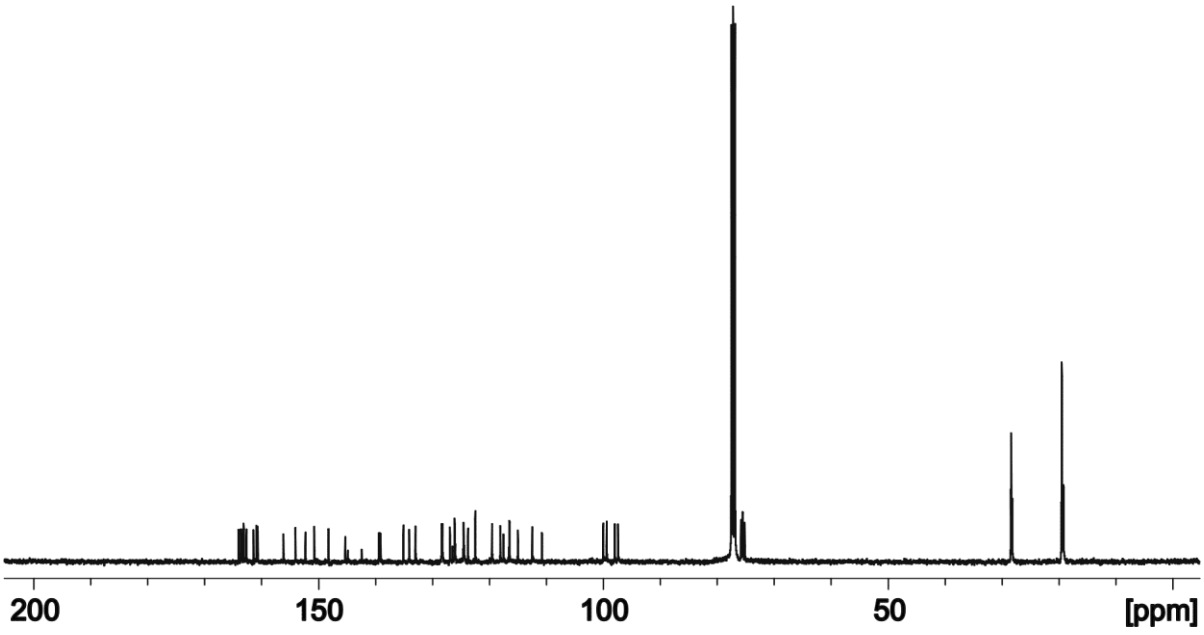

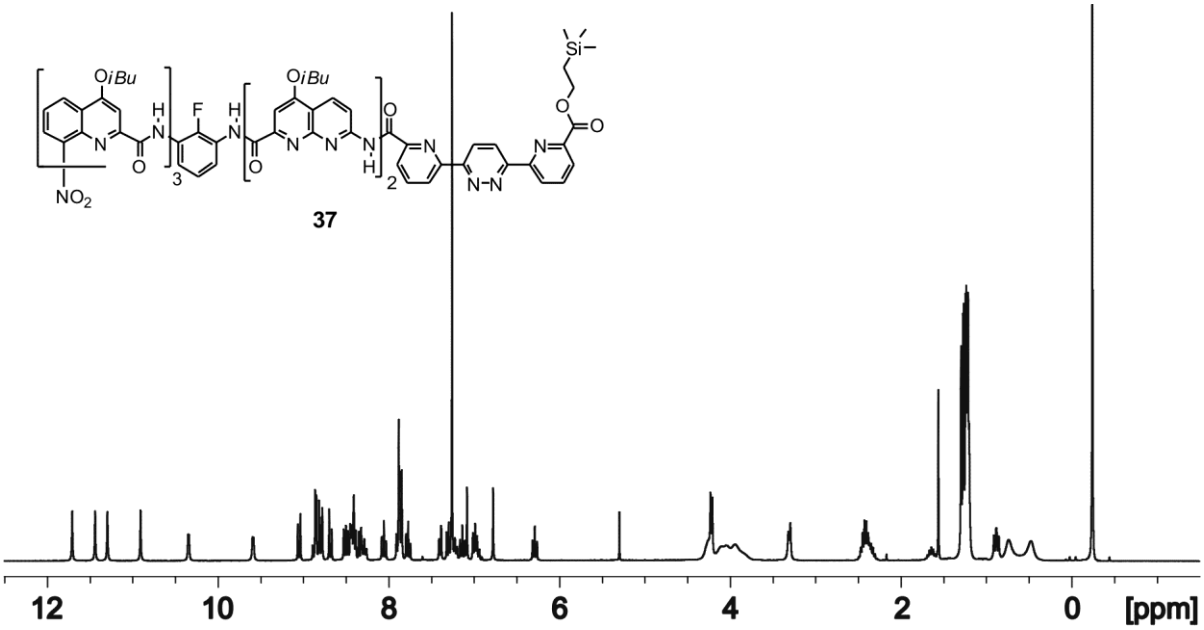

37

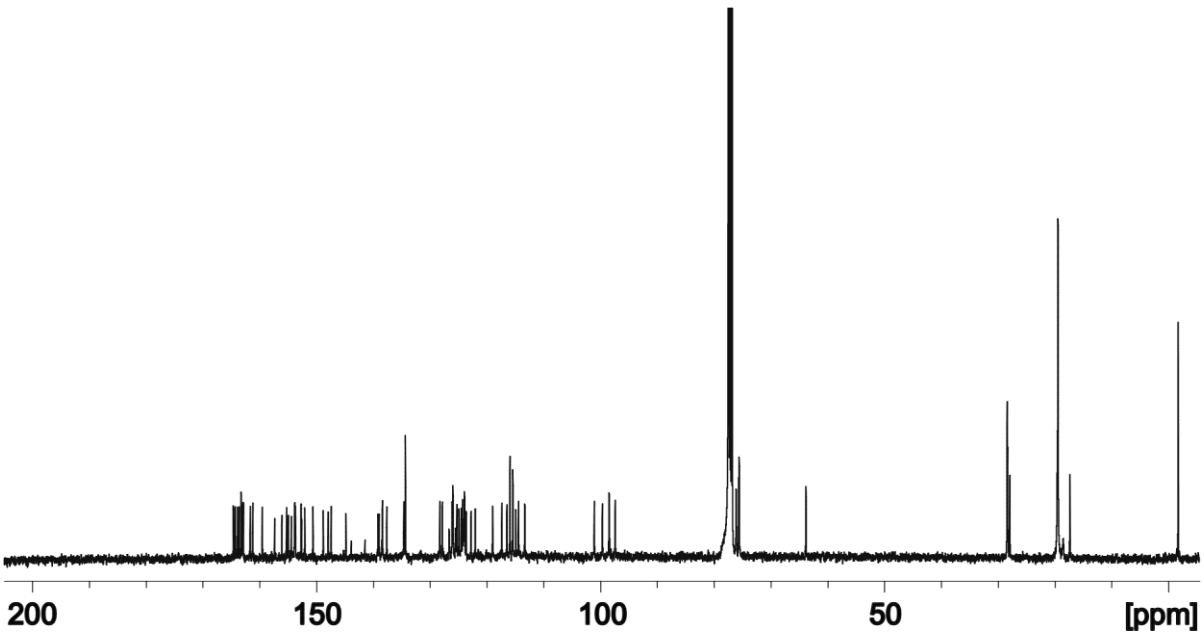

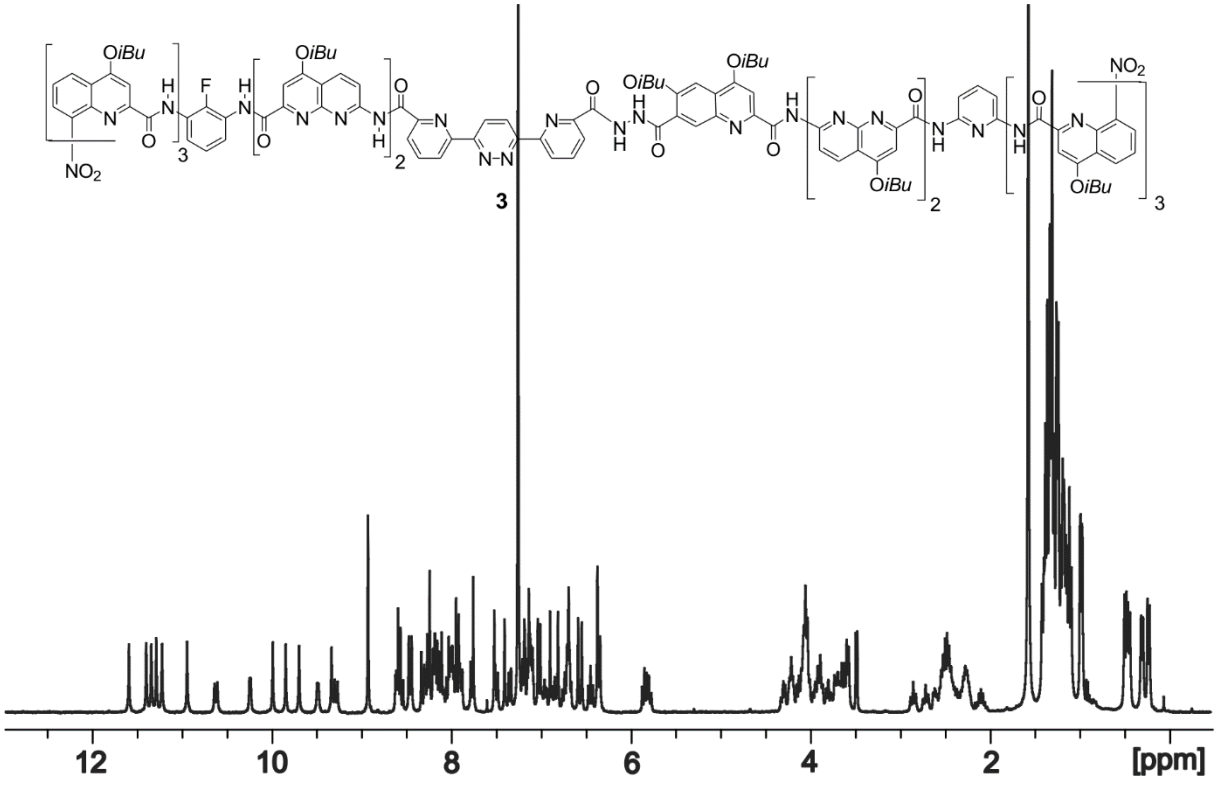

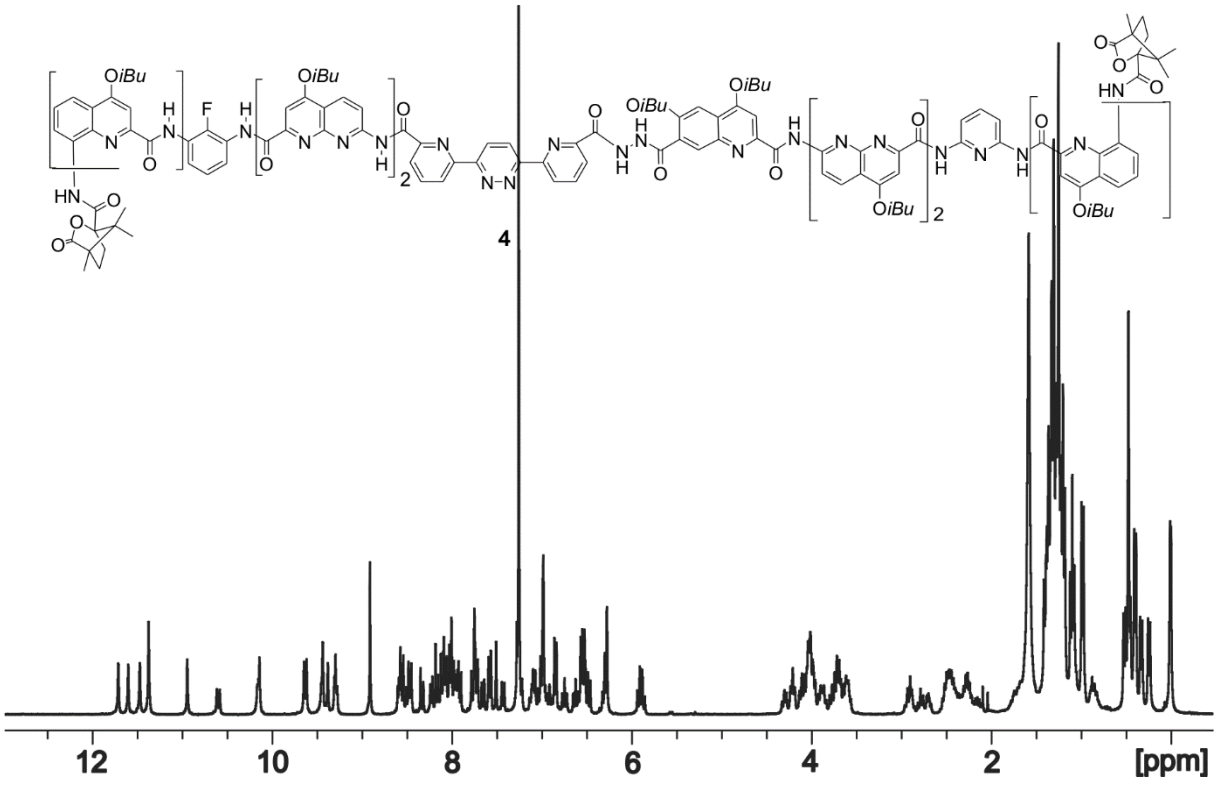

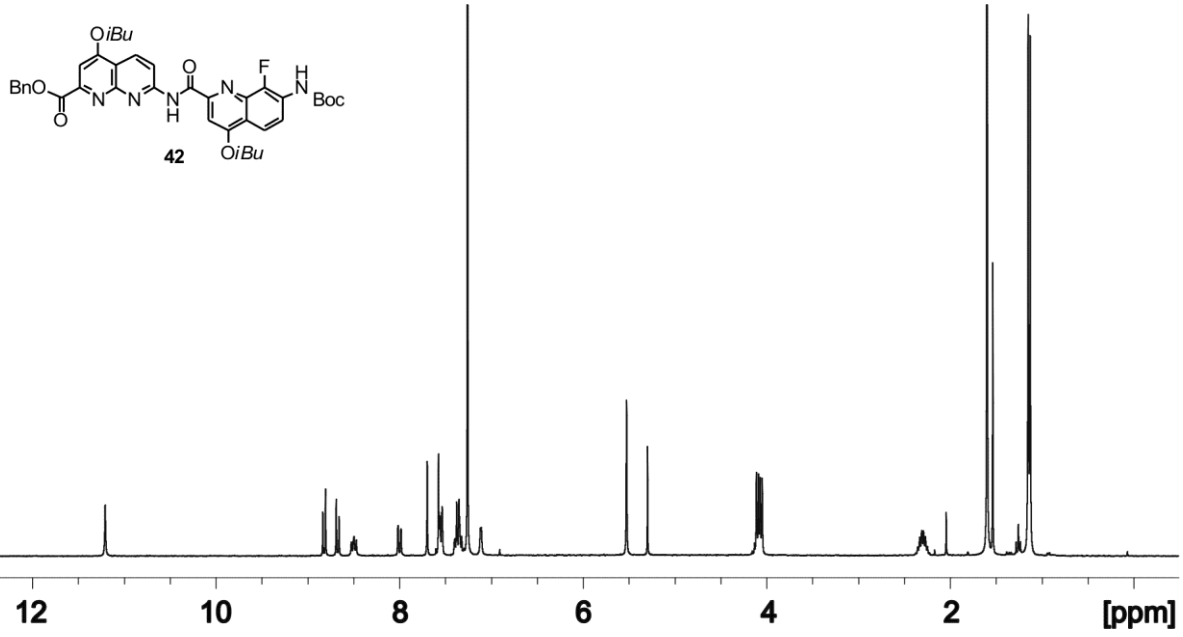

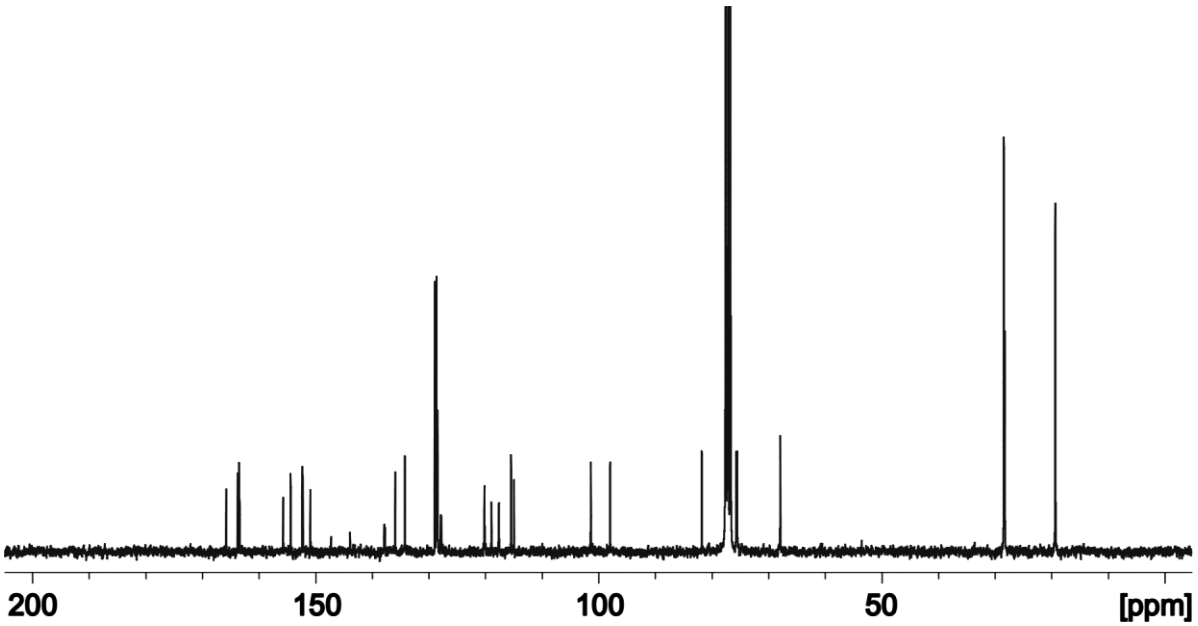

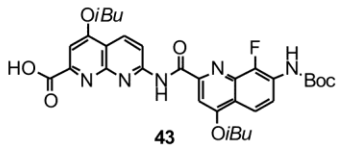

43

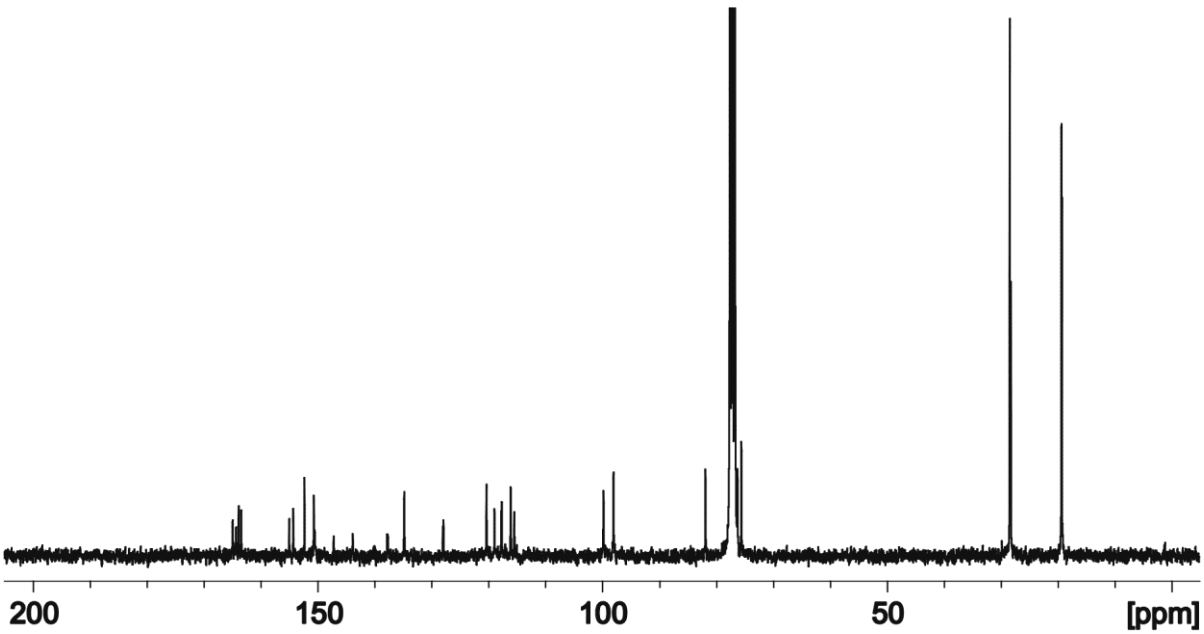

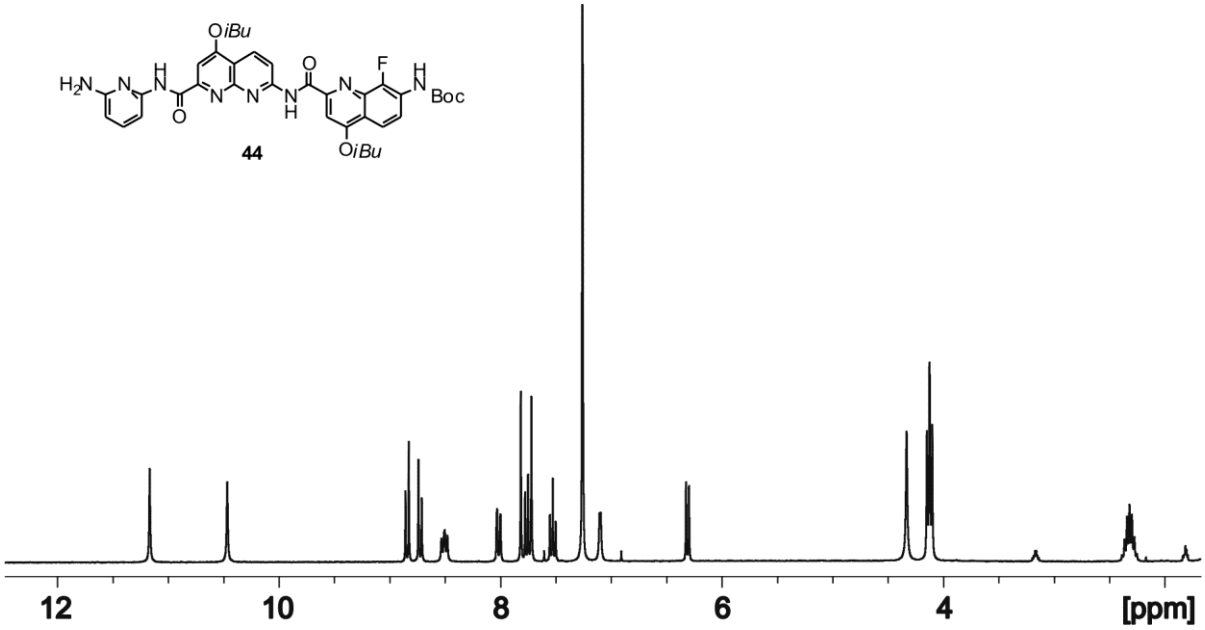

44

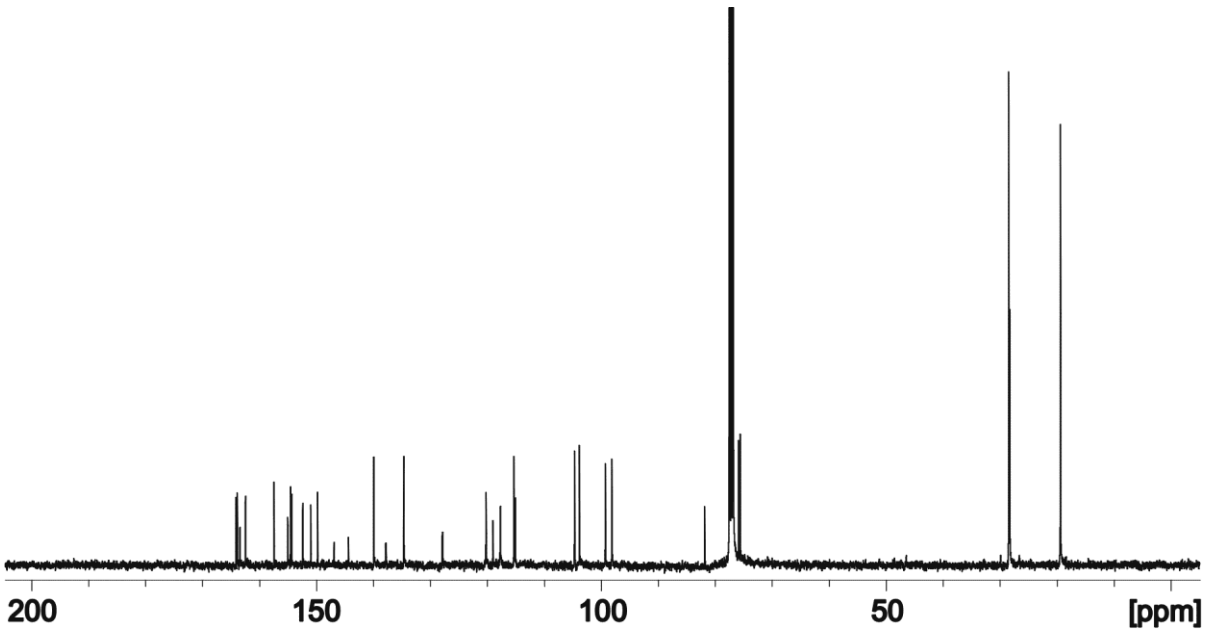

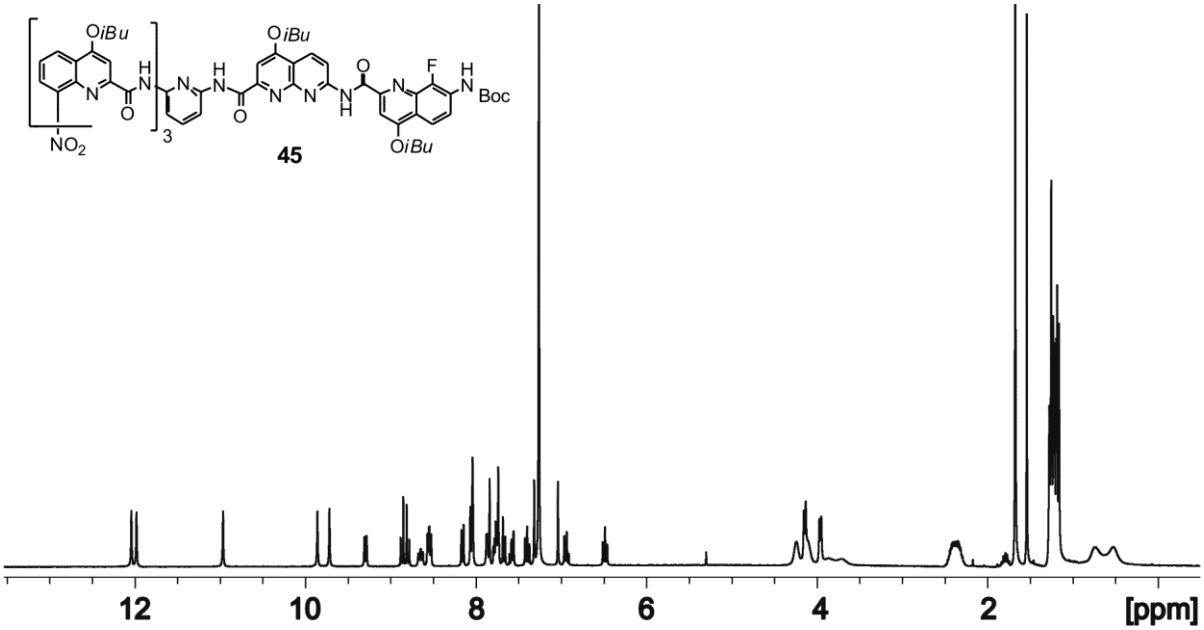

45

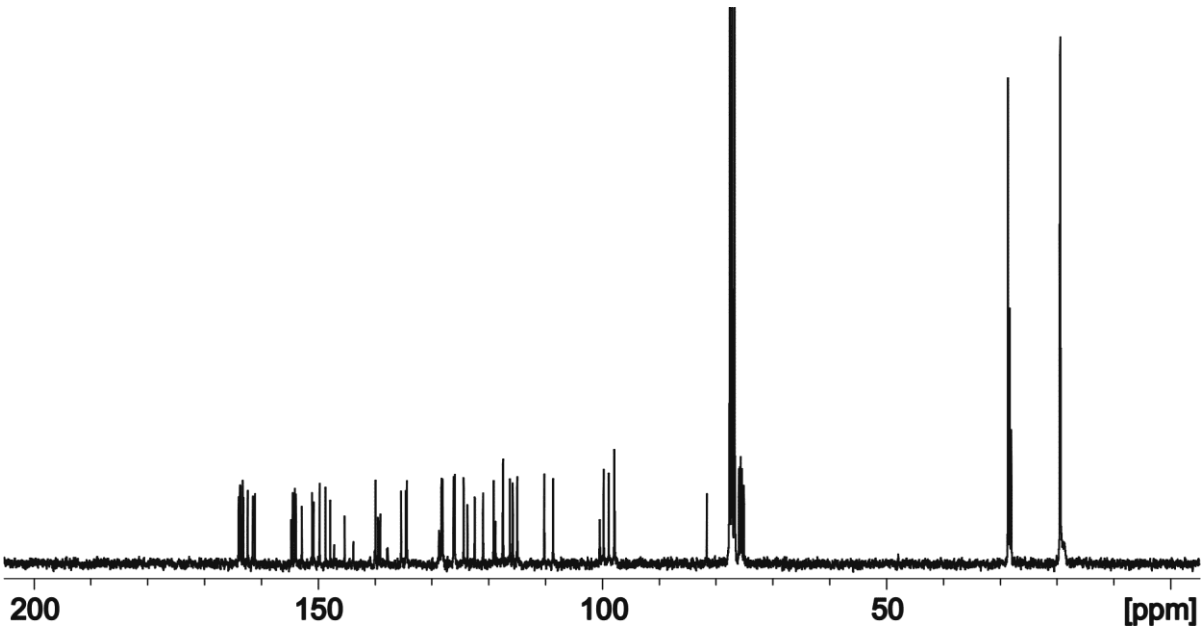

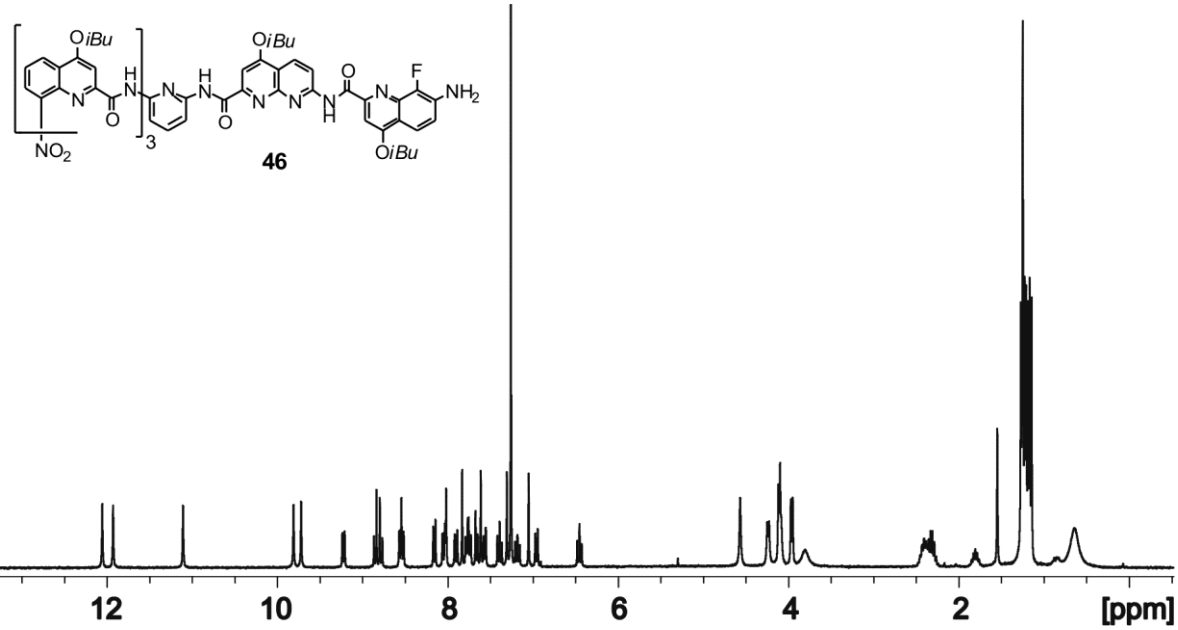

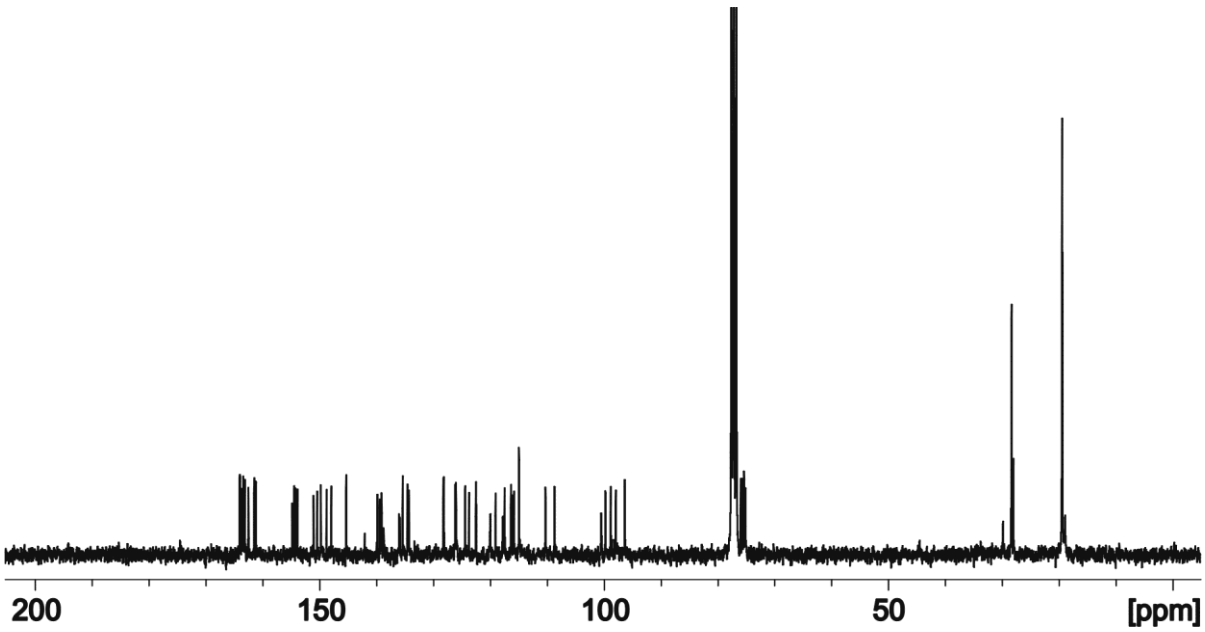

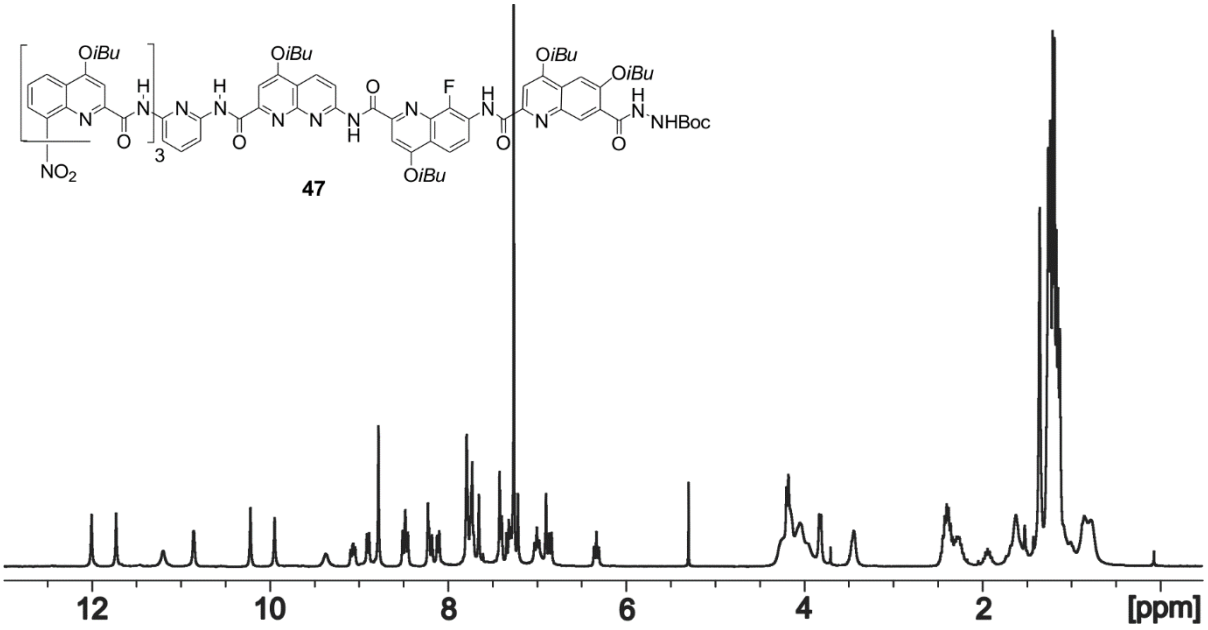

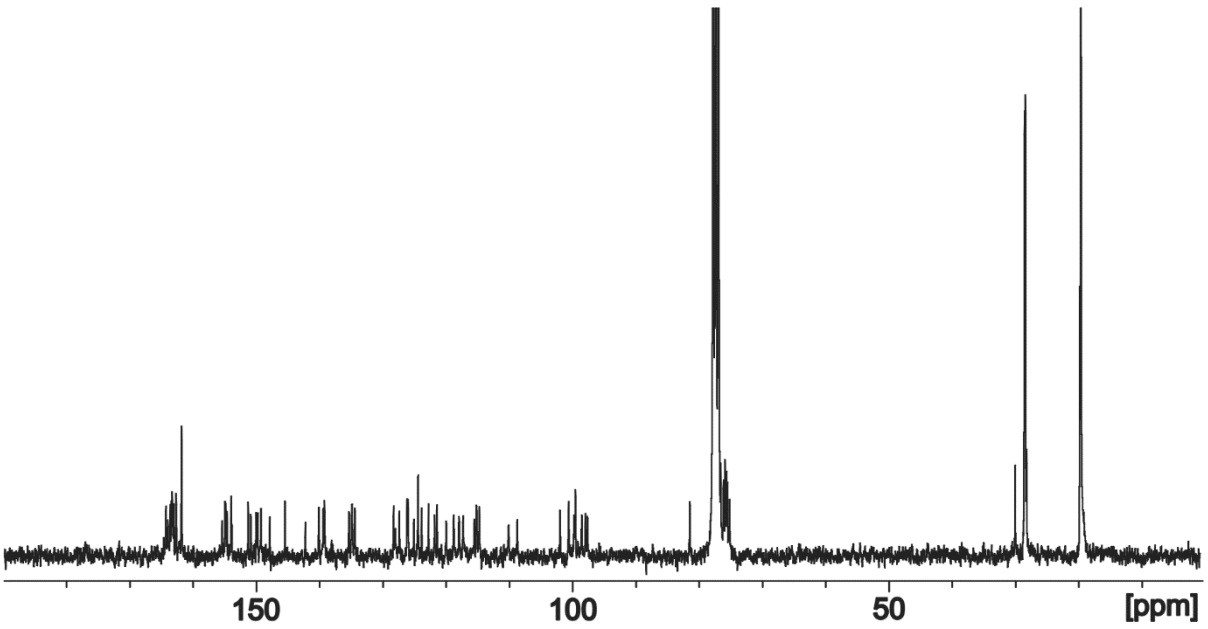

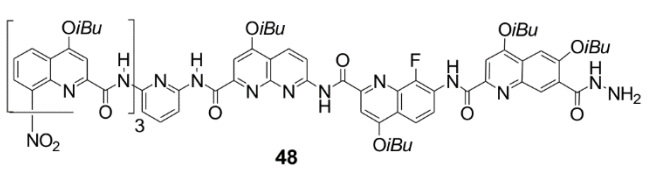

48